University of Alberta

Predicting the Elastic Properties of Two Dimensionally Braided Tubular Composite Structures Towards the Design of Braid-Reinforced Polymer Medical Catheters

by

Cagri Ayranci

A thesis submitted to the Faculty of Graduate Studies and Research
in partial fulfillment of the requirements for the degree of

Doctor of Philosophy

Department of Mechanical Engineering

©Cagri Ayranci
Fall 2010
Edmonton, Alberta

Permission is hereby granted to the University of Alberta Libraries to reproduce single copies of this thesis and to lend or sell such copies for private, scholarly or scientific research purposes only. Where the thesis is converted to, or otherwise made available in digital form, the University of Alberta will advise potential users of the thesis of these terms.

The author reserves all other publication and other rights in association with the copyright in the thesis and, except as herein before provided, neither the thesis nor any substantial portion thereof may be printed or otherwise reproduced in any material form whatsoever without the author's prior written permission.

EXAMINING COMMITTEE

Dr. Jason P Carey, Mechanical Engineering

Dr. Derek Emery, Radiology & Diagnostic Imaging

Dr. Pierre Mertiny, Mechanical Engineering

Dr. Samer Adeeb, Civil and Environmental Engineering

Dr. Frank K. Ko, Materials Engineering, Advanced Materials and Process Engineering Laboratory (AMPEL), University of British Columbia

DEDICATION

Dedicated to my Stephanie and my soon to be born child.

Also dedicated to my mom, Dr. Guler Ayranci, my dad, Dr. Erol Ayranci, my brother, Korhan, and sister, Inci.

A special dedication to my grandfather:

Aslan Dedem, Mehmet Sukru Seval, you always said that the most important thing in life is scientific knowledge and education. You did your part in this world, three children and eight grandchildren all of which have received, or in the process of receiving, the highest levels of education in their fields. Now, rest in peace. You are deeply missed.

ABSTRACT

Two-dimensionally (2D) braided tubular composites have been utilized in a wide range of applications including medical equipment such as braided stents and catheters.

Catheters are long flexible tubes used in catheterization procedures, such as angiography and ablations. In this thesis, angiographic catheters were specifically targeted; which are referred as “catheters” for the remaining of the document. Catheters are typically used with guidewires which provide structural support to the often low rigidity catheters. In some catheterization procedures, it may be beneficial to use a 2D braided catheter for increased control and maneuverability in the body. The 2D braided catheter, if designed properly, may provide all the required rigidities for a successful procedure and decrease the dependency to the guidewire compared to conventional catheters. Hence, use of 2D braided catheters may decrease the procedure time, may provide superior control of the device due to its design, and may also decrease the inherent patient discomfort. A thorough understanding of 2D braided composites is of absolute necessity considering the delicate use of medical equipment, such as catheters, in the human body. The aim of this PhD thesis is to address the shortcomings of the available models in the literature by developing an analytical model geometrically consistent with small braided tubular structures and provide all the necessary tools possible to design a target specific braided catheter.

An analytical model that accounts for the effect of diameter of a braided tubular product on the elastic properties, needed for catheter design, was developed. Parametric studies were conducted to highlight the effects of the change in radius on elastic properties of braided composites. Case studies that underline the important geometrical parameters that affect predictions were conducted and findings discussed.

Effect of increased undulation length on elastic properties of braided composites was also investigated. The findings were compared to experimental work using three different fiber/matrix system composites. As predicted by the model, a decrease in the properties was observed experimentally; however, this decrease was found to be more important than predicted. Possible reasons for this behavior are discussed in the view of composite materials and geometrical factors.

The experimental findings of the open-mesh composites were also used to further validate a regression based model available in the literature. Lower linearity limit values for the regression based model were calculated for longitudinal elastic and shear moduli predictions.

PREFACE

The thesis is presented in paper-format and contains six chapters. Chapter 1 is an introduction to the work done and outlines the thesis objectives. Amongst the remaining five chapters, Chapters 2, 3, 4, and 5 were accepted or in-print in scientific journals, Chapters 6 has been submitted to a scientific journal and is under review.

This PhD study was geared towards design of braided catheters. It was aimed to provide an accurate predictive model to designers and provide all necessary tools to be able to have good control over the design of said catheters by having a wide range for design tailorability. This was done by dividing the PhD thesis into two main research streams to analyze the braided structure's unit cell. The unit cell was analyzed in terms of (a) effect of curvature of the unit cell on the elastic properties of braided structures, and (b) effect of undulation length, and thus closed versus open mesh braided architectures, on the elastic properties of the braided structures.

Chapter 2 is a review paper that serves as the literature review of the study. The relevant models are presented and developed in the papers published in Chapters 3 and 4 of this thesis. In Chapters 3 and 4 the curved-unit cell model is developed. In Chapters 5 and 6 open mesh structures are investigated.

ACKNOWLEDGEMENTS

I postponed writing this section until the end. I wanted to make sure that this is really happening, and this long journey is really coming to an end. I enjoyed it. It was not always easy or fun, but people around me always made it easier to put a smile on my face.

I would like to start with Dr. Jason Carey. Jason, I have enjoyed your supervision, guidance, and friendship tremendously during this journey. I think we worked really well together, and I am looking forward to contributing much more to this field together in the coming years. I can only hope to be as good as a supervisor to my students in the future as you were to me. I learned a lot from you, benefited a lot from your knowledge and experience, and I am going to be always thankful for this. You always went above and beyond your duties as a supervisor, like you do to all of your students, and prepared me for the life of an academic, thank you. I would like to also thank you for your continuous financial support during this journey.

I would like to thank my supervisory committee members, Dr. Pierre Mertiny and Dr. Derek Emery, and to my Ph.D. defense examination committee members, Dr. Frank Ko and Dr. Samer Adeeb, for their valuable contributions to my work and for their time.

Stephanie'cigim, my beautiful wife, I thank you for all your support, and understanding. I know it was not an easy journey for you either, but I promise I will have more time for us after this.

I would like to thank my parents, Guler and Erol, for their support throughout all my studies. Their help, support, and confidence in me made it possible for me to complete this journey, thank you. My brother and sister, Korhan and Inci, you have always been there for me and I thank you for all your support, help, and understanding.

Dan Romanyk, the lab would have been very boring if we did not have our daily coffee breaks and "nice" conversations. I would like to also thank you and Mr. Troy Awid for your help in conducting some of the experiments of this thesis.

I would like to extends my thanks also to the University of Alberta and the Mechanical Engineering Department for their financial support, and the Mechanical Engineering machine shop for their technical assistance during this study.

TABLE OF CONTENTS

LIST OF TABLES

LIST OF FIGURES

Glossary :

- Braiding : A two dimensional, automated composite prefom manufacturing technique.
- Braid angle : Angle between the longitudinal direction of the braided composite and deposited fiber strand.
- Catheter : A small diameter flexible polymeric tubular product used in catheterization procedures.
- Closed mesh braid : A braid architecture with a tight mesh due to minimal undulating and matrix-only regions.
- CLPT : Classical Laminated Plate Theory
- Cross-over regions : Sub-regions of a unit cell where braided strands crosses over each other.
- Diamond braid : A braid architecture where braided fiber strands crosses each other in a 1x1 pattern.
- Lamina : A single layer of a thin composite.
- Laminate : A composite that is composed of multiple laminae.
- Marix-only region : Sub-regions of a unit cell where there are no fibers.
- Open mesh braid : A braid architecture with long undulating regions and large matrix-only regions.
- Stent : A medical device that has a meshed structure used to provide additional support to damaged vessels in the body.
- Undulating regions : Sub-regions of a unit cell where the fiber strands travel from one crossover region to the other.

- Unit cell : A small (imaginary) repeating element in a braided composite that is assumed to represent the behavior of the overall structure.
- Mandrel : A cylindrical rod or tube device used during braiding to deposit fibers on to form the preform.

Nomenclature : :

- 1, 2, 3 : Lamina coordinate system
- x, y, z : global coordinate system of the unit cell.
- a_u : Undulation length.
- β: Undulation angle of a strand.
- $\boldsymbol{\varepsilon}^0$: Strains of the midplane of a laminate, CLPT.
- $\boldsymbol{k}^0$: Curvature of the midplane of a laminate, CLPT.
- $\boldsymbol{\phi}$: arch angle
- ν : Poisson's ratio.
- A : Extensional stiffness matrix, CLPT.
- B : Coupling stiffness matrix, CLPT.
- D : Bending stiffness matrix, CLPT.
- E_{11} : Longitudinal elastic modulus of a lamina.
- E_{22} : Transverse elastic modulus of a lamina.
- E_m : Elastic modulus of matrix.
- E_{xx} : Longitudinal elastic modulus of a braided structure.
- E_{yy} : Transverse elastic modulus of a braided structure.
- G_{12} : Shear modulus of a lamina.
- G_m : Shear modulus of matrix.

- G_{xy} : Shear modulus of a braided structure.
- h_c : Strand thickness.
- I : Moment of inertia.
- J :Polar moment of inertia.
- K_t : Stress concentration factor.
- LLL : Lower linearity limit.
- M : Bending moments per unit length, CLPT.
- N : Normal forces per unit length, CLPT.
- $\boldsymbol{Q}$: Stiffness matrix of a lamina.
- $\overline{\boldsymbol{Q}}$: Stiffness matrix of the laminate defined with respect to the global laminate coordinates.
- V_f : Fiber volume fraction of a strand.
- V_{fo} : Fiber volume fraction of a unit cell.
- W_y : Strand width.

CHAPTER 1: INTRODUCTION

Catheters are tubular products utilized in arterial and venous circulation of patients to deliver or withdraw fluids, including blood and medication, and collect data [1]. Catheters are generally used along with a guidewire [2] as they are stiffer compared to catheters. Guidewires provide support and increased stiffness during a procedure as well as guide the catheter to its target in the body.

Although a very common procedure, catheterization can be uncomfortable for patients. In some procedures, it may be possible to improve catheterization procedures by designing an alternative catheter that has all the required rigidities for a specific procedure [3, 4] with increased controllability and maneuverability. Use of 2D braided catheter may shorten the catheterization procedure time, decrease the inherent patient discomfort, and may also provide superior control of the device due to its design. The 2D braided catheters may be designed to be stiff and torquable but also flexible enough to obtain optimal catheterization parameters.

Carey et al, [3, 5], listed axial (AE), flexural (EI), and torsional (GJ) rigidities as important parameters for catheter characterization; where E and G are the longitudinal elastic and shear moduli, and A, I and J are the area, first moment and polar moment of inertia, respectively. 2D braiding provides the designer good control over parameters that affect rigidities and thus on a successful catheter design and end product.

There are many different types of catheters and guidewires with many different specifications and materials [2]; hence, the braided catheters must have a wide range of design tailorability to be able to compete with the existing catheters and guidewires. A previous study, [4], has documented the catheterization procedure, different types of currently available catheters and their materials [4].

When designing a braided composite catheter, a designer may control three major parameters, namely, fiber/matrix properties, angle of the fiber yarn with respect to the longitudinal direction (braid angle), and geometry of the braid architecture (unit cell).

Selection of fiber and matrix is a matter of the specified design requirements given that they must adhere to medical equipment standards such as sterilization and biocompatibility. Schneider [2], Carey et al [3], and many others, listed a number of materials that may be used for conventional as well as braided catheters.

Changing the braid angle of a braided composite has a direct effect on the mechanical properties of the end product. Due to available computerized systems used in the braiding machines, operators have good control over the braid angle of the end products.

2D braided composites have a repeating structure called “unit cell”. Many identical unit cells come together to form the braided structure; therefore, properties of one unit cell is assumed to be representative of the entire structure that has the same unit cell configuration. Control over the geometry of the unit cell provides one level of control over the rigidities.

1.1. Thesis Objectives

There are a number of available models in the literature that were proposed to predict the elastic properties of braided composites; however, these models are mostly developed for high stiffness applications and large structures. Hence, they were developed either for flat-braided structures or researchers assumed that using a flat unit cell would be sufficient accurate for large tubular braided structures. This assumption may be acceptable for large diameter tubular structures because a unit cell on a large diameter tubular structure may be considered almost flat as its radius of curvature will be minimal. On the other hand, if the diameter of the tubular structure is small, the effects of the geometry on the unit cell may play an important role in predicting elastic properties.

The objective of this thesis is to develop a model that addresses the shortcomings of the previous models and give the braided catheter designer a better understanding and control of the braided composites to design with accurate predictions.

In this Ph.D. thesis, the unit cell of a braided structure was analyzed from two different points of view to have a thorough understanding of the unit cell architecture effects on elastic properties. First, the effect of unit cell curvature, and second, the effects of the undulation length between overlapping strands in the unit cell on the properties are investigated. It is hypothesized that including curvature in an analytical model will account for some of the variation found between existing models and experimental data. It is further hypothesized that there are differences in elastic properties between open and closed mesh braids.

1.1.1. Curved-Model

An analytical model, which considers the effects of radius of curvature of the unit cell on the elastic properties as a function of braid angle will be developed and compared to predictions of the flat-unit cell models. Validation will be performed using experimental data. Case studies will be conducted to understand the sensitivity of the model to unit cell geometry.

1.1.2. Open-mesh Structures

Unit cells can be divided into two main types, namely: closed-, and open-mesh structures. Increasing the undulation length in a unit cell, would consequently introduce regions that do not have any reinforcing fiber into the structure hence creates an "open-mesh" structure and eventually causes a decrease in the properties. Although in many applications of braided composites, this decrease is undesirable and avoided by using closed-mesh structures (consequently, this may be the reason why open-mesh structures were not investigated a lot in the literature), for design of braided catheters, this presents an invaluable tool to be able to target specific rigidities. Hence, as part of this PhD thesis, a parametric study that outlines the effect of having different sizes of open mesh structures will be conducted and results will be compared to experimental data. Finally, experimental results of open-mesh structures will be used to further validate a previously developed regression based model for braided composites. An objective will be to determine the model lower linearity limit.

1.2. References

[1] Ratner, B. D., Hoffman, A. S., Schoen, F. J., Lemons, J. E., "Biomaterials science an introduction to materials in medicine", Academic press, Chapter 7, 1996.

[2] Schneider, P.A., "Endovascular skills: guidewires, catheters, arteriography, balloon angioplasty, stents", Quality Medical Publishing, St. Louis, Missouri, 1998.

[3] Carey, J., Fahim, A., Munro, M., Design of braided composite cardiovascular catheters based on required axial, flexural, and torsional rigidities, Journal of Biomedical Materials Research - Part B Applied Biomaterials 70 (1), pp. 73-81, 2004.

[4] Carey, J., "Axial, flexural and torsional rigidities of two-dimensional braided fibre composite medical catheters", PHD thesis, University of Ottawa (Canada), 2003.

[5] Carey, J., Emery, D., McCracken, P., Buckling test as a new approach to testing flexural rigidities of angiographic catheters, Journal of Biomedical Materials Research - Part B Applied Biomaterials 76 (1), pp. 211-218, 2006.

CHAPTER 2: 2-D BRAIDED COMPOSITES: A REVIEW FOR STIFFNESS CRITICAL APPLICATIONS

A version of this chapter was published as:

Ayranci, C., Carey, J., 2D braided composites: A review for stiffness critical applications, Composite Structures 85 (1), pp. 43-58, (2008).

2.1. Introduction

Braiding has been used since 1800's to produce textile fabrics. New demands for high production rate manufacturing of high quality composite materials have focused attention on braiding. A conventional braiding machine has fiber carriers moving in a circular pattern [1]. Half of the carriers move clockwise, the others counterclockwise, in an intertwining serpentine motion producing a desired braid pattern, such as 2-dimensional tubular and flat braids.

The braiding process competes with other composite material or composite preform manufacturing, techniques such as filament winding, pultrusion, and tape lay-up. The advantages and disadvantages of 2D are discussed in the following sections.

2.2. Common terminology

Braiding: A composite material preform (Figure 2. 1 (a)), manufacturing technique. A braiding machine is used to intertwine fibers to create desired braid architecture before or during the impregnation of the fibers.

Braid angle: The angle between the longitudinal direction of the braided preform and the deposited fiber, Figure 2. 1 (b).

Volume fraction: Relative amount of one constituent of the composite to the remaining constituents.

Unit cell: An imaginary small repeating element on a braided composite, Figure 2. 1 (b).

Crossover regions: Regions where intertwining fiber tows are deposited on top of each other in a unit cell.

Undulation region: The region where fiber tows undulate from one crossover region to the other, Figure 2. 1 (b).

Matrix only region: Remaining parts of the unit cell where fiber undulations or fiber crossovers do not exist, Figure 2. 1 (b).

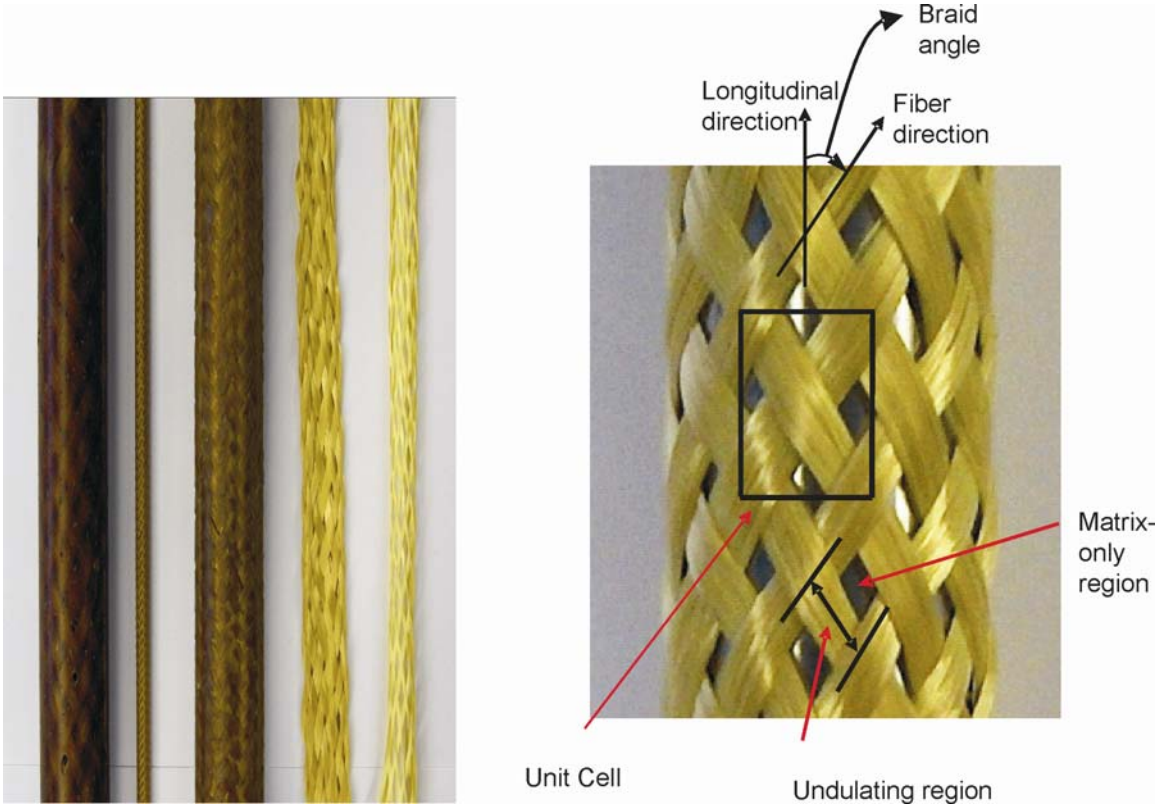

(a) **(b)**

Figure 2.1: (a) various braided composites (first three from the left), different preform sizes (last two on the right); (b) braid architecture (i.e., unit cell, braid angle, undulating region, matrix only region).

2.3. Braid Architecture

Braiding is a composite material preform manufacturing technique where a braiding machine deposits continuous, intertwined, fiber tows to create desired reinforcing braid architecture before or during the impregnation of the fibers.

There are three commonly used braid architectures: Hercules braid, regular braid, diamond braid. Hercules braid is a braid where each yarn passes over and then above three other yarns, where in regular braid each yarn crosses over and below two yarns, and finally if each yarn crosses over and below one other yarn in a repeating manner, it is called a diamond braid [2, 3]. Adding axial fibers along the mandrel axis is called a triaxial braid, and it increases bending and tension strength and also stiffness of braided composite materials. Triaxial braids need to be formed/braided on a mandrel due to the geometric nature of the process, whereas it is sometimes possible to produce a biaxial braided preform without the use of a mandrel. Tubular triaxial braids resist to radial shrinkage, and flat triaxial braids resist to shrinkage in width under tensile loads. Hence, these preforms are compatible as reinforcements in pultrusion process [3].

2.4. Introduction to 2-D Braids

The most common commercial applications of braided composites are, but not limited to, over-braided fuel lines, braided air ducts, rocket launch tubes, and aircraft structural parts [1]. Other possible applications are catheters, automotive shaft reinforcement, sporting equipment, etc.

Conventional braiding machines produce preforms either vertically or horizontally. Most braiding machines are said to be Maypole-type machines due to the serpentine or maypole strand carrier path. There are also Rotary braiders which use two rotating tables. Although they have higher production rates than Maypole braiders, they can not produce flat braids. Flat braids must be produced by carriers following two intersecting serpentine paths; however the intersecting paths form a single path by removal of the horn-gear. This forces the carriers to reverse their motion at the end of the track and form a flat braid instead of completing a circular track on the machine to form a tubular braid [2, 3]. Maypole and Rotary tubular braid preforms are the same in terms of their architectures [2]. Fibers used to produce braided preforms can be dry or prepreg [1]. The braiding process competes well with filament winding, pultrusion, and tape lay-up. Braiding compares favorably in terms of structural integrity of components, design flexibility, damage tolerance, repair ability, and low manufacturing cost [4]. Braiding advantages are high rate of strand deposition on the mandrel, ability to produce complex shapes, low capital investment cost [1], and minimal labor cost [3]. The most important braiding process disadvantage is the difficulty in producing low braid angle preforms.

Munro et al [5] presented a direct comparison of braiding to one of its major competitors, filament winding. Advantages and disadvantages of both high production rate reinforced composite manufacturing techniques were highlighted with respect to design and manufacturing methodology and manufacturing aspects. They emphasized that it was not possible to determine the better process

since both have similarities, advantages and disadvantages compared to the other and the selection of the manufacturing technique would largely be product dependent [5]; however, ease of conformability of preforms of braiding technology can be seen as an advantage over mostly geodesic path dependent filament winding technique.

The kinematic analysis of the braiding process has been studied since 1950's [6, 7, 8, 9]. Du and Popper [7] proposed a detailed time dependent model that predicts the microgeometry of a fiber preform braided on an axisymmetric mandrel in terms of the relationship between braid angle, fabric cover factor, yarn volume fraction, convergence zone length and rate of braid formation. The model also outlines limits of the braiding process as a result of jamming of yarns [7].

Early studies showed that the crimp angle and braid angle affect the strength and stiffness of the braided composites. Phoenix [10] presented experimental findings that verify that an increase in the crimp angle or the braid angle causes decrease in the strength of the braided composite [10]. Smith and Swanson [11] investigated the stiffness and strength properties of 2D braided carbon/epoxy composites under biaxial tension and compression loading. Influential factors on stiffness were fiber volume, braid angle, percentage of fibers in the braid and axial directions [11].

Braided composites are usually used in applications that require high shear and torsional strength and stiffness. A ±45° braid angle was proven suitable for such applications [3, 12]. They also offer increased transverse moduli, transverse strength, damage tolerance, dimensional stability and near net shape

manufacturing capabilities [13]. The transverse moduli and strength, and dimensional stability of braided composites arise from off-longitudinal-axis oriented fibers. Damage tolerance results from the locking mechanism between the intertwined fibers of the braid architecture that prevents or limits yarn delamination. Low velocity impact damage tolerance capability of laminated composites has long been recognized and methods of further improving the damage tolerance of the composites have been studied [14]. Braiding is listed as one of the manufacturing techniques to produce aircraft primary structures at lower cost and with better damage tolerant properties. Jackson and Kuykendall [15, 16] reported on studies investigating resin transfer molding (RTM) impregnated 2D braided preforms as one manufacturing technique used to produce aircraft primary structures at lower cost and with better damage tolerant properties. They indicated that RTM technique makes possible to achieve up to 60% fiber volume fractions. Thicker parts can be achieved by adding any desired number of braided layers; this is an advantage of 2D braiding. Lack of through the thickness tows and long manufacturing times for multi-lamina stacking procedures were listed as the disadvantages of the 2D braids [15, 16]. The authors indicated that 3D braiding addressed these disadvantages; however, the high cost of the 3D braiding machinery was a major disadvantage. As an example, for their study, authors indicated that the 2D braided components cost 10% less than that of the 3D braided components, and hence 2D braiding was chosen as the manufacturing technique [15].

2.5. Resin Impregnation of 2D Braided Fibers

2.5.1. Manual impregnation

One of the limiting factors of broader use of composite materials is from inconsistent mechanical properties due to stress concentrations originating from the voids that occur in the materials as a result of non-homogeneous impregnation of fibers.

During the manufacturing process of the braided composites, fiber impregnation is as important as preform production. Manual impregnation of the preform, such as brushing or massaging resin into the preform, is the simplest and least expensive method but has its limitations [17, 18]. In this type of impregnation, to avoid premature cure, resins with long gel time must be selected. Furthermore, product quality depends highly on the skill level of the operator applying the resin onto the preform, and this can lead to inconsistent mechanical properties. This can be addressed by using preimpregnated (prepreg) fibers [17, 18]. Kruesi et al [19] suggested use of an impregnation ring that preimpregnates fibers prior to their deposition onto the mandrel. This is done by a controlled amount of resin applied to the fibers through small pores while they are passing through the proposed impregnation ring. It was reported that very low void content, ranging from 3.71% and 1.74%, was achieved. Also high fiber volume fractions in excess of 60% were achieved [19]. This process may provide consistent specimen fiber volume fraction while also decreasing production time.

2.5.2. Commingled fibers

In some applications thermoplastic (TP) resins may be preferred over thermosetting resins. One of the reasons for using TP resins is to decrease composite manufacturing time, because TP resins do not need chemical reaction time as the thermoset resins. Fujita et al [20] investigated commingled and un-commingled yarns as impregnating systems to increase the uniformity of mechanical properties of braided composites. In commingled yarns, reinforcing fibers and matrix fibers are commingled together, while for un-commingled yarn, the reinforcing fibers and matrix fibers are placed next to each other. Specimens were manufactured by compression molding. The commingled yarn specimens required lower pressures and shorter holding times compared to un-commingled specimens [20]. Additional advantage of thermoplastic resins is the greater fracture toughness compared to thermosetting resins [21].

Bechtold et al [22] modeled the impregnation process for braided and pultruded tubes. Due to the difficulty in braiding preimpregnated thermoplastic tapes, powder impregnated or commingled yarns were used. Braided commingled yarns are preheated slightly above the thermoplastic melting temperature prior to entering the heated pultrusion die. The complete melting process of the thermoplastic and subsequent impregnation of the fibers occurs in the heated die, which is followed by a pressurized cooling stage through a die for calibration purposes [22].

2.5.3. Resin transfer molding based processes

Brookstein [17, 18] underlined that consistency in fiber volume fractions and hence mechanical properties may also be achieved by using other automated impregnation techniques such as Resin Transfer Molding (RTM) [17, 18]. RTM creates high fiber volume composites with very low void content. This leads to homogeneous products. In addition, near net shape products are possible to produce. Circumferential frames, keel frames, and window frames are some examples of RTM manufactured braided composites [23, 24].

In RTM, a completed preform is put in a tool or mold. The part and the resin are heated to optimal temperature for the resin to have minimal viscosity. Resin is then applied to the preform under pressure. Later the necessary curing procedure for the specific resin is followed [25]. Minimal machining requirement of these products decrease the end cost. It also avoids the negative effects of machined composite parts, such as stress concentration factors introduced at the machined location of the part. Also due to the damage of matrix in the machined region, environmental effects such as moisture and other existing chemicals effect the fibers, matrix, and the interface and hence this effect the strength and elastic properties of the machined composites.

Michaeli et al [26] used RTM to manufacture a braid reinforced tubular composite where the reinforcement was placed over a flexible tubing and inserted into the RTM mold. The tube was pressurized and resin injected. Good fiber placement and controlled impregnation as well as good surface finish were achieved.

However, resin permeability through the preform plays a major role in the quality of products manufactured by RTM. Charlebois et al [27] reported on permeability characteristics and mechanical properties of braided fabrics. Authors investigated permeability of 2D biaxial braided glass fibers at three braid angles ±35°, ±45°, ±50°, and found that change in braid angle effect the fiber volume fraction and thus permeability. Permeability of ±45° and ±50° angles decreased as the fiber volume fraction was increased. However, permeability of ±35° angle was not affected from the fiber volume fraction change [27].

Vacuum assisted resin transfer molding (VARTM) has also been used to manufacture braided composites [28]. VARTM offers low cost for high volume production, large and complex shapes capabilities and high fiber volume fractions compared to hand lay up [29]. VARTM process requires that a dry preform be placed in a mold (or tool), low viscosity resin be transferred to the preform under vacuum, followed by the resin curing procedure. It is used by many industries [30]. Some other advantages of VARTM and RTM are their low volatile organic chemical (VOC) emission and good part surface quality production ability [31].

RTM and VARTM provide cost reductions in composite materials compared to using prepregs. Prepreg materials offer good toughness to the composites; however, the resins used have high viscosities that can not be used with the RTM/VARTM techniques. Pederson et al [28] addressed this issue and proposed to achieve better toughness using RTM. For this, the resin system toughening agent that is used in the prepreg materials had to be manufactured in a fiber form and directly braided into the preform along with the reinforcing fibers

(without compromising braid structural integrity). Experimental results demonstrated similar mechanical properties between proposed RTM and conventional prepreg autoclave manufactured composites [28].

Uozumi et al [32] proposed a new technique to manufacture near-net-shaped composites using RTM impregnated 2D braiding, followed by a forging process to minimize cost as compared to 3D braiding. “I”, “J”, “T”, “Z” shaped composites are listed as producible. Authors found superior tensile properties with the braided specimens compared to equivalent aluminum specimens, suggesting possible aircraft applications for weight savings. Also, the braiding/RTM process was reported to have approximately 34% cost savings compared to the hand-lay-up/ autoclave process [32].

2.6. Applications

Braid reinforced composite materials have a broad range of industrial applications. Based on the aforementioned advantages, such as the specific strength, these materials are preferred increasingly over the conventional engineering metals. This section outlines some of the broad applications of braided composites.

Brookstein [17, 18] listed structural columns, rods, shafts, pressure vessels, and plates as some classical applications where braid reinforcement had replaced conventional materials. Brookstein suggested, with no theoretical or experimental evidence to support the claims, the structural limits of braided structure. It was stated that braided structure could be used for tensile load carrying applications if the braid angle did not exceed 15°. In the cases of

compression loading and thin-wall buckling, delamination could be overcome by the circumferential reinforcing nature of braided fabrics (if 20 % of the fiber placement was at a ±45° braid angle). Shafts were listed as ideal components manufactured using composite materials, where axially placed fibers provide stiffness, and ±45° braid provided torque transmission reinforcement. He showed, through modeling, that 54.74° braided pressure vessels are also good candidates for braided composite applications [17, 18].

2D braiding may be used to manufacture structural components as well. Kobayashi et al [33] reported manufacturing a T-shape braided graphite epoxy composite truss joint. Authors proposed a different continuous production manufacturing method for structural components such as T-shaped trusses. At the end of the process the whole T-Shape had two layers of continuous triaxial braiding. In this study EPIKOTE 828 epoxy resin with an amin system hardener (KC1118). Fibers were impregnated in a vacuum and an autoclave was used for curing. It was reported that the braided T-shaped truss joint had higher strength than a similar cloth tape component [33].

Hamada et al [34, 35] reported a new technique to produce tubular braided products that are more resistant to interlaminar delamination, also referred to as through-the-thickness toughness. The technique uses a conventional 2D braider in a multireciprocal fashion to produce a multi-layer braided laminate. Through-the-thickness fibers were simultaneously added to the braid through a three track system where the spindles travel from one track to the other creating a three dimensional structural network of strands. It was observed that propagation of

interlaminar delamination was impeded during lateral compression tests of said manufactured tubular braided specimens [34, 35].

Due to their specific strength and tailorable mechanical properties, composites have long been the preferred materials for aviation [15, 23, 24, 32, 36]. White [36] reported on manufacturing, testing, and cost analysis of a Kevlar 49©/epoxy blade spar. Ballistic tests were done to evaluate the structural damage. After complete armor penetration, static retesting of spar section did not show any detectable changes in the elastic behavior, which was attributed to the braided fabric delamination resistance. Also, ultrasonic C-scan inspection of the structure was assessed and satisfactory results were observed. Finally, the cost evaluation of the braided structure revealed 33% savings compared to filament wound glass blade spar [36].

The sports equipment industry highly utilizes the benefits offered by braided composite materials. Casale et al [37] reported on design and fabrication of a braided bicycle frame using Kevlar/graphite braided hybrid preforms impregnated with Epon 828 epoxy resin and D-230 curing agent. The frame was manufactured by braiding the four-piece frame over a foam core and subsequent joining process. Five prototype bicycles were produced [37].

Production of braid reinforced laminated wood baseball bats have been reported by Axtell et al [38, 39]. Reversed balloon molding was used to manufacture the bats. During this process an elastomeric tube was inflated and the molded component pushed onto it. The tube was subsequently deflated to

wrap the part for the curing process. Following curing, the tube was again inflated forcing the cured product out.

Neogi et al [40, 41] published their findings on design analysis and fabrication of a self deployable structural element, constructed of a foam core, internal bladder, braided load carrying preform and an outer jacket, which was originally developed to minimize payload volume on space shuttle missions. The proposed structure had a minimum volume at the onset; using a resistance wire embedded in the foam core as a heat source, the structure expanded and cured. A carbon/epoxy system was chosen for the braid because of low coefficient of thermal expansion, high longitudinal and torsional stiffness and interlaminar strength. As a result of the study, 80% volume savings were achieved compared to original designs. The authors suggested using a triaxial braid structure due to the lower specific stiffness of the final product compared to aluminum structures. They also listed emergency sailboats, deployable antennas and tent frames as other possible applications of deployable structures [40, 41].

Braided composites have also been suggested for use with structural reinforced concrete components since flexural strength and ductility of reinforced concrete members can be improved with braided composite jackets [42]. Life spans of reinforced concrete structures can be improved by using corrosion resistant and high specific strength braided fiber reinforced polymer (FRP) rebars instead of conventional steel rebars. The non-ductile behavior of braid reinforced FRP rebars were also addressed by researchers: Hampton et al [43], and Lam et al [44] reported on hybrid Kevlar-Carbon FRP rebars manufactured using a

braiding/pultrusion process exhibiting desirable ductile behavior similar to conventional steel rebars [43, 44].

Karbhari et al [45, 46] studied crush performance and energy absorbing capabilities of braided composites. Braid energy absorbing capabilities could be eventually used in industrial applications such as car bumpers. They reported that triaxially braided composites increased the energy absorbing performance of the braided composites [45], and the occurrence of damage prior to onset of crushing affected crush performance [46].

Braid reinforced composite materials have been extensively studied for biomedical applications. Hudgins et al [47, 48] suggested replacing the natural intervertebral disc with a prosthetic intervertebral disc. The proposed disc had a core of elastomeric polymer and a braid reinforced outer shell. Braided shells proved to provide compressive strength to the design [47, 48]. Moutos et al [49] reported tubular braided structures with elastomeric cores that were manufactured and tested to mimic the properties of anterior cruciate ligaments [49]. Reinhardt et al [50] underlined the high numbers of hip replacement surgeries conducted every year in the world, and the need for a design that would have tailorable mechanical properties, enhanced fatigue life, and biocompatibility. Authors proposed a design that consisted of balsa wood core with six layers of braided carbon preforms manufactured by RTM using a vinyl ester matrix. The study was designed as a basis for future studies but early mechanical performance of the design were reported to be excellent; however, resin biocompatibility issues were left for future studies [50]. Another example of biomedical application of braided

composites, braided carbon/PEEK composite bone plates, were fabricated and tested by Fujihara et al [51]. Braided fabric reinforcement was chosen for this work based on better in plane properties and out of plane delamination resistance. Promising results encouraged researchers to further investigate the effect of the braid angles and plate thicknesses on the bending performance of the composite plates; braid angle was identified as important for thick plates. For example, it was suggested that a 2.6 mm thick plate with a 10° braid angle was suitable for forearm treatments [51, 52, 53]. Finally in dentistry, braided composites were used in dental posts that require varying stiffness along the shaft. This was obtained by varying the braid angle along the post shaft [54].

Braided tubular products can also be used as catheters in medical field. Carey et al published a study about the design of fiber reinforced composite catheters [55]. They analyzed the required rigidities of conventional catheters and set design objectives to achieve these targets by use of braided composites [55].

2.7. Typical challenges in applications: Joining Methods - Braided and Machined Holes in 2D Braided Composites

Composite materials, including braided composites, may be manufactured to near net shape to avoid any post-manufacturing processes; however, there are also numerous applications that require multi-part assembly with other composite or non-composite components. Assembly may be accomplished through adhesive or polymeric bonding as well as mechanical joints. Use of adhesives involves studying adhesive shear strength, surface finish of substrates and coupling agents.

For the purposes of this review, mechanical joints were investigated since they require holes or other shape openings in the structures and will have effects on the integrity of the parts.

Composite materials are susceptible to develop stress concentrations around holes and cutouts. Tsiang et al [56] and Brookstein [57] compared the effect of integrally formed braided holes and machined holes on strength of cylindrical braided composites. Specimens with braided and machined holes were tested under tensile loads. In average, specimens with braided holes were observed to bear loads that were 1.23 times higher than that of machined holes. Observations on specimen failure modes were presented; however, limited micromechanical discussions to explain the observed phenomena were provided. In another set of tensile experiments, load was applied through pins inserted into the braided and machined holes. On average, specimens with braided holes supported 1.8 times greater loads than those with machined holes. This was associated to the fiber discontinuity at the machined holes [56, 57].

Following the study of Brookstein et al, Wang and his co-workers published contradictory findings [58, 59, 60]. Authors outlined that, in the previous studies, the overall wall thickness of the tube specimens were not controlled due to excess resin surrounding the holes. It was suggested that these thicker resin rich regions contributed to the increased the local bearing strength. In Wang and his co-workers' studies, wall thickness was kept constant. Change in fiber angles in the surrounding regions of the holes resulted in decreased bearing strength. They concluded that similar or greater bearing strengths were found for

machined holes as compared to braided holes. Other studies on 3-D braided composites support their findings [58, 59, 60, 61].

However, Fujita et al [62] published studies on comparison of machined holes versus braided holes on flat braided bars, and they found results parallel to that of Brookstein et al. They stated that machined holes have lower bearing strengths; however, their work concentrated on the effect of hole diameter on bearing strength. Smaller diameters caused more local disturbance on the orientation of fibers than larger diameters leading to resin rich regions and lower bearing strengths than their larger counterparts. Results were validated using numerical analysis. They concluded that fiber orientations around the holes significantly affected the bearing strength and failure mode [62]. They did not comment on the issue (i.e. the resin-rich regions surrounding the holes) raised by Wang et al.

Ohki et al [63], Ohki et al [64], and Nakai et al [65] evaluated the effect of machined versus braided holes in end loaded flat-braided specimen with a centralized hole. Specimens with braided holes had higher strength properties during both static and fatigue testing. From microscopic observations, authors conclude that the damage mechanism of the machined holes is related to the fiber-resin interface, while the damage mechanism of the braided holes is related to the reorientation of the continuous fibrous strand path caused by the presence of the hole [63, 64, 65].

2.8. Elastic Constant Predictive Models

Mechanical behavior of 2D braided composites can be discussed in terms of elastic behavior, plastic behavior, and failure behavior such as ultimate strength and failure mechanism [66]. This review, due to the broadness of the topic, focuses on elastic behaviors of braided composites. Important publications about the remaining two categories are listed for bibliographical purposes but not detailed.

Elastic property prediction of 2-D braided composites has been studied far more than their plastic behavior and failure behavior. Braided structures are assumed to behave linearly in the elastic range. In the plastic region, a non-linear behavior is observed which increases the complexity of the problem. Nevertheless, a number of studies have been published regarding plasticity behavior and failure characteristics of braided composites [67, 68, 69, 70, 71, 72, 73, 74]. Other papers that have dealt with elastic properties, as well as strength and failure mechanisms, will be covered in detail.

The majority of braid analysis developed to date can find its origins in earlier woven fabric composite and laminated composite analysis; hence, this review also outlines major studies published in these fields to create a basis for the overall discussion. In this view, braided composites can be seen as a specific form of woven fabric composites, or textile composites [75].

Some of the models discussed are based on the well known Classical Laminate Plate Theory (CLPT). During the discussions of this review, it is

assumed that readers are familiar with the well documented CLPT analysis, such as by Jones [76].

In early 1970s, Halpin et al [77] developed a model predicting elastic stiffness and thermal expansion properties of short fiber composites from a laminate analogy. This laminate analogy was extended to 2 and 3 dimensional woven fabric composites. Authors reported that predicted and experimental results for woven fabric composites were compared and found to be "*qualitatively correct"*.

Whitney and Halpin [78], analyzed laminated anisotropic tubes subjected to combined tension or compression, internal pressure, and torque. Authors listed the governing equations as equilibrium, compatibility, strain and curvature displacement, and constitutive relations. The analysis was done using Donnel's approximations.

Some of the most influential studies that followed were published by Ishikawa and Chou [79, 80, 81] who proposed and compared three stiffness and strength predictive models that formed the basis to many subsequent textile fabric composite models, namely, the "mosaic", "fiber undulation", and "bridging" models. The models study the smallest repeating unit of the fabric, the unit cell. The properties of the unit cell are assumed to be representative of the overall composites. Mosaic model treats the system as an assemblage of asymmetric cross-ply laminates. The model uses the Classical Laminate Plate (CLPT) theory as the basis of the analysis. The model was analyzed using both iso-strain and iso-stress assumptions to respectively obtain upper and lower bound composite

stiffness properties. The fiber undulation model was developed to validate and improve the mosaic model. Undulation (crimp) and continuity characteristics of the fibers in woven fabric composites omitted in the mosaic model were considered. Due to physically occurring matrix only regions, this model also allowed the recognition of changes in the overall fiber volume fraction of the unit cell. The undulating fibers, assumed to follow a path described by a sinusoidal function, were used to calculate stiffness matrices of CLPT analysis. The local stiffness matrices used in the calculation of the CLPT A, B, D matrices were computed as a function of the local undulation angle (called "local off-axis angle" by Ishikawa and Chou). The authors stated that the undulation of the fibers reduced the effective stiffness of the composite in the longitudinal direction, and that the maximum strain occurs at the mid-point of the undulating fiber. The bridging model was developed for satin weave fabrics and is therefore out of the scope of this review [79, 80, 81].

Ishikawa and Chou also characterized geometric and material properties of hybrid woven fabrics [82], and investigated effects of these fabric parameters on elastic properties by using the mosaic model. In this model, due to the hybrid nature of the fabric, in-plane and bending moduli (A_{ij}, and B_{ij} matrices) are no longer uniform in the repeating region. Gaps that may exist between the fibers were neglected and a close mesh configuration was adapted. In this report, Ishikawa and Chou also investigated the thermal expansion coefficients and thermal bending coefficients. Investigation was conducted using the mosaic

model and one dimensional fiber undulation model. Agreement was found between experimental and theoretical results [82].

Tsiang et al [83] investigated the longitudinal and transverse mechanical properties of triaxial braided graphite/epoxy cylinders using a simple micromechanics theory based model. The braid architecture was modeled as a structure composed of unidirectional-ply and bias-angle ply yarns. The brief description of the model provided stated that material properties were calculated by applying the principle of superposition to the two sub-layers. Results for the longitudinal and transverse elastic modulus and Poisson's ratio were provided, and were stated to be in reasonable agreement with experimental results.

Yang et al, [84], proposed a predictive model for triaxially braided composites elastic properties. Unlike woven fabric models (45° fiber deposition angle), this model, based on the Ishikawa and Chou's fabric undulation model [79], assumes 60° fiber deposition angle. The model utilizes the geometrical characterization of the braid architecture where the triaxial fabric composite is treated as an assemblage of three laminae; bias and longitudinal yarn laminae. The corrugated yarns impregnated with matrix are taken into account in the initial calculation, and the contribution of the matrix only regions are subsequently considered using a Rule of Mixtures prediction. The upper bound is calculated from a laminate that consists of three laminae stacked together with fibers in the bias braid and longitudinal angles, and the lower bound is calculated from the proposed model. As a result of the analysis, the stiffness of the non-orthogonal

woven fabrics was determined to be strongly influenced by the fiber deposition angles. The model was not verified experimentally [84].

In a later study, Yang et al [85] proposed the "Fiber Inclination Model" based on a modified CLPT to predict the elastic properties of three dimensional textile (woven and braided) composites. Here, the unit cell used for the analysis is assumed to be composed of an assemblage of inclined unidirectional laminae. The idealized unit cell was described as fiber bundles oriented in four body diagonal directions. All the yarns in one direction were assumed to form inclined laminae after matrix impregnation. The rest of the analysis was explained as an extension of the fiber undulation model developed by Ishikawa and Chou. In the analysis, contribution of pure matrix regions to the stiffness matrices were neglected (interested reader may refer to the original text for the modifications and necessary assumptions). Authors recognized and underlined that the CLPT ignores the interactions of fiber yarns at the interlocking points and stated that it is still a convenient technique for the analysis. Predictions and experimental findings were in good agreement [85].

Whyte [86] proposed an analytical model, the Fabric Geometry Model (FGM), to predict the properties of three dimensionally braided structures. FGM is based on a modified CLPT where the unit cell is defined as repeating volumes. The stiffness matrix is developed for each yarn in the unit cell by calculating the stiffness matrix of the equivalent unidirectional lamina and transforming it into the structural coordinate system. The contributions of each yarn are superimposed with respect to their volumetric contribution. Authors also suggest calculating the

strain at every new strain level to account for the non-linear behavior of the materials [86]. Pastore and Gowayed [87] underlined two major disadvantages of the FGM model presented earlier. First, the theoretical mathematical derivation is not compatible with the basic transverse isotropy used in the model. Secondly, the transformation matrices used for the stiffness calculations are not consistent. In their paper, authors address these problems. They compared stiffness averaging and compliance averaging techniques, and they compared predicted and experimental results for triaxially braided, as well as orthogonal glass reinforced composites. The self consistent FGM model, as it was called, was used to predict elastic properties results using both stiffness averaging and compliance averaging technique. Authors highlighted that in all cases the stiffness averaging technique provided better predictions.

Ko et al and Lei et al, [2, 88], presented the Finite Cell Model (FCM) in which the unit cell for the structure was defined as an assemblage of brick-shaped elements. The FCM defines the composite as a "space truss" and hence each yarn is considered individually. The yarns are assumed to be diagonals of the unit cell and analyzed as pin-jointed two-force truss members, which makes this model suitable for finite element analysis.

Soebroto et al [89] published a design framework for braided tubular composites. The objective was to fill a gap in the field by creating a link between textile preform manufacturers and structural designers creating design curves such as effect of braid angle on fabric diameter and transverse speed required for a given braider to achieve a certain diameter tubular braided preform. They also

used FGM model by Whyte [86], to predict elastic properties and strength of 2D braids. Soebroto et al theoretical predictions, taken approximately from a graphic, were reported in the range of 5 to 85 degrees. Experimental verification was done for 20 and 70 degrees braid angles and appear to follow the general trend with the models published after them, such as the longitudinal elastic modulus decreases as the braid angle changes increases. However, for the region between 30 to 60 degrees, their predictions appear nearly linear compared to other models that have a more curved shape. Again, FGM was originally developed for three dimensionally braided composites and does not include undulating fiber strands. Hence, following the comparison of linear versus curved predictions of the different models, it may be concluded that for two dimensionally braided composites more sensitivity in the results may be obtained by methods that account for fiber undulation [89].

A woven fabric study was published by Naik and Shembekar [90, 91, 92] as a series of three publications, namely, lamina and laminate analysis and laminate design. Naik and Shembekar indicated that the early elementary laminate theory models developed, such as mosaic and undulations models by Ishikawa and Chou, were simple but not accurate because of the one dimensional nature of these models leading to large discrepancies between predicted and experimental results. Conversely, authors indicated, numerical models were accurate but complex. To address early model concerns, Naik and Shembekar proposed simple but accurate generalized two-dimensional models to predict the elastic properties of woven fabric composites. Their models account for fiber continuity and

undulation in both the weft and warp directions, matrix only regions and cross sectional geometry of the yarns in the unit cell. The Naik and Shembekar two dimensional model was an extension of the Ishikawa and Chou one dimensional model. Only non-hybrid two-dimensional plain weave fabric lamina was considered. The unit cell was divided into straight cross ply, undulated cross ply, and matrix only regions. The undulating tow paths were modeled using sinusoidal functions. The elastic constants were calculated using a Cylindrical Assemblage Model (CAM) in the principal material directions. Each infinitesimal region of the unit cell was analyzed using CLPT [90, 91, 92].

In the analysis, the unit cell is assumed to be comprised of sub-sections along and perpendicular to the loading directions. Each sub-section is comprised of infinitesimal pieces. A uniform, unidirectional, in-plane load was assumed to be applied to the woven fabric. The infinitesimal sub-sections in the unit cell, which are in series with the loading direction, were assumed to be under constant stress. On the other hand, the infinitesimal sub-sections that are parallel to the loading axis were assumed to have constant strain in their mid-planes [90, 91, 92]. Following this approach, they created two models: Series Parallel Model (SPM) and Parallel Series Model (PSM). The SPM was created by assembling all the infinitesimal pieces in series with the loading direction under iso-stress condition, and then assembling all the sections along the loading direction under iso-strain condition. The PSM was created by following the same approach in the reverse order. Naik and Shembekar stated that the SPM provides the lower bounds of the in-plane stiffness constants, whereas the PSM provides the upper bounds of the

stiffness constants. Following experimental verification PSM was recommended for woven fabric composites. It should be underlined that PSM was developed for woven fabric composites, which can not be generalized to include braided structures that may have different angle orientations [90, 91, 92].

Finally, Naik and Shembekar [92] underlined the superior properties and advantages of woven fabric composites to that of unidirectional composites such as shorter build time, complex shape capability and ease of mold impregnation because of the intertwined structure. Authors highlighted the fact that the elastic behavior of a unidirectional lamina and a thin laminate are the same, whereas this may not be necessarily true for a woven fabric lamina and thin woven fabric laminate because of the macroscopically heterogeneous nature of the woven fabric lamina; they also outlined the limited number of studies published in this field [92]. Authors studied the effect of stacking sequence or shift of laminae to obtain optimal laminates. Since this is beyond the scope of this review, interested readers are referred to the original publication [92].

Masters et al [93] studied the mechanical properties of triaxially braided composites both analytically and experimentally, which could serve as a database of experimental results for comparison purposes with predicted results of models available at the time. The experiments used 2x2 braided AS4/epoxy resin composite flat panels impregnated by RTM. Braid angle, size of the braided yarn and size of the longitudinal yarn were varied to obtain three different architectures. A processing science model was used to construct the braided unit cell geometry. Mechanical properties of the braided composites were predicted

using four different approaches, namely, laminate, corrected laminate, diagonal brick, and finite element model. Laminate model was the simplest model where all the tows were treated as unidirectional plies in a symmetric laminate. A correction factor was applied to this model to compensate for the ignored fiber undulations to create the corrected laminate model. Diagonal brick model [94] is an extension of the above FCM. The finite element model was based on a previous model proposed by one of the authors of the paper, Foye R.L., where the unit cell was analyzed as a combination of sub-cells. They found that all model predictions were comparable to experimental findings and the differences between them were not significant; however, finite element method predictions were best. Also studied was the sensitivity of experimental measurements to strain gage sizes. Findings concluded that large gage sizes, such as the 2.54 cm gage length of some extensometers, were preferable [93]. Master and Ifju [95] later published a detailed study where they outline Moire interferometry, X-Ray radiography, and surface replication techniques as alternatives to inspecting or testing methods for braided composites [95].

A review paper that utilizes experimental results to compare stiffness predictive models available at the time was published by Falzon et al in 1993, [96]. Authors categorized the models into three types, namely, the elementary models such as fabric geometry model (FGM); the laminate theory models such as “fiber undulation model” and “mosaic model”; and, finally numerical models. Authors stated that the elementary models are unsuitable for strength calculation; the laminate models are unable to predict out-of plane elastic properties; while

finite element models are complex [96]. Although these observations were true at the time, in subsequent years, improvements were made to these models to address these concerns.

Redman and Douglas [97] proposed a simple analytical model to determine the elastic properties of triaxially braided composites. The model utilizes a unique combination of Rule of Mixtures prediction and CLPT. Unlike many of the previous models presented, the Redman and Douglas model, due to this unique modeling approach combination, does not require the use of a unit cell. The length between neighboring fibers was assumed to be big enough to neglect the effect of undulating fibers. The triaxial braid is considered to have three separate plies that all coexist in the same space. Each ply is assumed to have a thickness equal to the full braid layer and assumed to have primary fiber tows and effective matrix material. Effective matrix material is assumed to be composed of two secondary fiber tows and matrix material, and is analyzed using CLPT as a symmetric laminate. This model may be a good alternative to obtain fast preliminary design results prior to a detailed analysis [97].

Following Masters et al, [93], Naik et al [98] conducted an analytical and experimental study on the effects of braiding parameters on 2-D triaxially braided composites. Braiding parameters were listed as braid angle, yarn size and axial yarn content. A Repeating Unit Cell (RUC) was isolated and used for the analysis. Each yarn in the RUC was discretely modeled and sliced. The three dimensional effective stiffness of the RUC was calculated using a volume averaging technique under iso-strain assumption. Although the analysis was conducted in three

dimensions with respect to the XYZ global coordinate axis, the predicted elastic properties mainly showed sensitivity to braiding parameter in the longitudinal and transverse directions. The elastic properties in the thickness direction were much less sensitive to changes in braid angle or percent axial yarn content. This may be the underlying reason to why many braiding models following this study analyzed braids only in the axial and transverse direction, such as Carey et al, [75]. Stiffness properties were not affected by yarn sizes, but were affected by braid angle and axial yarn content. Increasing the braid angle increased transverse and shear elastic moduli, but decreased longitudinal elastic modulus. It was also reported that the out of plane elastic and shear moduli were insensitive to these parameters [98].

Following Naik et al, Naik [99] published a study to extend on the previous work. He implemented the analysis in a program code called TEXCAD used for braided as well as other textile composites. The work was also extended to predict strength of woven and braided composites [99, 100, 101].

Raju and Wang [102] reported a detailed study about classical laminate theory models for woven fabric composites derived from, but not limit by the simplification of, the Ishikawa and Chou models [79]. They first identified a repeating unit in the woven fabric composite, which was further divided into unit cells. This geometrical characterization was done for plain weave, 5-and 8-harness satin weave structures; this review covers only the plain weave case. A uniform membrane strain and curvature are assumed at the midplane of the unit cell. The unit cell was divided into four regions, each subsequently divided into four sub-

regions composed of undulating and non-undulating regions. As was the case for Ishikawa and Chou's fiber undulation model, Raju and Wang's model accounts for the undulating fibers; however, they use a more accurate geometry to characterizes undulating fibers in the fill and warp directions than its predecessor. The undulating fibers are assumed to follow a sinusoidal shape function as with the model by Naik and Shembekar [90]. CLPT stiffness matrices A, B, and D of the unit cells are calculated as follows. First the A, B, and D matrices of all four sub-regions are calculated by integrating the Stiffness matrix, $\boldsymbol{Q}$, over the volume of each sub-region. Then, these are summed over each sub-region to obtain A, B, D matrices for each region in the unit cell. Finally, all four regions are summed to obtain unit cell A, B, D matrices. Authors state that the integrals involving the undulating strand stiffness were calculated numerically without specifying the method selected. In the model, coefficients of thermal expansions were also obtained. Predicted results were compared to many other available models; most matched favorably. It should be noted that, as mentioned, the study was conducted for woven fabrics; hence, fill and warp strands were always perpendicular [102].

Gowayed et al [103] proposed a finite element model to predict the elastic properties of textile composites. This model addresses the short comings of the Unit Cell Continuum Model (UCCM) by Foye [104]. The UCCM utilizes a unit cell that is divided into subcells. Displacements of the subcells are calculated using Virtual Work, and summed to calculate the total displacement. However, Gowayed et al suggested that the UCCM does not clearly differentiate between fiber and matrix material properties in the analysis. They state that if the

difference between the properties of fiber and matrix materials is large, such as for the case of fiber reinforced composites, the solution becomes inaccurate. Authors suggested correcting this by using the UCCM along with Whyte's FGM model [86], where composite material fibers and matrix constituents are treated separately and their contribution to the global stiffness matrix are calculated through superimposing each contribution with respect to their relative volume fraction. The model was verified experimentally [103].

Nakai et al [105], Hamada et al [106], and Nakai et al [107] attempted to use the unit cell predictions to design and predict behavior of braided cylinders upon loading using numerical analysis. The analysis was comprised of a micro analysis, modeling individual resins and fibers as straight lines, and of a macro analysis, which combined the micro models, to form structural elements. They also studied the influence of braiding structure on torsional properties of braided composite tubes.

Naik and Ganesh [108] studied two dimensional orthogonal plain weave fabric laminae through a thermoelastic analysis. The authors claimed that most of the models developed until then, [90, 109, 110], do not consider the actual strand geometry and cross section; hence, the fiber volume fraction was not included in the models. The few models that included these were complex. Consequently, they outlined a two dimensional closed form analytical method which takes into consideration the strand undulation and continuity in fill and warp directions, strand cross section, fiber volume fraction, and possible gaps between two adjacent strands. In their model, a unit cell that is composed of three layers, fill

and warp fibers and matrix, is used. Strand cross section, strand cross sectional shape in woven form and the strand undulations are defined by shape functions. Authors compared both circular and sinusoidal functions for strand undulations and concluded that the sinusoidal functions offered better predictions. As many before, Naik and Ganesh defined the unit cell of the composite as an asymmetric cross-ply laminate. This laminate is assumed to consist of one pure matrix and two unidirectional laminae. The thermoelastic properties of woven fabric lamina were calculated using CLPT under the assumptions that CLPT is applicable to a unit cell and the bending deformations of a unit cell are constrained by the surrounding unit cells. The undulating angle of the strands is assumed to vary linearly [108]. In their study, twelve material systems with different strand and weave geometries were analyzed. The results were compared to a previous model by the same author and experimental data. They concluded that the proposed model provides acceptable and quick results. The effect of the ratio of strand thickness to strand width on elastic constants was also investigated in the study and the results are provided in a graphical form. They also suggested that the twist of the strand along the fiber undulation direction should be investigated; however, later, Carey et al, [75], calculated this to be negligible in 2-D braided structures [108].

Byun et al [111] proposed a novel braiding and pultrusion manufacturing technique during which the fiber tows are preimpregnated and subsequently braided on a Teflon mandrel. Impregnated preforms are cured in a curing die and cut into pieces. Authors proposed an analytical model for elastic properties of

braided products that first calculates the effective compliance matrix of a yarn based on its length then uses this information to obtain the effective stiffness of the composite by averaging the stiffness constants of the axial yarn, braided yarn, and matrix as functions of their volume fraction in the composite. The model does not allow for open-mesh braid configuration. Limited experimental data was provided [111].

A three dimensional tow inclination model was proposed by Branch et al [112] to calculate elastic constants of two dimensional textile and three dimensional braided composites. The global constitutive equation of the composite material is derived using an iso-strain approach for the unit cell and averaging all tow segments and matrix within the unit cell [112].

Tsai et al [31] used a CLPT-based model to predict stiffness and strength of braided tubular composites. They introduced two models, bridge and crimp, that are similar to those of Ishikawa and Chou [79]. The experimental and predicted values were generally not in god agreement; however, better agreement was found with the crimp model.

Robitaille et al [113] stated the importance of realistically characterizing preform geometry for use in predictive models. They proposed a method to describe preform interlacing geometrical patterns by a series of vectors. Authors indicate that the geometries can be used in predictive models as well as permeability studies of preforms to obtain optimal impregnation of fibers. In a subsequent study [114], the group underlined the difficulty in characterizing the complete structures for such purposes; hence, they presented an algorithm to

generate geometric characterization of unit cells for textile and composite materials. Possible useful applications were calculation of local permeability values and local stress distributions in these materials. Their examples are mostly aimed towards permeability calculations.

Wong et al [115] investigated permeability models and proposed two new numerical models, namely, grid average and stream surface methods. Grid average simplifies the unit cell domain to a rectangular grid in the longitudinal and transverse directions plane from which the permeability tensor components are calculated. In the Stream Surface model the unit cell domain is first divided into basic volumes that consisted of open channels and porous tows from which permeability can also be calculated.

Aggarwal et al [116] proposed an analytical model for their braided dental post and bone plate calculations. It was stated that many current models for braided composites ignored unit cell inter-yarn gap for which they proposed a micromechanical model. Here undulating fibers and yarn cross sections were considered. The geometrical characterization was based on a unit cell, authors called *Repeating Unit Cell (RUC)*. Each sub-cell in the RUC is treated as assemblage of spatially oriented unidirectional laminates of transversally isotropic properties. The stiffness of the RUC was calculated using a modified CLPT. They assumed that the CLPT is applicable in infinitesimal subcells generated within the RUC. The subcells consisted of two braiding yarns and a single matrix lamina. Experimental results were used to validate the model. Only longitudinal elastic

modulus results were provided; good agreement between predicted and experimental results was found.

In another work, Aggarwal et al [117] proposed an analytical model based on a repeating unit cell (RUC) approach for in-plane elastic constants of two-dimensional braided composites. The geometric model considers yarn undulations and inter-yarn gap using a sinusoidal shape functions. Under iso-stress and iso-strain assumptions engineering constants of each sub-cell is calculated and averaged over the RUC volume. The paper considers flat braids. Both upper and lower braiding yarns follow the same undulation path but have different cross sectional area shapes. Yarns in the unit cell were calculated as an assemblage of small straight yarns. This approach was also followed in the local undulating yarn segments. They performed a sensitivity analysis of the yarn thickness/yarn width (t/a) ratio and concluded that in-plane elastic constants decrease slightly as the ratio increases. Intern yarn gap was found to affect the RUC volume fraction and consequently mechanical performance. Also, changes in yarn aspect ratio affect the undulation and therefore mechanical performance [117].

Byun [118] proposed a detailed model to predict geometrical characteristics, undulation yarn angle, fiber volume fraction and three dimensional engineering constants of 2D braided composites. Byun underlined the simplicity of the calculation procedures compared to lamination theory [93] and yarn-discretization [98] models. First, a geometric model of the triaxial braid is developed; yarn shape parameters measured from photomicrographs are used to characterize yarn geometric relationships within the unit cell, which lead to the

prediction of the undulation angle, fiber volume fraction and elastic constants. The resin impregnated yarns are modeled as unidirectional composite rods. The effective compliance matrix of the unidirectional composite is found through simple transformation through the undulation angle and subsequent averaging of the transformed compliance matrix. The author stated that after transformation the specific geometry of the yarn is no longer significant and it can be treated as layers of orthotropic materials. It is assumed that, once loaded, each layer undergoes iso-strain. The effective stiffness of the composite is found by averaging the stiffness of each layer based on volume. The stiffness matrix is inverted to get the compliance matrix, from which engineering constants of the triaxially braided composite are obtained. The model was experimentally verified: predicted and experimental fiber volume constants were in good agreement; however, the undulation angle was under-predicted. In the conclusions author suggested more experiments were needed to support the model predictions.

Harte and Fleck [119, 71] studied the necking and tensile behavior of braided tubes. Elastic moduli of which were predicted using laminate plate theory. The mechanics of neck propagation was investigated; the authors concluded that braided structures can be very effective in energy absorbing applications because they deform in tension at constant stress for large extensional strains. Failure mechanisms of braided composites under compression and torsion were also investigated.

Huang [66, 120, 121, 72] underlined that, for woven and braided fabrics, many of the available models were developed for elastic behavior (i.e. small

displacements) and there are very few models for plastic behavior and strength predictions. Authors proposed a micromechanical model, the bridging model, for woven and braided fabrics capable of determining elastic, plastic and ultimate strength behavior of fiber composites under any arbitrary load condition. Concisely, in the model the overall applied load on the composite is explicitly correlated with the stress states developed in the fiber and matrix constituents. Huang [66, 120, 121, 72] divided the woven/braided composite into a repeating unit cell (RUC) further divided into four sub-elements consisting of two yarns and pure matrix regions. Each sub-element component, assigned a local coordinate system, can be locally treated as a unidirectional composite. Relative coordinate transformations are provided with respect to the global axes. Yarn undulations are defined by sinusoidal functions. Following the iso-strain assumption, an average stiffness/compliance of the sub-element is determined. Based on the iso-stress assumption, the overall stiffness/compliance matrix of the unit cell is obtained using the contributions of each sub-element. To be more comprehensive on the approach, Huang uses a "bridging matrix", to correlate the volume averaged stress increments in the fiber and matrix of the representative volume element. This matrix represents the load carrying contribution of one of the constituents in the composite with respect to the other constituent (i.e. contribution of fiber with respect to matrix). The model utilizes this relationship in the calculation of the volume averaged stress relationship. The bridging matrix is populated differently when finding elastic or plastic response, or ultimate tensile strength. The results compared favorably to the experimental studies and other models available in the

literature. Here, Huang also studied the effect of gap-ratio of braided fabrics on the predicted properties via a parametric study [66, 120, 121, 72]. Huang's model is correlated with experimental data and results. Differences between experimental and predicted results are less than 13% [122, 123].

A computational micromechanical model was developed by Ivanov and Tabiei [124] to predict elastic properties of woven fabric composites. The model is based on a micromechanical approach and homogenization technique. It is claimed that due to the efficiency of the model it is suitable for large scale finite element analysis. Similar to other models, a unit cell of the composite is divided into four sub-cells with respect to its fill and warp yarns. Direction of the yarns in each cell is characterized by the braid and undulation angles. The homogenization technique used was summarized in three steps by the authors: first, partitioning the constituent stiffness matrices by choosing iso-strain and iso-stress components; second, calculating the interim matrices; and, finally, calculating the partitions of the effective stiffness matrix [124].

Yan and Van Hoa [125] developed a macrostructure model to predict the mechanical behavior of 2-D triaxially braided composites. Authors used the elastic deformation energy of a unit cell to calculate the effective stiffness of the braided composites. They used this model to predict elastic properties and to conduct a parametric study [126]. The elastic property predictions were compared to results of Master et al [93]. In their parametric study, they separated independent parameters (yarn and composite geometrical parameters, and constitutive material constants) that affect the analysis of braided composites.

These parameters can be used for guidance in designs using triaxial braided composite structures.

Tabiei and Yi [127] compared several numerical analysis methods and proposed a new one to predict the elastic properties of woven fabric composites. Their model is a simplified version of the earlier "method of cells" for woven composites by Tabiei et al [128]. The authors claimed that the new method is more computationally efficient and requires less memory than the previous methods that were too complex and required high numbers of calculations; thus addressing one of the major disadvantages of analyzing braided composites using numerical analysis.

Quek et al [129] proposed an analytical model for the effective elastic stiffness of a 2D triaxially flat braided composite capable of investigating the effect of imperfections on stiffness. A Representative Unit Cell (RUC) comprised of two braid tows, one axial tow and one matrix layer is developed for the braid geometry. The model uses a Concentric Cylinder Model (CCM) to predict, with respect to local coordinate axes of the fibers, the elastic constants of the tows in the composite. The contribution of the undulating fibers, which affect the stiffness in the ply direction, is calculated by averaging transformed local fiber stiffness over one complete undulation cycle, called *wavelength* in the paper. Finally, the stiffness in the ply directions is transformed to the global coordinate system. Stiffness contributions of each ply are assembled together as a function of their volume fraction within the RUC to predict overall RUC elastic constants. The predicted results are compared to experimental and finite element model results;

results are in agreement. Based on their results, the authors underline the advantages of using the proposed model in terms of time and computational memory savings compared to finite element models, which they state should only be used if ultimate strength is required. Analytical models are preferable for elastic properties. Finally, a parametric study revealed that braid fiber plies in the RUC have the largest effect on elastic properties.

Carey et al, [75], proposed a model to predict elastic constants of 2D-diamond-braided fiber composites. The model is a generalization of the model developed by Raju and Wang in which the geometry of a braid unit cell is analyzed by dividing the unit cell into thirteen regions. These regions are categorized as overlapping strands, strand undulation, and matrix only regions. Model was capable of limiting the physically possible braid angles for a unit cell based on strand geometry. In the model, unidirectional lamina elastic constants are found using micromechanical models. The longitudinal modulus and major Poisson's ratio are calculated using Rule of Mixture predictions. Transverse and in-plane shear moduli are calculated with Halpin-Tsai equations, while out-of-plane shear modulus and Poisson's ratio were calculated using stress partitioning parameter and a method proposed by Ko, respectively [75]. The macro model is based on a modified CLPT where a volume weighted stiffness matrix is calculated using the thirteen regions. Stiffness matrices of undulation regions are calculated using the Gauss-Legendre numerical iteration. Stiffness matrices are subsequently transformed to the loading direction axis. Comparison of the predicted results to results of other models and experimental findings were in god agreement. Later

they performed a sensitivity analysis of the effect of constituent elastic constants on braid elastic constants. The model is found to be mainly sensitive to longitudinal fiber elastic modulus, and matrix elastic and shear moduli. Authors later used the findings of the model to design a braided composite catheter through calculations of axial, flexural and torsional rigidities of braided composites [75, 130, 55].

In another publication, Carey et al, [131], claimed that, although accurate and promising, available elastic property predictive models for woven/braided structures are lengthy. They proposed a regression based model simpler than other available models, for use in the preliminary stages of design with braid/woven composites. The geometrical characterization of the braid unit cell was done in a generalized manner that compensates for different braids angles and open-mesh braids. Using previously developed analytical models, elastic constants of braids and laminates possessing the same angle-ply geometry are calculated. A unit cell fiber volume fraction was determined. Normalized elastic modulus values are plotted with respect to unit cell fiber volume fractions. A linear relationship was observed between braid and laminate longitudinal and transverse elastic moduli values and fiber volume fractions. This model is underlined to be a very promising pre-design tool for such composites [131].

Recently, finite element models used for predicting engineering properties of 2x2 braided composites were developed by Tang et al [132], Goyal et al [133], and Goyal and Whitcomb [134]. Tang et al and Goyal et al studied the effect of waviness ratio, a relation between the thickness of lamina with an undulating yarn

and the undulation length, and the braid angle on the elastic properties of braided 2x2 braided composites. Transverse properties were found to be more sensitive to these parameters. On the other hand, the out-of-plane modulus was found to be almost insensitive. Later, stress concentrations of 2x2 braided composites were investigated by researchers from the same group Goyal and Whitcomb [134].

Potlori and Mannan [135], and Potlori et al [136] used finite element analysis to determine the mechanics of non-orthogonal structures such as braided structures [135]. Flexural and torsional behaviors of biaxial and triaxial braided composite structure were also investigated. Flexural and torsional rigidities, calculated using a modified CLPT, analysis were in good agreement with experimental findings [136].

Very recently, Lomov et al, [137], published a detailed work on finite element analysis (FEA) of textile composites that provides an algorithm of the necessary steps to textile composites FEA [137]. Since 2007, Tsai et al, [138], Zheng and Binienda [139], and Pickett et al, [140] also published studies to predict the elastic properties of braided composites using FEA analysis.

Ayranci and Carey [141] indicated that almost none of the models used for predicting tubular braided structure elastic constants consider tube diameter in the geometric definition of the unit cells. Authors modified the analytical models developed by Raju and Wang, [102], and Carey et al., [75] to compensate for the curvature in the unit cell [141].

2.9. Conclusion

In this report, braiding technique used for composite materials manufacturing was reviewed. Advantages and disadvantages of 2D and 3D braiding were outlined. Resin impregnation of fibers and different methods to achieve proper impregnation were listed. A broad range of applications of 2D braided composite materials were listed to show the nearly endless possibilities and advantages of 2D braids, which reinforce the notion of braiding as a strong alternative to other types of composite manufacturing techniques available. A large number of analytical models used to predict the elastic properties of braided composites were outlined and discussed.

2D-Braided composite materials offer numerous advantages over the conventional materials. The recent improvements in their fabrication techniques and understanding of their mechanical behaviors through predictive models contribute to the increasing popularity of these materials.

The investigation conducted in this chapter help to underline the gaps existing in the literature crucial for this thesis. Very limited data exist related to the investigation of the effect of radius of curvature of unit cells and the effect of undulation lengths of unit cells (i.e. open versus closed mesh braided structures) on the elastic properties of 2D braided composite materials.

The works presented in Chapters 3 to 6 were conducted to address these shortcomings. Chapters 3 reports on development and verification of an analytical model that utilizes a curved-unit cell for the predictions, and important parameters that affect the elastic properties using case studies. Chapter 4 was written to

outline the important parameters of the developed model using a sensitivity study, and also to document the experimental verification of the shear modulus predictions of the model.

Chapters 5 and 6 investigate the open-mesh braided composites by comparing analytical versus experimental findings. Chapter 5 was written to outline the comparison of analytical and experimental findings of open-mesh braided composites by analyzing the effects of undulation length on elastic properties of 2D braided tubular composites. Also, the applicability of the proposed model in Chapters 3 and 4 to stent-like structures, another medical device that may be manufactured using braiding, was investigated. Chapter 6 was written to further validate a previously developed regression based model using open-mesh experimental data, and determine Lower Linearity Limits of the model for practical design applications.

2.10. References

[1] Sanders, L. R., 1977, "Braiding - A Mechanical Means of Composite Fabrication", SAMPE Q, 8(2) pp. 38-44.

[2] Ko, F.K., Pastore, C.M., Head, A.A., “Atkins and Pearce Handbook of Industrial Braiding”, Atkins and Pearce, Covington, Kentucky, 1989.

[3] Sainsbury-Carter, J. B., 1985, "Braided Composites: A Material Form Providing Low Cost Fabrication Techniques" National SAMPE Symposium and Exhibition (Proceedings), 30pp. 1486-1497.

[4] Munjal, A. K., and Maloney, P. F., 1990, "Braining for Improving Performance and Reducing Manufacturing Costs of Composite Structures for Aerospace Applications” National SAMPE Technical Conference, 22pp. 1231-1242.

[5] Munro, M., and Fahim, A., 1995, "Comparison of Helical Filament Winding and 2D Braiding of Fiber Reinforced Polymeric Components” Materials and Manufacturing Processes, 10(1) pp. 37-46.

[6] Brunnschweiler, D., 1954, “The structure and tensile properties of braids”, Journal of Textile Institute (45), T55-87.

[7] Du, G., Popper, P., and Chou, T., 1990, "Process Model of Circular Braiding” American Society of Mechanical Engineers, Materials Division (Publication) MD, 19pp. 119-133.

[8] Du, G. W., and Popper, P., 1994, "Analysis of a Circular Braiding Process for Complex Shapes”, Journal of the Textile Institute, 85(3) pp. 316-337.

[9] Zhang, Q., Beale, D., Broughton, R.M., August 1999, “Analysis of circular braiding process, Part 1: theoretical investigation of kinematics of the circular braiding process”, Vol. 121, n3, 345-350.

[10] Phoenix, S. L., 1978, "Mechanical Response of a Tubular Braided Cable with an Elastic Core" Textile Research Journal, 48(2) pp. 81-91.

[11] Smith, L. V., and Swanson, S. R., 1994, "Selection of Carbon Fiber 2D Braid Preform Parameters for Biaxial Loading”, American Society of Mechanical Engineers, Materials Division (Publication) MD, 48pp. 33-44.

[12] Croon, C., 1984, "Braided Fabrics Properties and Applications" National SAMPE Symposium and Exhibition (Proceedings), pp. 611-624.

[13] Byun, J.H., and Chou, T.W., 1989, "Modelling and Characterization of Textile Structural Composites. A Review”, Journal of Strain Analysis for Engineering Design, 24(4) pp. 253-262.

[14] Maass, D., Hoon, D., March 1985, “Design of Composite Tubular Structures for Impact Damage Tolerance”, 30th National SAMPE Symposium and Exhibition (Proceedings), 1294-1308.

[15] Jackson, A. C., 1994, "Development of Textile Composite Preforms for Aircraft Primary Structures”, Collection of Technical Papers - AIAA/ASME/ASCE/AHS/ASC Structures, Structural Dynamics and Materials Conference, 2pp. 1008-1012.

[16] Kuykendall, M. A., 1994, "Braided Frame Testing and Analysis”, International SAMPE Technical Conference, 26pp. 746-758.

[17] Brookstein, D., 1988, "Structural Applications of Advanced Braided Composites", In: Proceedings SPE/APC '88. Advanced Polymer Composites for Structural Applications. Los Angeles, 14-17 November, pp. 415-424.

[18] Brookstein, D. S., 1988, "Processing Advanced Braided Composites", American Society of Mechanical Engineers, Materials Division (Publication) MD, 5pp. 33-36.

[19] Kruesi, A. H., and Hasko, G. H., 1987, "Computer controlled resin impregnation for fiber composite braiging" Int SAMPE Symp Exhib, 32pp. 309-317.

[20] Fujita, A., Maekawa, Z., and Hamada, H., Matsuda, M., Matsuo, T. 1993, "Mechanical Behavior and Fracture Mechanism of Thermoplastic Composites with Commingled Yarn", Journal of Reinforced Plastics and Composites, 12(2) pp. 156-172.

[21] Ramasamy, A., Wang, Y., and Muzzy, J., 1996, "Braided Thermoplastic Composites from Powder-Coated Towpregs. Part III: Consolidation and Mechanical Properties", Polymer Composites, 17(3) pp. 515-522.

[22] Bechtold, G., Kameo, K., Langler, F., Hamada, H., and Friedrich, K. 1999, "Pultrusion of Braided Thermoplastic Commingled Yarn - Simulation of the Impregnation Process", Proceedings of the 5th International Conference on Flow Processes in Composite Materials, Plymouth, UK, July 1999, pp. 257-264.

[23] Jackson, A. C., 1996, "Application of Textiles to Aircraft Primary Structures", Proceedings of the American Society for Composites, pp. 969-978.

[24] Dexter, H. B., 1996, "Innovative Textile Reinforced Composite Materials for Aircraft Structures", International SAMPE Technical Conference, 28pp. 404-416.

[25] Krebs, N. E., and Rahnenfuehrer, E. W., 1987, "Kaman braided structures" Annual Forum Proceedings - American Helicopter Society, 2pp. 605-611.

[26] Michaeli, W., Dyckhoff, J., and Jehrke, M., 1993, "Production of Structural Hollow Fibre Reinforced Components using a Combined RTM and Blow-Up Technology", International SAMPE Symposium and Exhibition (Proceedings), 38(2) pp. 2092-2101.

[27] Charlebois, K. M., Boukhili, R., Zebdi, O., Trochu, F., and Gasmi, A. 2005, "Evaluation of the Physical and Mechanical Properties of Braided Fabrics and their Composites", Journal of Reinforced Plastics and Composites, 24(14) pp. 1539-1554.

[28] Pederson, C., Lo Faro, C., Aldridge, M., and Maskell, R., 2003, "Epoxy - Soluble Thermoplastic Fibers: Enabling Technology for Manufacturing High Toughness Structures by Liquid Resin Infusion", SAMPE Journal, 39(4) pp. 22-28.

[29] Kelkar, A. D., Tate, J. S., Whitcomb, J., and Tang, X., 2003, "Performance Evaluation and Modeling of Braided Composites", Collection of Technical Papers - AIAA/ASME/ASCE/AHS/ASC Structures, Structural Dynamics and Materials Conference, 1, 674-684.

[30] Tate, J. S., and Kelkar, A. D., 2003, "Fatigue Behavior of VARTM Manufactured Biaxial Braided Composites", American Society of Mechanical

Engineers, Pressure Vessels and Piping Division (Publication) PVP, 470pp. 177-180.

[31] Tsai, J. S., Li, S. J., and Lee, L. J., 1998, "Microstructural Analysis of Composite Tubes made from Braided Preform and Resin Transfer Molding", Journal of Composite Materials, 32(9) pp. 829-850.

[32] Uozumi, T., Kito, A., Yamamoto, T., 2005, "CFRP using braided preforms/RTM process for aircraft applications", Advanced Composite Materials: The Official Journal of the Japan Society of Composite Materials, 14, 4, 365-383.

[33] Kobayashi, H., Nakama, N., Maekawa, Z., Hamada, H., Fujita, A., and Uozumi, T. 1992, "Fabrication and Mechanical Properties of Braided Composite Truss Joint", International SAMPE Symposium and Exhibition, 37pp. 1089-1103.

[34] Hamada, H., Nakai, A., and Masui, M., 1996, "Mechanical Properties for Self-Reinforced Braided Composite Tube", Proceedings of the American Society for Composites, pp. 1026-1035.

[35] Nakai, A., Masui, M., and Hamada, H., 1996, "Fabrication and Mechanical Properties of Multi-Reciprocal Braided Composite Tube", Advanced Composites Letters, 5(3) pp. 77-79.

[36] WHITE, M. L., 1982, "Tubular braided composite main rotor blade spar" J Am Helicopter Soc, (N 4) pp. 45-48.

[37] Casale, N., Bristow, D., and Pastore, C. M., 1991, "Design and Fabrication of a Braided Composite Monocoque Bicycle Frame", In: High-Tech Fibrous Materials (ACS Symposium Series 457), pp. 90-101.

[38] Axtell, J. T., Smith, L. V., and Shenoy, M. M., 2000, "Effect of Composite Reinforcement on the Durability of Wood Baseball Bats", International SAMPE Technical Conference, 32pp. 687-697.

[39] Shenoy, M.M., Smith, L.V., Axtell, J.T., 2001, "Performance assessment of wood, metal and composite baseball bats", Composite Structures 52 (3-4), pp. 397-404.

[40] Neogi, D., and Douglas, C. D., 1993, "Advanced Composite Self Deploying Structures - Design, Analysis and Fabrication", International SAMPE Symposium and Exhibition (Proceedings), 38(2) pp. 1811-1825.

[41] Neogi, D., and Douglas, C. D., 1995, "Design and Development of a Self Deployable Structural Element", International Journal of Space Structures, 10(2) pp. 77-87.

[42] Nanni, A., and Norris, M. S., 1995, "FRP Jacketed Concrete Under Flexure and Combined Flexure-Compression", Construction and Building Materials, 9(5) pp. 273-281.

[43] Hampton, F. P., Lam, H., Ko, F. K., and Harris, H.G., 2001, "Design Methodology of a Ductile Hybrid FRP for Concrete Structures by the Braidtrusion Process", International SAMPE Symposium and Exhibition (Proceedings), 46 IIpp. 2421-2432.

[44] Lam, H., and Ko, F. K., 2001, "Composite Manufacturing by the Braidtrusion Process", International SAMPE Technical Conference, 33pp. 532-539.

[45] Karbhari, V. M., Falzon, P. J., and Herzburg, I., 1996, "Effect of Braid Architecture on Progressive Crush of Composite Tubes", International SAMPE Symposium and Exhibition (Proceedings), 41(2) pp. 1409-1416.

[46] Karbhari, V. M., Haller, J. E., Falzon, P. K., and Herszberg, I., 1999, "Post-Impact Crush of Hybrid Braided Composite Tubes", International Journal of Impact Engineering, 22(4) pp. 419-433.

[47] Hudgins, R. G., and Muzzy, J. D., 1998, "Analytical Stress Model for a Composite Prosthetic Intervertebral Disc", Polymer Composites, 19(6) pp. 837-845.

[48] Hudgins, R. G., and Muzzy, J. D., 2000, "Assessment of Compressive Strength of Flexible Composite Materials for Spinal Implantation", Journal of Composite Materials, 34(17) pp. 1472-1493.

[49] Moutos, F. T., and Gupta, B. S., 1999, "Development of Biomimetical Composite Prosthetic Ligaments using Mechanically Dissimilar Materials", Annual International Conference of the IEEE Engineering in Medicine and Biology - Proceedings, 2pp. 730.

[50] Reinhardt, A., Advani, S. G., Santare, M. H., and Miller, F., 1999, "Preliminary Study on Composite Hip Prostheses made by Resin Transfer Molding", Journal of Composite Materials, 33(9) pp. 852-870.

[51] Fujihara, K., Huang, Z. -., Ramakrishna, S., Satkunanantham, K., and Hamada, H., 2001, "Development of Braided carbon/PEEK Composite Bone Plates", Advanced Composites Letters, 10(1) pp. 13-20.

[52] Fujihara, K., Huang, Z. -., Ramakrishna, S., Satkunanantham, K., and Hamada, H., 2003, "Performance Study of Braided carbon/PEEK Composite Compression Bone Plates", Biomaterials, 24(15) pp. 2661-2667.

[53] Huang, Z. -., and Fujihara, K., 2005, "Stiffness and Strength Design of Composite Bone Plates", Composites Science and Technology, 65(1) pp. 73-85

[54] Fujihara, K., Teo, K., Gopal, R., Loh, P.L., Ganesh, V.K., Ramakrishna, S., Foong, K.W.C., and Chew, C.L. 2004, "Fibrous Composite Materials in Dentistry and Orthopaedics: Review and Applications", Composites Science and Technology, 64(6) pp. 775-788.

[55] Carey, J., Fahim, A., Munro, M., "Design of braided composite cardiovascular catheters based on required axial, flexural, and torsional rigidities", Journal of Biomedical Materials Research - Part B Applied Biomaterials 70 (1), 2004, 73-81.

[56] Tsiang, T., Albany Inst Research Co, Dedham, and Brookstein, D. S., 1985, "Load-Deformation Behavior of composite cylinders with integrally-formed braided and with machined circular holes" pp. 1283-1296.

[57] Brookstein, D. S., 1986, "Joining Methods for advanced braided composites." Composite Structures, 6(1-3) pp. 87-94.

[58] Wang, Y., Du, S., Zhao, D., and Ramasamy, A., 1992, "Study of Composites from Weaving, Braiding, and Pultrusion Processes", Proceedings of the American Society for Composites, pp. 3-11.

[59] Wang, Y., and Ramasamy, A., 1992, "Bearing Behavior of Fiber Reinforced Composites from Braiding, Pultrusion, and Fabric Lamination Processes", International SAMPE Symposium and Exhibition, 37pp. 727-737.

[60] Wang, Y., 1994, "Bearing Behavior of Triaxially Braided Flat and Tubular Composites", Applied Composite Materials, 1(3) pp. 217-229.

[61] Li, W., Hammad, M., Reid, R., El-Shiekh, A., 1990, "Bearing behavior of holes formed using different methods in 3-D braided Graphite/Epoxy composites", National SAMPE Symposium and Exhibition (Proceedings), 35 (pt 2), pp. 1638-1646.

[62] Fujita, A., Hamada, H., Maekawa, Z., Ohno, E., and Yokoyama, A., 1994, "Mechanical Behavior and Fracture Mechanism in Flat Braided Composites. Part 3: Mechanically Fastened Joint in Flat Braided Bar", Journal of Reinforced Plastics and Composites, 13(8) pp. 740-755.

[63] Ohki, T., Ikegaki, S., and Kurasiki, K., Hamada, H., Iwamoto, M. 2000, "Mechanical Properties of Flat Braided Composites with a Circular Hole", Journal of Engineering Materials and Technology, Transactions of the ASME, 122(4) pp. 420-424.

[64] Ohki, T., Nakai, A., and Hamada, H., 2000, Takeda, N. "Micro/macro Damage Evaluation of Flat Braided Composites with a Circular Hole", Science and Engineering of Composite Materials, 9(2) pp. 55-66.

[65] Nakai, A., Ohki, T., and Takeda, N., Hamada, H. 2001, "Mechanical Properties and Micro-Fracture Behaviors of Flat Braided Composites with a Circular Hole", Composite Structures, 52(3-4) pp. 315-322.

[66] Huang, Z.M., “The mechanical properties of composites reinforced with woven and braided fabrics”, Composites Science and Technology 60 (4), 2000, 479-498.

[67] Naik, N.K., Ganesh, V.K., “Failure behavior of plain weave fabric laminates under in-plane shear loading”, Journal of Composites Technology and Research 16 (1), 1994, 3-20.

[68] Smith, L. V., Swanson, S. R., ”Strength design with 2-D triaxial braid textile composites”, Composites Science and Technology, v 56, n 3, 1996, 359-365.

[69] Smith, L. V., Swanson, S. R., “Micro-mechanics parameters controlling the strength of braided composites”, Composites Science and Technology, v 54, n 2, 1995, 177-184.

[70] Bigaud, D., Hamelin, P., “Multi-scale approach for modeling mechanical behavior of 2D and 3D textile-reinforced composites”, Proceedings of the International Conference on Computer Methods in Composite Materials, CADCOMP, 1998, 127-136.

[71] Harte, A.-M., Fleck, N.A., “Deformation and failure mechanisms of braided composite tubes in compression and torsion”, Acta Materialia 48 (6), 2000, 1259-1271.

[72] Huang, Z.M., “A unified micromechanical model for the mechanical properties of two constituent composite materials. Part III: Strength behavior”, Journal of Thermoplastic Composite Materials 14 (1), 2001, 54-69.

[73] Aggarwal, A., Ramakrishna, S., Ganesh, V.K., "Predicting the strength of diamond braided composites", Journal of Composite Materials 36 (5), 2002, 625-643.

[74] Huang, Z.-M., Teng, X.C., Ramakrishna, S., "Fatigue behaviour of multilayer braided fabric reinforced laminates", Polymers and Polymer Composites 13 (1), 2005, 73-81.

[75] Carey, J., Munro, M., Fahim, A., "Longitudinal elastic modulus prediction of a 2-D braided fiber composite", Journal of Reinforced Plastics and Composites 22 (9), 2003, 813-831.

[76] Jones, R. M., "Mechanics of composite materials", USA, Taylor and Francis, Second Edition, 1999.

[77] Halpin, J.C., Jerine, K, Whitney, J.M., "Laminate Analogy for 2 and 3 Dimensional Composite Materials", Journal of Composite Materials, Vol. 5, Jan. 1971, 36-49.

[78] Whitney, J.M., Halpin, J.C., "Analysis of laminated anisotropic tubes under combined loading", Journal of Composite Materials, Journal of Composite Materials, Vol. 2, No. 3, July 1968, 360-367.

[79] Ishikawa, T., Chou, T-W., "Stiffness and Strength Behavior of Woven Fabric Composites", Journal of Materials Science, Vol. 71, No. 11, November 1982, 3211-3220.

[80] Ishikawa, T., Chou, T-W., "In-Plane Thermal Expansion and Thermal Bending Coefficients of Fabric Composites", Journal of Composite Materials, Vol. 17, Issue 2, March 1983, 92-104.

[81] Ishikawa, T., Chou, T-W., "One-Dimensional Micromechanical Analysis of Woven Fabric Composites" AIAA Journal (American Institute of Aeronautics and Astronautics), Vol. 21, Issue 12, December 1983, 1714-1721.

[82] Ishikawa, T., Chou, T-W., "Elastic Behavior of Woven Hybrid Composites", Journal of Composite Materials, Vol. 16, January 1982, 2-19.

[83] Tsiang, T.-H., Brookstein, D., Dent, J., "Mechanical Characterization of Braided Graphite/Epoxy Cylinders", Technology Vectors, Proc. 29th National SAMPE Symposium/Exhibition (Proceedings), April 1984, 880-890.

[84] Yang, J. M., Ma, C. L., Chou, T.-W., "Elastic stiffness of Biaxial and Triaxial Woven Fabric Composites", 29th National SAMPE Symposium and Exhibition (Proceedings), April 3-5, 1984, 292-303.

[85] Yang, J.-M., Ma, C.-L., Chou, T.-W., "Fiber Inclination Model of Three-Dimensional Textile Structural Composites", Journal of Composite Materials, Vol. 20, Issue 5, September 1986, 472-484.

[86] Whyte, D.W., " On the Structure and Properties of 3-D Braid Reinforced Composites", Ph.D. Thesis, Drexel University, June 1986.

[87] Pastore, C. M., Gowayed, Y. A., "A Self-consistent fabric geometry model: modification and application of a fabric geometry model to predict the elastic properties of textile composites", Journal of Composites Technology and Research 16 (1), 1994, 32-36.

[88] Lei, C.S.C., Wang, A.S.D., Ko, F.K., " Finite cell model for 3-D braided composites", American Society of Mechanical Engineers, Materials Division (Publication) MD 5, 1988, 45-50.

[89] Soebroto, H.B., Hager, T., Pastore, C.M., Ko, F.K., "Engineering Design of Braided Structural Fiberglas Composites", National SAMPE Symposium and Exhibition (Proceedings), Vol. 35, Issue pt 1, April 1990, 687-696.

[90] Naik, N.K., Shembekar, P.S., "Elastic behavior of woven fabric composites: I-lamina analysis", Journal of Composite Materials 26 (15), 1992, 2196-2225.

[91] Shembekar, P.S., Naik, N.K., "Elastic behavior of woven fabric composites: II-laminate analysis", Journal of Composite Materials 26 (15), 1992, 2226-2246.

[92] Naik, N.K., Shembekar, P.S., "Elastic behavior of woven fabric composites: III-Laminate design", Journal of Composite Materials 26 (17), 1992, 2522-2541.

[93] Masters, J. E., Foye, R. L., Pastore, C. M., Gowayed, Y. A., "Mechanical properties of triaxially braided composites: Experimental and analytical results", Journal of Composites Technology and Research 15 (2), 1993, 112-122.

[94] Ma, C.-L., Yang, J.-M., Chou, T.-W., "Elastic Stiffness of Three-Dimensional Braided Textile Structural Composites", ASTM Special Technical Publication, 1986, 404-421.

[95] Masters, J.E., Ifju, P.G., "A phenomenological study of triaxially braided textile composites loaded in tension", Composites Science and Technology 56 (3), 1996, 347-358.

[96] Falzon, P.J., Herszberg, I., Baker, A.A., “Stiffness analysis of textile composites”, National Conference Publication - Institution of Engineers, Australia 1 (93 pt 6), 1993, 219-224.

[97] Redman, C. J., Douglas, C. D., “Theoretical prediction of the tensile elastic properties of braided composites”, International SAMPE Symposium and Exhibition (Proceedings) 38 (1), 1993, 719-727.

[98] Naik, R. A., Ifju, P. G., Masters, J. E., “Effect of fiber architecture parameters on deformation fields and elastic moduli of 2-D braided composites”, Journal of Composite Materials 28 (7), 1994, 656-681.

[99] Naik, R.A., “Analysis of woven and braided fabric-reinforced composites”, ASTM Special Technical Publication 1274, 1996, 239-263.

[100] Naik, R.A.,, “Analysis of 2-D triaxial and 3-D multi-interlock braided textile composites”, Collection of Technical Papers - AIAA/ASME/ASCE/AHS/ASC Structures, Structural Dynamics and Materials Conference 3, 1996, 1804-1811.

[101] Naik, R. A., “Multiaxial stiffness and strength analysis of woven and braided composites”, Collection of Technical Papers - AIAA/ASME/ASCE/AHS/ASC Structures, Structural Dynamics and Materials Conference 2, 1997, 1148-1158.

[102] Raju, I.S., Wang, J.T., “Classical laminate theory models for woven fabric composites”, Journal of Composites Technology and Research 16 (4), 1994, 289-303.

[103] Gowayed, Y.A., Pastore, C., Howarth, C.S., “Modification and application of a unit cell continuum model to predict the elastic properties of textile composites”, Composites Part A: Applied Science and Manufacturing 27 (2), 1996, 149-155.

[104] Foye, R.L., Fiber Tex '90, (Ed. J. Buckley), NASA Langley Research Center, Hampton, VA, May, 1992, pp. 45-53.

[105] Nakai, A., Fujita, A., Yokoyama, A., Hamada, H., “Design methodology for a braided cylinder”, Composite Structures, v 32, n 1-4, 1995, 501-509.

[106] Hamada, H., Fujita, A., Maekawa, Z., Nakai, A., Yokoyama, A., “Design of braided composite tubes by numerical analysis method”, American Society of Mechanical Engineers, Pressure Vessels and Piping Division (Publication) PVP, v 302, Composites for the Pressure Vessel Industry, 1995, 69-73.

[107] Nakai, H., Hamada, Hoa, S.V., “Influence of braiding structure on torsional properties of braided composite tube”, American Society of Mechanical Engineers, Pressure Vessels and Piping Division (Publication) PVP 326, 1996, 125-130.

[108] Naik, N.K., Ganesh, V.K., “Analytical method for plain weave fabric composites”, Composites, v 26, n 4, Apr, 1995, 281-289.

[109] Naik, N.K., Ganesh, V.K., “Prediction of thermal expansion coefficients of plain weave fabric composites”, Composite Structures 26 (3-4), 1993, 139-154.

[110] Naik, N.K., Ganesh, V.K., “Prediction of on-axes elastic properties of plain weave fabric composites”, Composites Science and Technology 45 (2), 1992, 135-152.

[111] Byun, J.-H., Lee, S.-K., Kim, B.S., "Development of braided-pultrusion process and structure-property relationships for tubular composites", Acta Metallurgica Sinica (English Letters), v 9, n 6, Dec, 1996, 555-564.

[112] Branch, K. L., Shivakumar, K. N., Avva, V. S., "Three-dimensional tow inclination model for calculating elastic constants of three-dimensional triaxial braided composites", Collection of Technical Papers - AIAA/ASME/ASCE/AHS/ASC Structures, Structural Dynamics and Materials Conference 3, 1996, 1788-1803.

[113] Robitaille, F., Clayton, B.R., Long, A.C., Souter, B.J., Rudd, C.D., "Geometric modelling of industrial preforms: Woven and braided textiles", Proceedings of the Institution of Mechanical Engineers Part L: Journal of Materials: Design and Applications 213 (2), 1999, 69-83.

[114] Robitaille, F., Long, A.C., Jones, I.A., Rudd, C.D., "Automatically generated geometric descriptions of textile and composite unit cells", Composites Part A: Applied Science and Manufacturing 34 (4), 2003, 303-312.

[115] Wong, C.C., Long, A.C., Sherburn, M., Robitaille, F., Harrison, P., Rudd, C.D., "Comparisons of novel and efficient approaches for permeability prediction based on the fabric architecture", Composites Part A: Applied Science and Manufacturing 37 (6 SPEC. ISS.), 2006, 847-857.

[116] Aggarwal, A., Ganesh, V.K., Ramakrishna, S., "Analytical characterization of diamond braided fabric reinforced composites", International SAMPE Technical Conference 31, 1999, 431-443.

[117] Aggarwal, A., Ramakrishna, S., Ganesh, V.K., "Predicting the in-plane elastic constants of diamond braided composites", Journal of Composite Materials 35 (8), 2001, 665-688.

[118] Byun, J.-H., "The analytical characterization of 2-D braided textile composites", Composites Science and Technology 60 (5), 2000, 705-716.

[119] Harte, A.-M., Fleck, N.A., "On the mechanics of braided composites in tension", European Journal of Mechanics, A/Solids 19 (2), 2000, 259-275.

[120] Huang, Z.M., "Unified micromechanical model for the mechanical properties of two constituent composite materials. Part I: elastic behavior", Journal of Thermoplastic Composite Materials 13 (4), 2000, 252-271.

[121] Huang, Z.-M., "Unified micromechanical model for the mechanical properties of two constituent composite materials. Part II: Plastic behavior", Journal of Thermoplastic Composite Materials 13 (5), 2000, 344-362.

[122] Huang, Z.-M., Fujihara, K., Ramakrishna, S. "Tensile stiffness and strength of regular braid composites: Correlation of theory with experiments", Journal of Composites Technology and Research 25 (1), 2003, 35-49.

[123] Huang, Z.-M., Ramakrishna, S., "Towards automatic designing of 2D biaxial woven and braided fabric reinforced composites", Journal of Composite Materials 36 (13), 2002, 1541-1579.

[124] Ivanov, I., Tabiei, A., "Three-dimensional computational micro-mechanical model for woven fabric composites", Composite Structures 54 (4), 2001, 489-496.

[125] Yan, Y., Van Hoa, S., "Energy model for prediction of mechanical behavior of 2-D triaxially braided composites, Part I: Model development", Journal of Composite Materials 36 (8), 2002, 963-981.

[126] Yan, Y., Van Hoa, S., "Energy approach for prediction of mechanical behavior of 2-D triaxially braided composites Part II: Parameter analysis", Journal of Composite Materials 36 (10), 2002, 1233-1253.

[127] Tabiei, A., Yi, W., "Comparative study of predictive methods for woven fabric composite elastic properties", Composite Structures 58 (1), 2002, 149-164.

[128] Tabiei, A., Jiang, Y., Yi, W., "Novel micromechanics-based woven-fabric composite constitutive model with material nonlinear behavior", AIAA journal 38 (8), 2000, 1437-1443.

[129] Quek, S.C., Waas, A.M., Shahwan, K.W., Agaram, V., "Analysis of 2D triaxial flat braided textile composites", International Journal of Mechanical Sciences 45 (6-7), 2003, 1077-1096.

[130] Carey, J., Fahim, A., Munro, M., "Predicting elastic constants of 2D-braided fiber rigid and elastomeric-polymeric matrix composites", Journal of Reinforced Plastics and Composites 23 (17), 2004, 1845-1857.

[131] Carey, J., Munro, M., Fahim, A., "Regression-based model for elastic constants of 2D braided/woven open mesh angle-ply composites", Polymer Composites 26 (2), 2005, 152-164.

[132] Tang, X., Whitcomb, J.D., Goyal, D., Kelkar, A.D., "Effect of braid angle and waviness ratio on effective moduli of 2×2 biaxial braided composites",

Collection of Technical Papers - AIAA/ASME/ASCE/AHS/ASC Structures, Structural Dynamics and Materials Conference 6, 2003, 4364-4373.

[133] Goyal, D., Tang, X., Whitcomb, J.D., Kelkar, A.D., "Effect of various parameters on effective engineering properties of 2 × 2 braided composites", Mechanics of Advanced Materials and Structures 12 (2), 2005, 113-128.

[134] Goyal, D., Whitcomb, J.D., "Analysis of stress concentrations in 2 × 2 braided composites", Journal of Composite Materials 40 (6), 2006, 533-546.

[135] Potluri, P., Manan, A., "Mechanics of non-orthogonally interlaced textile composites", Composites Part A: Applied Science and Manufacturing 38 (4), 2007, 1216-1226.

[136] Potluri, P., Manan, A., Francke, M., Day, R.J., "Flexural and torsional behaviour of biaxial and triaxial braided composite structures", Composite Structures 75 (1-4), 2006, 377-386.

[137] Lomov, S.V., Ivanov, D.S., Verpoest, I., Zako, M., Kurashiki, T., Nakai, H., Hirosawa, S., "Meso-FE modelling of textile composites: Road map, data flow and algorithms", Composites Science and Technology 67 (9), 2007, 1870-1891.

[138] Tsai, K.-H., Hwan, C.-L., Chen, W.-L., Chiu, C.-H., "A parallelogram spring model for predicting the effective elastic properties of 2D braided composites", Composite Structures 83 (3), pp. 273-283, 2008.

[139] Zheng, X., Binienda, W.K., "Rate-dependent shell element composite material model implementation in LS-DYNA" Journal of Aerospace Engineering 21 (3), pp. 140-151, 2008.

[140] Pickett, A.K., Sirtautas, J., Erber, A., “Braiding simulation and prediction of mechanical properties”, Applied Composite Materials 16 (6), pp. 345-364, 2009.

[141] Ayranci, C., Carey, J. “Elastic constants of braided thick-walled tubular composites”, The Sixth Canadian-International composites Conference (CANCOM 2007), August 14-17 2007, Winnipeg, Manitoba, Canada.

CHAPTER 3: PREDICTING THE LONGITUDINAL ELASTIC MODULUS OF BRAIDED TUBULAR COMPOSITES USING A CURVED UNIT-CELL GEOMETRY

A version of this chapter was published as:

Ayranci, C., Carey, J.P., Predicting the longitudinal elastic modulus of braided tubular composites using a curved unit-cell geometry, Composites Part B: Engineering, 41 (3), 229-235, 2010.

3.1. Introduction

Braiding has been used for years to produce textile fabrics [1]. Increasing demand to produce fast, better, and automated composite material preforms forced researchers and engineers to utilize braiding as one of the techniques that fulfills this requirement. Braiding is one of the top choices of composite manufacturers for many applications due to the advantages it offers; such as increased toughness, control over fiber deposition angle and fast fiber deposition rate. Some of these applications can be listed as braided air ducts, aircraft structural parts, automotive shafts, braided catheters, braided stents and braided composite dental posts [1-5].

Optimal use of braided composites is possible via use of accurate models to predict their mechanical properties. Over the years, researchers developed both numerical and analytical models. Although accurate, numerical models are found to be rather lengthy due to the complex geometry requirements for stiffness calculations [6]. Analytical models, on the other hand, can provide sufficiently accurate data with less processing time and computer power requirements [5].

Many of the analytical models developed for woven-fabric and braided composites utilize Ishikawa and Chou's work developed for woven fabrics [7]. Authors proposed mosaic, fiber undulation, and bridging models that utilize the well-known Classical Laminate Plate Theory (CLPT) as a base for the calculations. The fiber undulation model was extensively modified and used by the braiding community as this model accounts for the undulation of the fibers between the cross-over regions of a braided structure for more accurate results.

Redman and Douglas predicted the tensile elastic properties of braided composites using a combination of rule of mixtures and Classical Laminate Plate Theory (CLPT) [8]. The authors neglected the undulating strand in their study by assuming the length between two neighboring strands to be large.

Soebroto et al. used Fabric Geometry Model (FGM) to predict the engineering properties of braids [9]. FGM uses a simplified geometry of the reinforcing elements and volumetrically combines the stiffness of these elements [9]. This model treats the reinforcement as a linear element hence may be seen as omitting the effect of undulation in the predictions.

Falzon et al. investigated a number of models to predict the stiffness of woven composites [6]. The authors divided the models into three main categories, namely, elementary models that rely on a generalized Hook's law, CLPT models, and numerical models (i.e. finite element models). The authors concluded that elementary models were simple but not suited for strength analysis, laminate theory models were limited to in-plane property predictions and not suitable for complicated architectures, and finite element models were suited for strength analysis but required detailed geometrical details [6].

Since, many new models have been published in the literature, and with the use of advanced computing capabilities both numerical and analytical models have developed to account for the limitations of the earlier models and to predict elastic properties of braided composites [10-16]. A detailed investigation of these works, along with others, has been published [5].

Many of these models were developed for flat-braided structures and predicted the properties through a flat unit-cell, or neglected the effects of curvature in tubular braids such as in works of Aggarwal et al. and Carey et al. [12,16]. This assumption may be acceptable for tubular structures with relatively large radii; however, it maybe not be for braided structures with smaller radii, such as braided catheters and stents.

Medical use of braided composites is rapidly increasing. The delicate use of braided tubular medical tubes in the human body requires thorough understanding of their mechanical properties. Hence, accurate models that predict composite material elastic properties must be developed and verified experimentally.

Carey et al. modified Raju and Wang's predictive model, developed for woven composites based on a generalized CLPT analysis, to predict elastic properties of diamond braided composites [16, 17]. Unlike some of the available simplified models, Carey et al.'s model included the possible effect of open-mesh regions (i.e. matrix only regions due to extensive undulating regions); however, the model neglected the effects of the curvature on the unit cell and assumed a flat unit cell even for tubular braided composites.

Potluri et al. (2006) and Potluri and Manan (2007) investigated the thicknesses of braided tows [18, 19]. The authors calculated the thickness of the tows to find the softened tow properties for use in a Modified Lamination Theory based model, which was also used by Byun in flat braided triaxial composites [10]. The authors suggested the thicknesses should be individually investigated.

Authors did not include the open mesh regions, although their unit cell indicates these regions, and did not study the effect of tube radius on the properties.

The proposed model is based on Carey et al.'s model; however, it is developed to evaluate and recognize the effects of the curvature on the elastic properties of the unit cell as a function of the tubular braided composite's diameter.

3.2. Proposed model

An initial version of the model was presented earlier [20]. Here, the detailed derivation, comparison of results with other available models and experimental results presented in the literature, and in-house experimental results are presented to validate the model.

In two-dimensional tubular braided composites, fibers are deposited on a cylindrical mandrel and impregnated by a matrix material. In this process, the diameter of the mandrel gains importance since each unit cell and the fiber-tow geometry in the unit cell would have a more pronounced effect depending on the diameter of the mandrel, i.e. curvature of the unit cell.

Figure 3.1 presents the top-view of an isolated unit cell. The unit cell is composed of three different regions, namely: crossover (where fiber tows lay on top of each other), undulating, and matrix-only regions. The strand thicknesses in the crossover regions of large-diameter tubular braids can be assumed almost identical as the radius of curvature of the unit cell can be assumed infinite; hence, the elastic properties of such structures can be predicted using flat-unit cell geometry.

In reality, the unit cell of a tubular braided structure has a curved geometry, (Figure 3.2), and the radius of curvature of the unit cell is a function of the tubular diameter. As the diameter of the tubular braid decreases, the thicknesses of the strands deposited on the mandrel become uneven, (Figure 3.3). The change in the curvature of the unit-cell and the un-even strand thickness must be accounted for through geometrical characterization of the unit cell to obtain more accurate elastic property predictions.

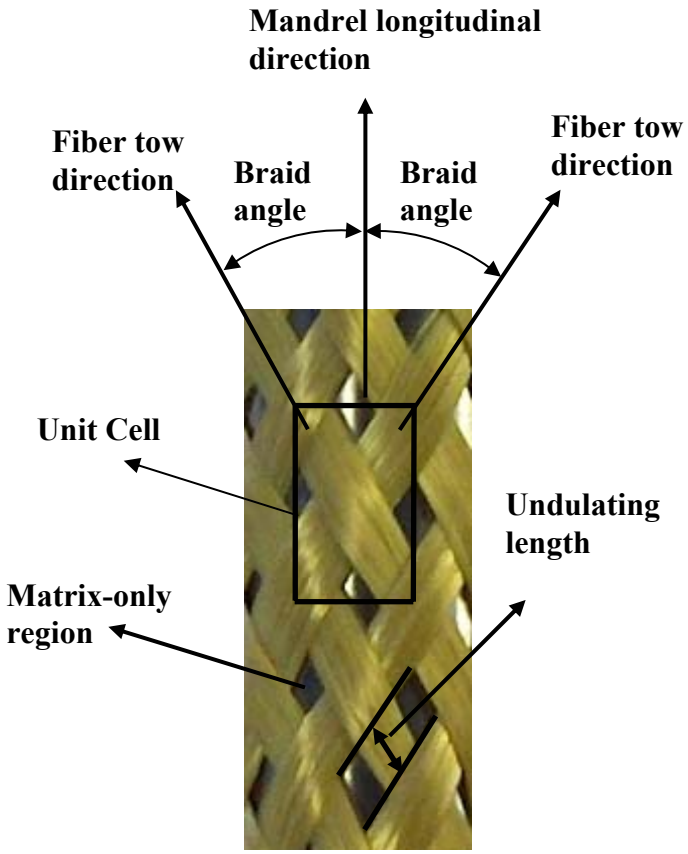

Figure 3.1: Top view of a unit cell.

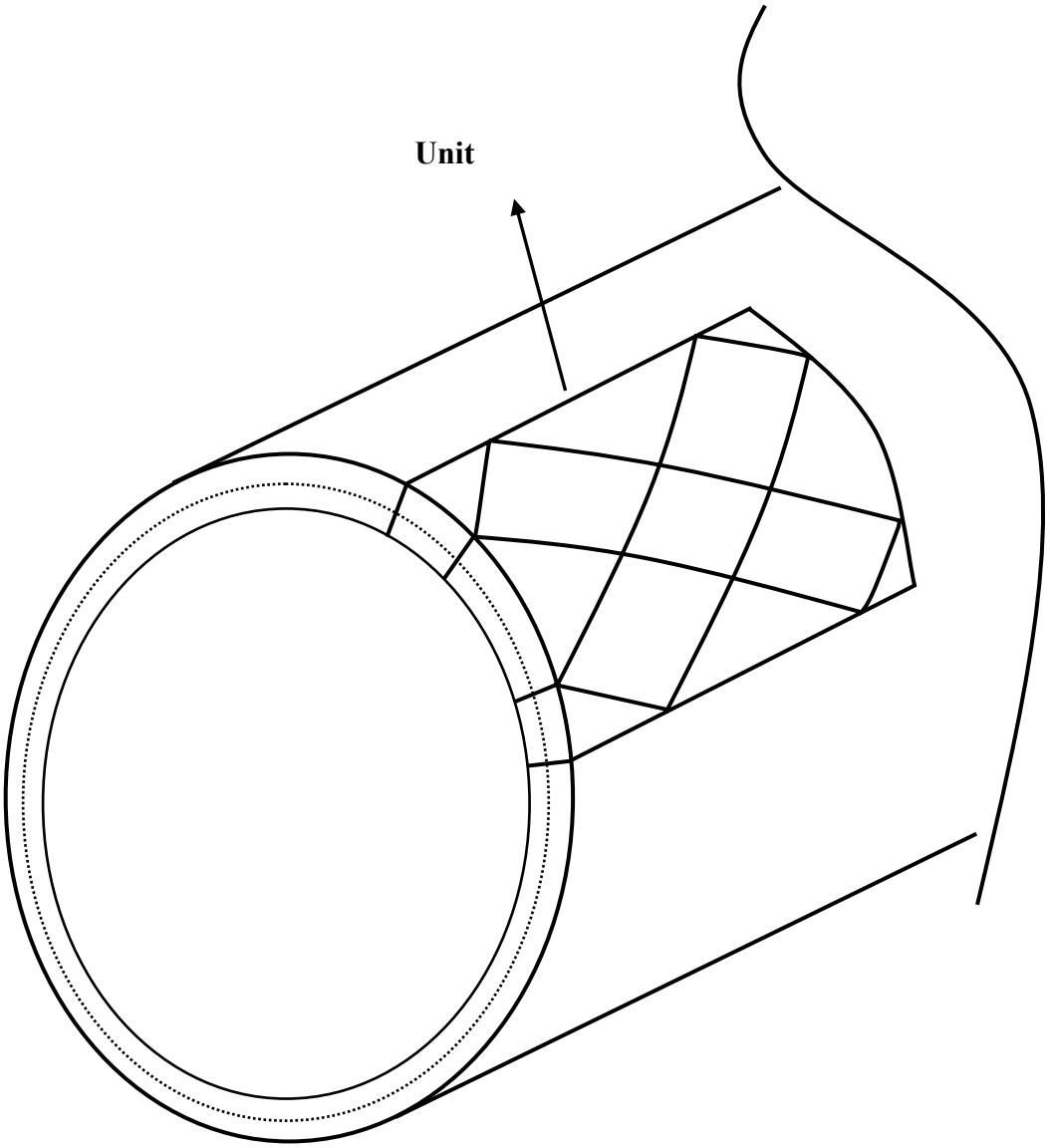

Figure 3.2: Schematic representation of a curved unit cell on a tubular braided composite.

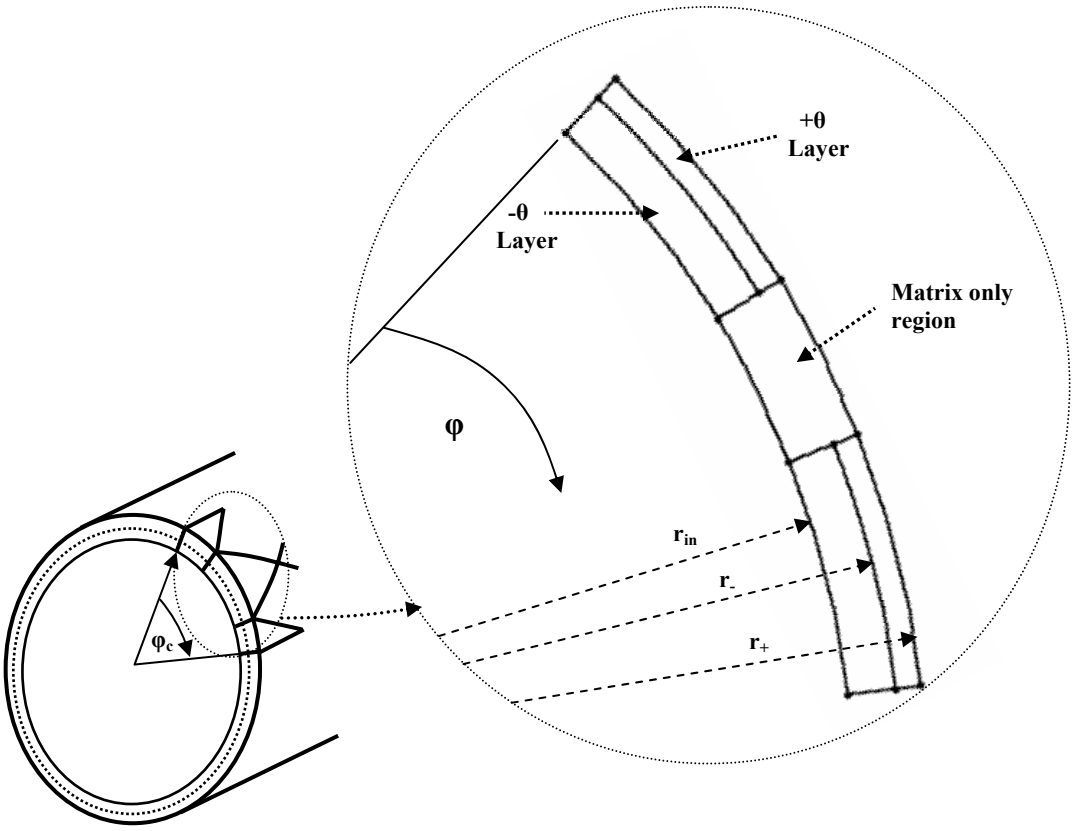

Figure 3.3: Zoomed-in section of the edge of the unit cell of Figure 3.2 **(exaggerated view). (in this figure φ is defined in the 0≤φ≤φc range)**

3.2.1. Geometric Characterization

Schematic representation of a curved unit cell is shown in Figure 3.4. The unit cell is characterized with respect to the radius (r) of the unit cell (i.e. radius of the tubular braided structure), the arc angle (φ_c) covered by the unit cell, and the longitudinal direction (y) of the unit cell/tubular braided structure. The braid angle (θ) is defined as the angle between the fibers and the longitudinal direction of the unit cell. The thirteen regions (defined as by Carey et al. [16]) of the unit cell are

shown using boxed-numbers in Figure 3.4. Regions 1 to 5 represent the crossover regions. In these regions there are no undulating fibers; therefore, the composite can be modeled as a cross-ply laminate. Regions 6 to 9 and 10 to 13 are the matrix-only regions and undulation regions, respectively.

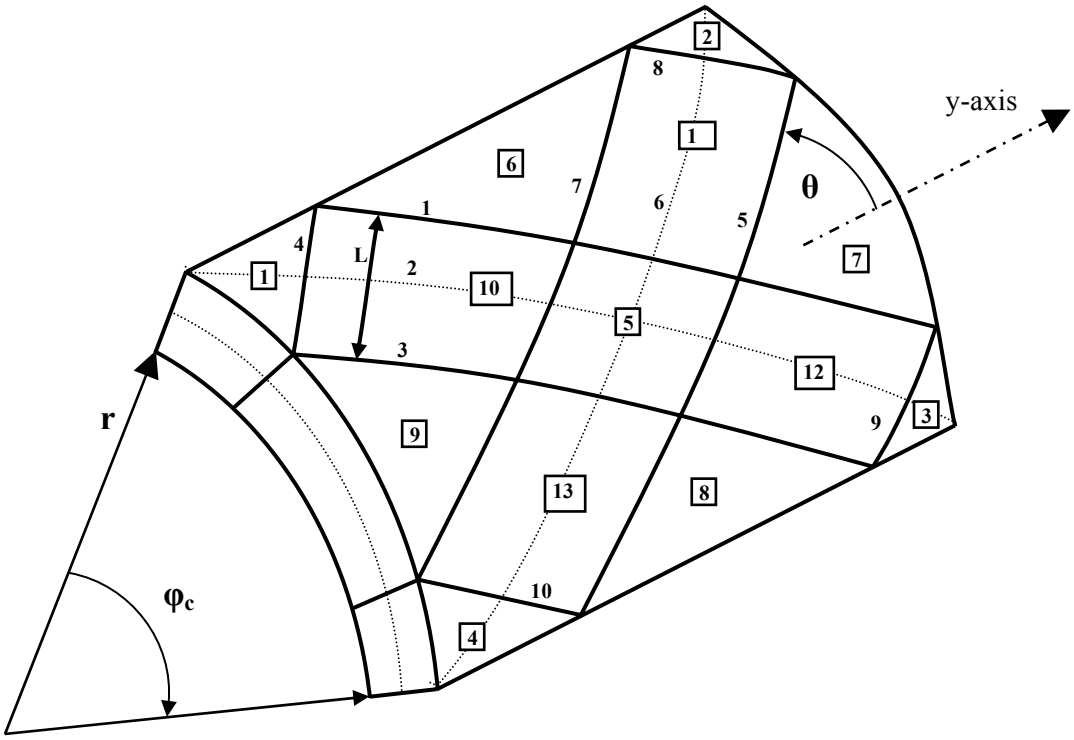

Figure 3.4: Geometric characterization of the curved unit cell.

Geometric boundaries of these thirteen regions are defined using lines 1 to 10 in Figure 3.4. As an example lines 1, 2 and 3 show the edges (lines 1 and 3) and mid-line (line 2) of the strand that is placed on the mandrel at a θ degree braid angle.

As the strands deposited on a mandrel are at the same angle, during the characterization of the unit cell, lines 1, 2, 3, 8, and 10 are assumed parallel to

each other. Similarly, lines 4, 5, 6, 7, and 9 are assumed parallel to each other. The magnitude of the lengths of lines 4, 8, 9 and 10 are same and equal to L, where L is a function of the strand width, W_y:

$$L = \frac{W_y}{\cos(2\theta - (\pi / 2))} \tag{1}$$

In the case of an unfolded and flattened unit cell, a Cartesian coordinate system, x-y, can be defined (x-direction being perpendicular to the previously defined y-direction). For this flat unit cell, for example, line-2 can be defined via angle γ, the complementary angle of the braid angle θ, as [16]:

$$y_2 = x \cdot \tan(\gamma) \tag{2}$$

The thicknesses of the tows used in most of the braiding applications are relatively small. Hence, it is assumed that upon unfolding the curved unit cell, the top layer of the unit cell does not buckle and Equation (2) can be modified and written as Equation (3) with $(r \cdot \varphi)$ being the arch length of the curved unit cell:

$$y_2 = (r \cdot \phi) \cdot \tan(\gamma) \tag{3}$$

The unit cell was geometrically characterized by defining lines 1 to 10 using the aforementioned approach. The layers that create the thickness of the unit

cell, fiber tows and the matrix, were projected onto a mandrel surface. In the model, an area-weighted approach was used to calculate unit cell elastic constants; therefore, defining the geometry of the unit cell plane which lies on the mandrel is assumed to be sufficient.

The difference between the thicknesses of the layers of the unit cell has to be defined. With respect to Figure 3.3 and Figure 3.4, the inner radius of the curved unit cell was defined as r_{in}. The radius of the top of the –θ ply, and top of the +θ ply were defined as r_{-} and r_{+}, respectively. The outer radius of the curved cell is assumed to have a thin layer of matrix rich region (omitted in Figure 3.4) and this radius was defined as r_m. Equation (4) can be geometrically derived using these radii and h_c as the thickness of the wet strands, and t_m as the thickness of the matrix layer. (i.e. Equation 4 is derived by assuming a constant cross sectional area and parametrically calculating the radii as the inner radius changes).

$$\begin{aligned} r_{-} &= \sqrt{(2 \cdot r_{in} \cdot h_c + r_{in}^2)} \\ r_{+} &= \sqrt{(2 \cdot r_{in} \cdot h_c + r_{-}^2)} \\ r_m &= \sqrt{(2 \cdot r_{in} \cdot t_m + r_{+}^2)} \end{aligned} \tag{4}$$

3.2.2. Theoretical approach

In the model, the undulating strands were assumed to follow a sinusoidal path defined by the function $h_{(d)}$ [16, 17]:

$$h_{(d)} = (1 + \cos(\pi \frac{d}{a_u})) \cdot \frac{h_c}{2} \tag{5}$$

where a_u is the length of the entire undulating region projected onto the mandrel surface, and d is the projected length of the undulation as $0 \le d \le a_u$. Hence, the undulation angle, β, was calculated from the derivative of $h_{(d)}$ with respect to the projected length, d.

Following the calculation of laminae properties using micromechanical models, properties are transformed into the y-direction for all regions except matrix-only regions.

Transformations of the non-undulating regions were done using Equation (6) [16];

$$\left[\bar{Q}\right] = [T_\theta]^{-1}[Q][T_\theta]^{-T} \tag{6}$$

$[Q]$ and $\left[T_\theta\right]$ matrices of Equation (6) are given by:

$$[Q]=\begin{bmatrix} \dfrac{E_{11}}{1-\nu_{12}\nu_{21}} & \dfrac{E_{11}\nu_{21}}{1-\nu_{12}\nu_{21}} & 0 \\ \dfrac{E_{11}\nu_{21}}{1-\nu_{12}\nu_{21}} & \dfrac{E_{22}}{1-\nu_{12}\nu_{21}} & 0 \\ 0 & 0 & G_{12} \end{bmatrix} \tag{7}$$

$$[T_\theta]=\begin{bmatrix} \cos^2\theta & \sin^2\theta & 2\sin\theta\cos\theta \\ \sin^2\theta & \cos^2\theta & -2\sin\theta\cos\theta \\ -\sin\theta\cos\theta & \sin\theta\cos\theta & \cos^2\theta-\sin^2\theta \end{bmatrix} \tag{8}$$

Similarly, stiffness matrices ($\left[\bar{Q}_u\right]$) of regions 10 to 13, i.e. undulating regions, were calculated using Equations (9) and (10) [16, 17, 21];

$$\left[\bar{Q}_u\right]=[T_\theta]^{-1}[Q_{(\beta)}][T_\theta]^{-T} \tag{9}$$

$$\left[Q_{(\beta)}\right] = \begin{bmatrix} E_{\phi(\beta)} / D_v & E_{y(\beta)}\nu_{21(\beta)} / D_v & 0 \\ E_{y(\beta)}\nu_{21(\beta)} / D_v & E_{y(\beta)} / D_v & 0 \\ 0 & 0 & G_{12(\beta)} \end{bmatrix}$$

$$E_{\phi(\beta)} = 1 / \begin{bmatrix} (\cos^4 \beta / E_{11}) \\ + \left[(1 / G_{13} - 2\nu_{31} / E_{11}).(\cos^2 \beta . \sin^2 \beta)\right] \\ + (\sin^4 \beta / E_{33}) \end{bmatrix} \qquad (10)$$

$$\nu_{21(\beta)} = E_{\phi(\beta)}\left[\nu_{31} \cos^2 \beta / E_{11} + \nu_{23} \sin^2 \beta / E_{33}\right]$$

$$G_{12(\beta)} = \left[\cos^2 \beta / G_{12} + \sin^2 \beta / G_{23}\right]^{-1}$$

$$E_{y(\beta)} = E_{22} = E_{33}$$

$$D_v = 1 - \left[(\nu_{21(\beta)})^2 E_{22} / E_{\phi(\beta)}\right]$$

If the unit cell is divided into small finite intervals, it was assumed that each of these intervals is tangent to the mandrel; therefore, other than the ones listed above, the undulating and non-undulating regions do not need any additional transformation to match the unit cell curvature.

Earlier, the Classical Laminate Plate Theory (CLPT) was modified for woven structures, Raju and Wang, [17], and it was generalized for braided structures, Carey et al., [16], to predict the elastic constants. These works were

taken as a base for the proposed model. The general equation of the CLPT can be written as:

$$\begin{Bmatrix} N \\ M \end{Bmatrix} = \begin{bmatrix} [A^*] & [B^*] \\ [B^*] & [D^*] \end{bmatrix} \begin{Bmatrix} \varepsilon^0 \\ k^0 \end{Bmatrix} \tag{11}$$

where volume weighted matrices are defined as:

$$[A^*, B^*, D^*] = \frac{1}{P_A} \sum_{n=1}^{13} [A, B, D]_n \tag{12}$$

where A, B and D are the well known extensional stiffness, coupling stiffness, and bending stiffness matrices, respectively. P_A is the projected cross sectional area of the unit cell onto the mandrel surface. The A, B and D matrices are defined and calculated separately for the thirteen regions of the unit cell using the general Equation (13).

$$\begin{aligned} [A] &= \int_{\phi} \left(\int_{y} \left(\int_{r} \left[\bar{Q} \right] dr \right) dy \right) d\phi \\ [B] &= \int_{\phi} \left(\int_{y} \left(\int_{r} \left[\bar{Q} \right] r dr \right) dy \right) d\phi \\ [D] &= \int_{\phi} \left(\int_{y} \left(\int_{r} \left[\bar{Q} \right] r^2 dr \right) dy \right) d\phi \end{aligned} \tag{13}$$

Here, as an example, formulae used for the calculations of Region 1 is provided via Equations 14 to 16. These equations provide a more detailed look at Equation (13), where $[Q_{c(\theta)}]$, $[Q_{c(-\theta)}]$ and $[Q_m]$ are the stiffness matrices for $+\theta$ strand ply, $-\theta$ strand ply, and matrix ply, respectively. The integration limits for equations 14 to 16 are provided in Table 3.1 as an example for Region 1. The limits, i.e. *a* to *j*, are derived from the geometrical boundaries of Region 1 as seen in Figure 3.4.

$$[A]=\int_b^a\left(\int_d^c\left(\left[\int_f^e[Q_{c(-\theta)}]dr\right]+\left[\int_h^g[Q_{c(\theta)}]dr\right]+\left[\int_j^i[Q_m]dr\right]\right)dy\right)d\phi \tag{14}$$

$$[B]=\int_b^a\left(\int_d^c\left(\left[\int_f^e[Q_{c(-\theta)}]rdr\right]+\left[\int_h^g[Q_{c(\theta)}]rdr\right]+\left[\int_j^i[Q_m]rdr\right]\right)dy\right)d\phi \tag{15}$$

$$[D]=\int_b^a\left(\int_d^c\left(\left[\int_f^e[Q_{c(-\theta)}]r^2dr\right]+\left[\int_h^g[Q_{c(\theta)}]r^2dr\right]+\left[\int_j^i[Q_m]r^2dr\right]\right)dy\right)d\phi \tag{16}$$

Table 3.1: Limits of the integrals for Equations 14 to 16.

Integration limits		Integration limits	
a	$L\sin\theta$	**f**	$-\left(\frac{r_m - r_{in}}{2}\right)$
b	0	**g**	$-\left(\frac{r_m - r_{in}}{2}\right)+\left(r_- - r_{in}\right)+\left(r_+ - r_-\right)$
c	$y_A = -\left(r_{in}\phi\right)\tan\gamma + L\cos\theta$	**h**	$-\left(\frac{r_m - r_{in}}{2}\right)+\left(r_- - r_{in}\right)$
d	0	**i**	$\left(\frac{r_m - r_{in}}{2}\right)$
e	$-\left(\frac{r_m - r_{in}}{2}\right)+\left(r_- - r_{in}\right)$	**j**	$-\left(\frac{r_m - r_{in}}{2}\right)+\left(r_- - r_{in}\right)+\left(r_+ - r_-\right)$

Remaining eight regions (i.e. regions 2 to 9) can be derived following the same procedure described. For undulating regions (i.e. regions 10 to 13), Gauss-Legendre numerical integration method was used with n=10 as data was not changing after the tenth order.

The elastic constants of the curved unit cell are determined using the inverse of the overall stiffness matrix of Equation (11) as outlined in Equations 17 and 18 [16, 22], where *t* is the thickness of the unit cell and assuming in plane loading:

$$\begin{bmatrix} [A^*] & [B^*] \\ [B^*] & [D^*] \end{bmatrix}^{-1} = \begin{bmatrix} a & b \\ b & d \end{bmatrix} \tag{17}$$

$$\begin{aligned} E_\phi &= ((a_{1,1})(t))^{-1} \\ E_y &= ((a_{2,2})(t))^{-1} \\ \nu_{\phi,y} &= -a_{1,2} / a_{1,1} \\ G_{\phi y} &= ((a_{3,3})(t))^{-1} \end{aligned} \tag{18}$$

3.3. Results

In this section, the proposed "curved model" is first compared to other models available in the literature. Then, it is validated using experimental data available in the literature and in-house experimental results.

Table 3.2: Yarn and resin properties used by Naik, R.A. (1996) [adopted from [13]].

	E_{11} (GPa)	E_{22} (GPa)	G_{12} (GPa)	ν_{12}	ν_{23}
Hercules 3501-6 epoxy	3.45	3.45	1.28	0.35	0.35
AS4 graphite yarn	144.8	11.73	5.52	0.23	0.30

Note: *E*, *G*, and *v* are used for Elastic Modulus, Shear Modulus, and Poisson's ratio, respectively. Directions *1*, *2*, and *3* indicate longitudinal, transverse, and thickness directions, respectively.

Naik, R.A. (1996) published a study that included stiffness prediction of two dimensionally braided composites [13]. The model was implemented in a personal-computer based code, TEXCAD. Naik used AS4 graphite fibers and Hercules 3501-6 epoxy matrix for the analysis. Table 3.2 outlines the yarn and matrix elastic properties used by Naik (1996). Yarn width and yarn thickness were 1.411 mm and 0.09 mm, respectively. Results of Naik,, which were read off a graph, are compared with the proposed model (Figure 3.5) [13]. During the prediction, the curvature of the unit cell was set to be near infinite to omit the effects of curvature and to properly compare the results to that of Naik's flat cell model. This was done by setting the radius of curvature for the curved model to near relative infinity using a 500 mm diameter (as the model becomes insensitive to the changes in radius at this radius, i.e. infinite radius).As can be seen in Figure 3.5, the two models are in agreement. This gives confidence to the results of the proposed model for flat braided structures (i.e. infinite radius of curvature).

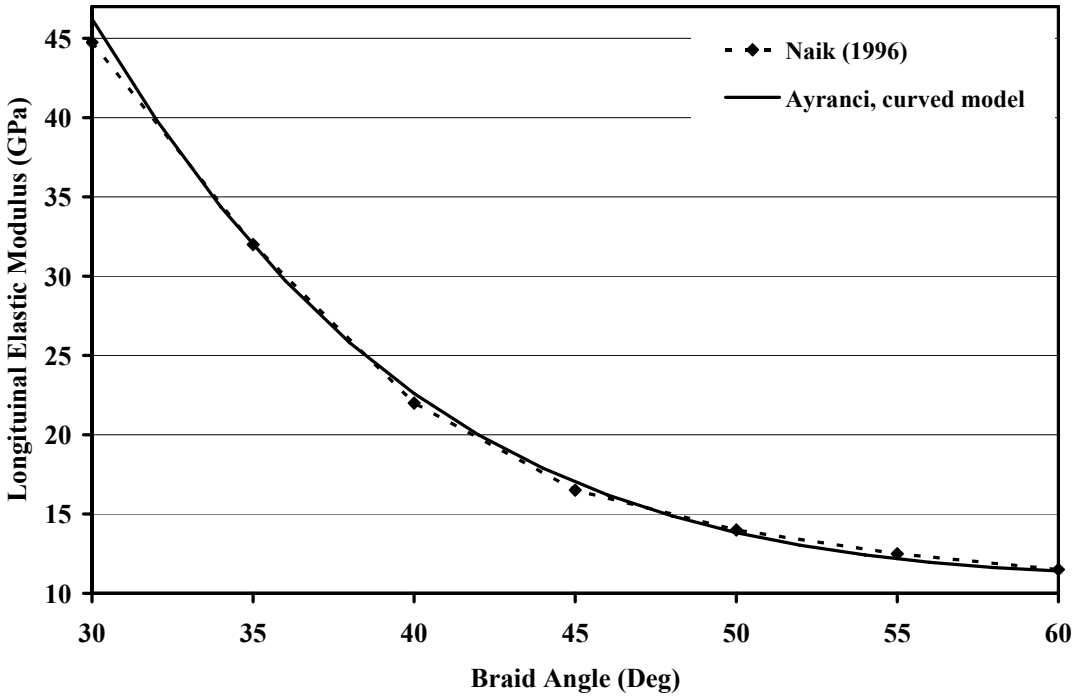

Figure 3.5: Comparison of results of the proposed study (with infinite radius) to that of Naik, R.A. (1996) [13]. Line is used for Naik data for visual purposes of overlapping trends only.

Table 3.3: Elastic properties used for Figures 3.6 and 3.7, respectively (data adopted from Carey et al. (2003), [16], for direct comparison purposes).

	E_{11} (GPa)	E_{22} (GPa)	G_{12} (GPa)	ν_{12}	ν_{23}
AS4 fiber	228	40	24	0.26	0.1
Epoxy Resin	4.2	4.2	1.62	0.3	0.3

Figure 3.6 presents the effect of curvature for a case presented by Carey et al. [16]. Yarn width and yarn thickness for this case were taken as 3.14 mm and 0.16 mm, respectively. The unit cell was composed of AS4 carbon fibers, and epoxy polymer resin matrix; the specific name of the epoxy was not provided, only the properties were listed. The fiber volume fraction of the yarns was taken as 0.43. The elastic properties, (Table 3.3), used for the calculations, are adopted from Carey et al. for direct comparison purposes with the results. Figure 3.6 presents the predictions for the flat model versus curved model. Curved unit cell results were obtained by setting the radius of curvature as 10 mm. Due to the relatively thin strand thickness assumed by Carey et al., 0.16 mm, the predicted effects of curvature had only approximately 1.6% difference in results compared to the flat unit cell model. It is difficult to visualize the difference for the given 30 to 60 degrees braid angle range, in Figure 3.6; therefore, an inset image zooming-in between 30 to 34 degrees braid angles was added, highlighting the small difference between the models. Although one might argue that a difference of 1.6% is not significant, this is due to the very small strand thickness of the investigated case of Carey et al. Using a different case study in which every parameter above is maintained with the exception of the strand thickness, which is increased to 0.5 mm, this effect is more noticeable. Results are presented in Figure 3.7; the effect of curvature becomes much more pronounced as the strand thickness increased, leading to a difference between predictions of the flat- and curved-unit cell of 4.7%. During the design of braided tubular products, such as

medical catheters, 4.7% difference in predictions may offer additional valuable tailorability in the design parameters and prevent critical arterial damage.

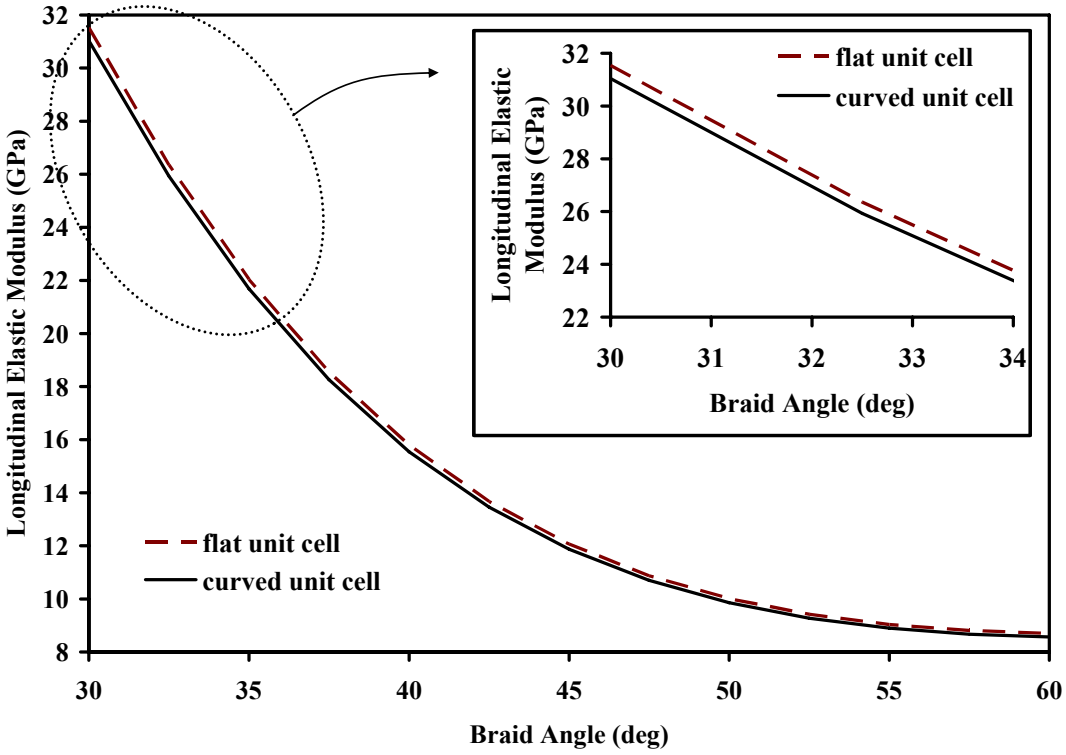

Figure 3.6: Effect of curvature on Carey et al.'s prediction, [16], for hc = 0.16mm (inner figure is a zoomed-in section).

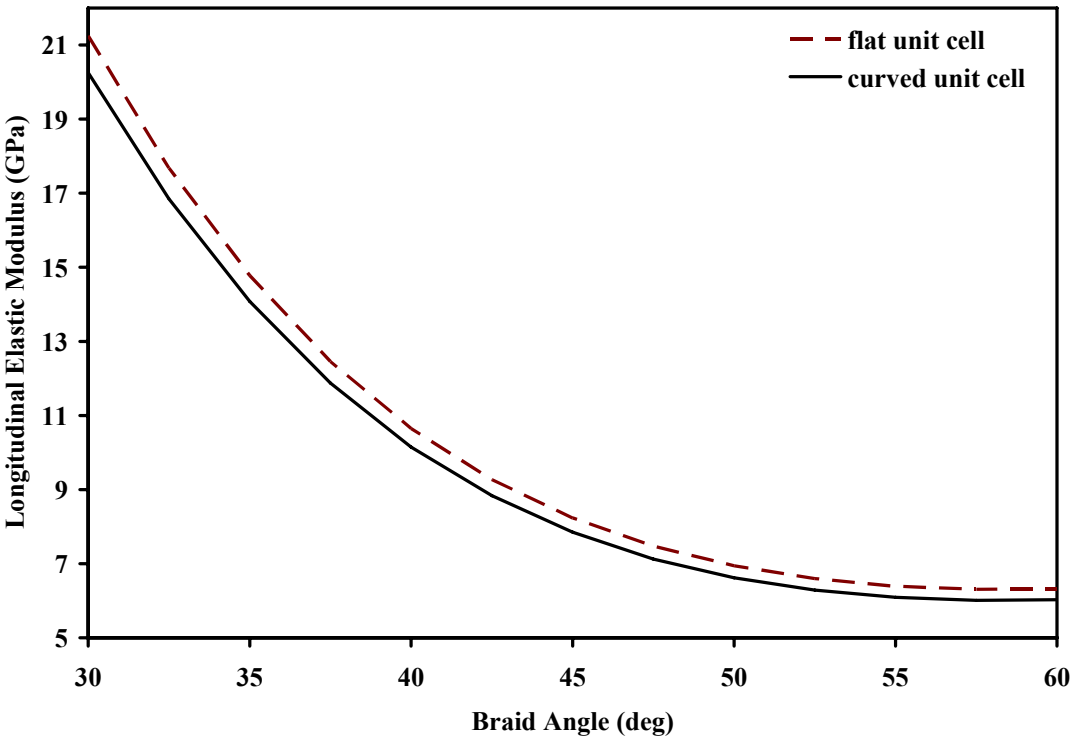

Figure 3.7: Effect of curvature on Carey et al.'s, [16], prediction for hc= 0.5mm.

Table 3.4: Elastic properties used in the calculations for Figure 3.8.

	E_{11} (GPa)	E_{22} (GPa)	G_{12} (GPa)	ν_{12}	ν_{23}
Epon 825 – Ancamine 1482	3.5	3.5	1.35	0.3	0.3
Kevlar 49 fiber	130	7.3	2.86	0.35	0.1

Kevlar 49 – Epoxy Lamina (Experimental properties based on Flanagan and Munro (1986) [24])	79.7	5.9	1.5	0.33	-

The proposed model has also been compared to the experimental findings of Carey et al. and in-house experiments for validation purposes. Carey et al. reported experimental longitudinal elastic modulus findings of 42.5 and 50 degree braided composite tubes. The specimens were braided on 11.1 mm and 12.7 mm outer diameter mandrels. The properties of the materials used for the specimens are tabulated in Table 3.4 [16]. The unit cells for the specimens were reported to have a strand width and thickness of 3.1 mm and 0.38 mm, respectively [23]. Using these values, flat model of Carey slightly over-predicted the results [16]. The experimental longitudinal modulus was reported as 6.3 GPa (±0.11 standard deviation) and 4.7 GPa (±0.085 standard deviation) for 42.5 and 50 degrees braid angles, respectively. Results of the experimental findings, flat-unit cell, and the curved unit cell for the diameters reported in the said study are plotted in Figure 3.8. The over-prediction of the flat unit cell model is clearly seen; however, the predictions for the two different diameters of the curved unit cell are in much better agreement with the reported experimental results. The percent difference, for the 42.5° braid angle, between the experiments versus flat-model and the experiments versus the curved model were, 8.10% and 2.41%, respectively.

Similarly, the percent difference, for the 50° braid angle, between the experiments versus flat-model and the experiments versus the curved model were, 4.33% and 2.37%, respectively.

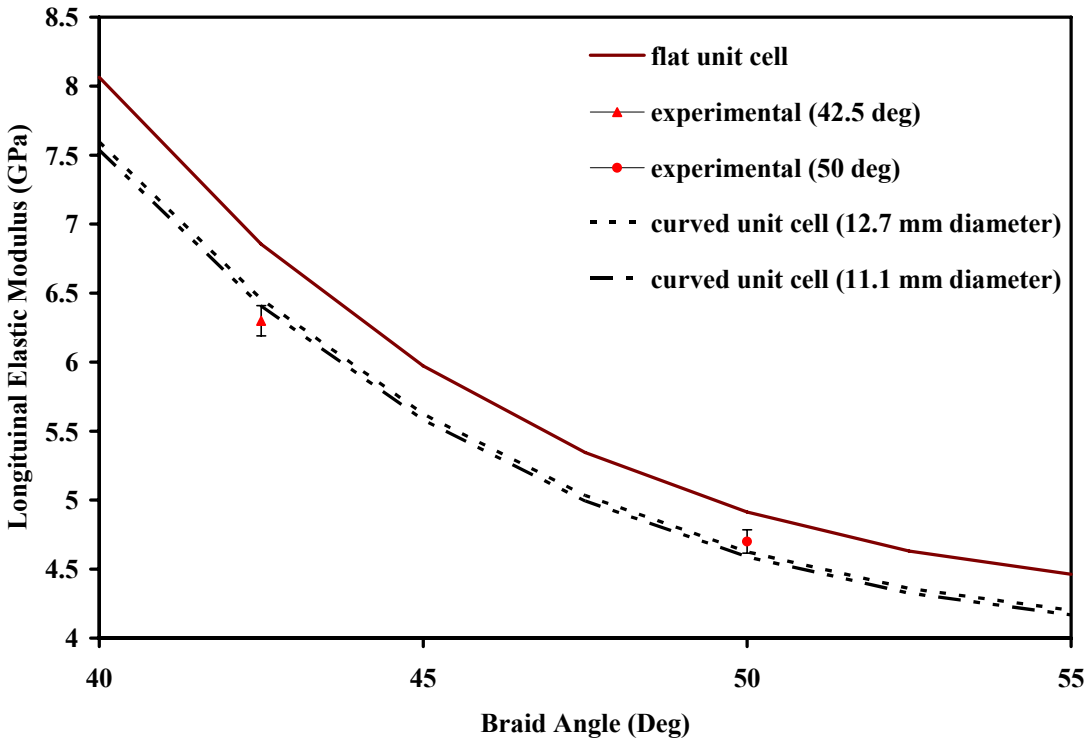

Figure 3.8: Comparison of the curved and flat model for Carey et al.'s experimental results [16, 23].

In house experiments for three different diameter braided tubular specimens were also conducted to validate the proposed curved-unit cell predictive model. Kevlar 49 fiber and Epon 825/Ancamine 1482 curing agent matrix system (Table 3.4) was used in preparation of the specimens. The curing cycle of the composites is detailed by Munro and Flanagan [24]. Three different size Teflon-mandrels were used for the specimens. Teflon-mandrels enabled easy

removal of the cured specimens from the mandrel. Specimens were tested using a MTS-810 testing machine (MTS Systems Corporation Eden Prairie, MN, USA) along with a 25.4 mm (1-inch) gage length extensometer (MTS 634.12E-24). During the experiments 1 mm/min loading rate was used to obtain a failure of the specimen within 1 to 10 minutes (ASTM D 3039/D 3039M – 08).

For ease of discussion, in this text, the specimens are referred to as KLTE (Kevlar - Large diameter - Tensile test specimen), KMTE (Kevlar -Medium diameter - Tensile test specimen), and KSTE (Kevlar - Small diameter - Tensile test specimen). Table 3.5 lists the geometric measurements taken from the specimens as well as the number of specimens tested for each diameter. Braid angle was measured by wrapping transparent paper on the specimens to trace the yarn paths using a marker and measuring the angle using a protractor. Measurements were taken for five different yarns to obtain a standard deviation.

Table 3.5: Geometric measurements of the specimens used for validation.

	Number of Specimens	**Braid Angle (θ, deg) (±Standard Deviation)**	**Strand width W_y (mm) (±Standard Deviation)**	**Outer Diameter OD, (mm) (±Standard Deviation)**	**Thickness t (mm) (±Standard Deviation)**
KLTE	5	54.1 (±0.5)	1.99 (±0.06)	10.22 (±0.05)	0.28 (±0.01)
KMTE	5	51.4 (±0.7)	1.85 (±0.03)	8.61 (±0.05)	0.30 (±0.13)
KSTE	5	48.1 (±0.9)	1.74 (±0.07)	7.14 (±0.01)	0.30 (±0.01)

Figure 3.9 shows the longitudinal elastic modulus values for the KLTE, KMTE, and KSTE specimens and includes experimental results and corresponding curved-model prediction results for the dimensions listed in Table 3.5. The error bars in the figure refer to standard deviations in the case of experimental findings, and to upper and lower predictions in the case of the curved model. The predictions for the curved model were obtained for the average values of the geometrical measurements for the unit cell. The upper and lower value predictions for the curved unit cell were obtained using one standard deviation above and one standard deviation below the average unit cell measurements, respectively. Very good agreement between the experiments and predictions can be observed.

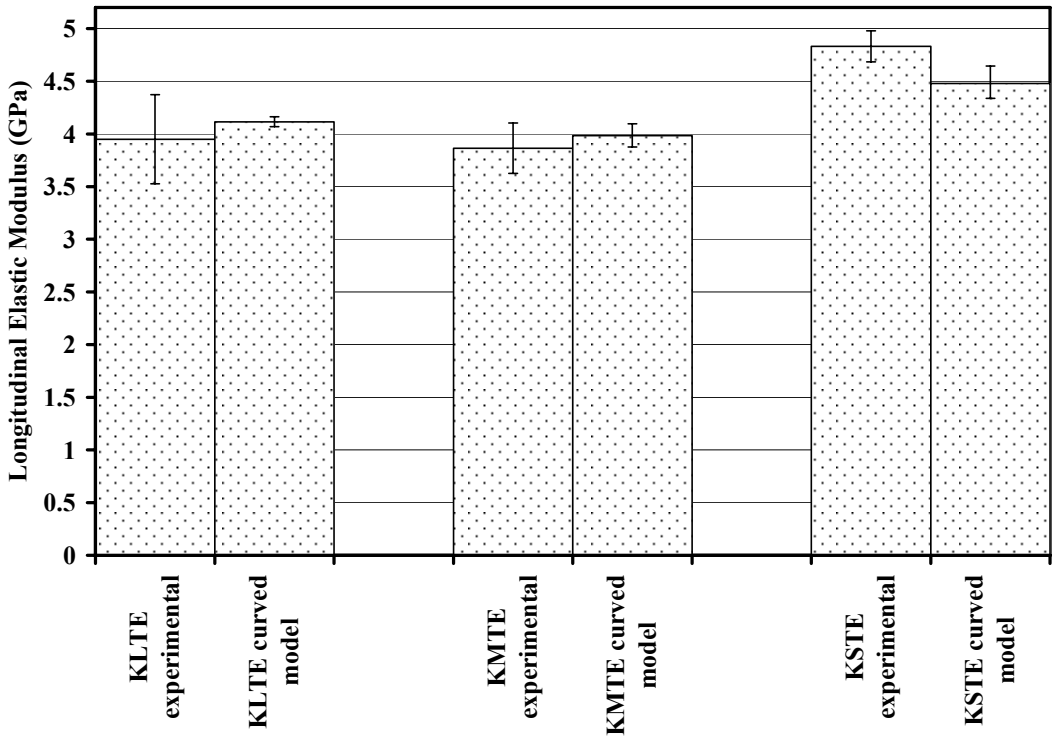

Figure 3.9: Experimental and corresponding curved model prediction results of KLTE, KMTE, and KSTE specimens. (Error bars indicate the standard deviations for the experimental results and upper/lower predictions in the curved model results.)

For KLTE specimens, average experimental longitudinal elastic modulus was found as 3.95 GPa (± 0.42 Standard Deviation) whereas the curved model predicted 4.12 GPa. Predicted value falls within the spread of standard deviation of the experimental finding; hence, the results are in very good agreement.

For KMTE specimens, average experimental longitudinal elastic modulus was found as 3.87 GPa (± 0.24 Standard Deviation) whereas the curved model

predicted 3.98 GPa. Predicted value falls within the spread of standard deviation of the experimental finding hence the results are in very good agreement.

For KSTE specimens, average experimental longitudinal elastic modulus was found as 4.83 GPa (± 0.15 Standard Deviation) whereas the curved model predicted 4.48 GPa. The upper level prediction from the model for KSTE is 4.64 GPa. The lower value of the experimental finding of 4.68 GPa (i.e. 4.83-0.15 = 4.68) and the upper level prediction of the curved model (4.64 GPa) has only 0.85% difference, which is an excellent agreement.

The effect of radius of curvature observed on the longitudinal elastic modulus values are similarly observed in shear modulus predictions and are currently being verified using experiments.

3.4. Conclusions

This paper outlines the development and validation of an analytical model to predict the longitudinal elastic modulus of two-dimensionally braided tubular composites.

1. The analytical model recognizes the effects of curvature on the unit cell via the thicknesses of the braided yarns to predict the properties.
2. The model was first compared to the available flat models in the literature by setting the radius of curvature of the proposed unit cell large enough to prevent the effect of curvature to obtain comparable results.
3. Effects of the tube curvature on the predicted elastic modulus were evaluated; the flat and curved models showed 1.6% and 4.7% differences

in the predictions for strand thicknesses of 0.16 mm and 0.5 mm, respectively.

4. In the final step, the curved model findings were compared to reported experimental findings in the literature and in-house experiments and excellent results were obtained.
5. The findings of this work are a valuable tool for design of medical equipment manufactured using two-dimensional braiding.

3.5. References

[1] Sanders, L. R., Braiding - A Mechanical Means of Composite Fabrication. SAMPE Q (Society of Aerospace Material and Process Engineers), 1977; 8(2) pp. 38-44.

[2] Carey, J., Fahim, A., Munro, M., Design of braided composite cardiovascular catheters based on required axial, flexural, and torsional rigidities, Journal of Biomedical Materials Research - Part B Applied Biomaterials; 2004; 70 (1), 73-81.

[3] Irsale, S., Adanur, S., Design and characterization of polymeric stents, Journal of Industrial Textiles, 2006; 35 (3), pp. 189-200.

[4] Fujihara, K., Teo, K., Gopal, R., Loh, P.L., Ganesh, V.K., Ramakrishna, S., Foong, K.W.C., and Chew, C.L., Fibrous Composite Materials in Dentistry and Orthopaedics: Review and Applications, Composites Science and Technology, 2004; 64(6) pp. 775-788.

[5] Ayranci, C., Carey, J. 2D braided composites: A review for stiffness critical applications, Composite Structures, 2008; 85 (1), pp. 43-58.

[6] Falzon, P.J., Herszberg, I., Baker, A.A., Stiffness Analysis of Textile Composites, National Conference Publication - Institution of Engineers, Australia 1 (93 pt 6), 1993; pp. 219-224.

[7] Ishikawa, T., Chou, T-W., Stiffness and Strength Behavior of Woven Fabric Composites, Journal of Materials Science, November 1982, Vol. 71, No. 11, 3211-3220.

[8] Redman, C., J., Douglas, C. D., Theoretical Prediction of the Tensile Elastic Properties of Braided Composites, 38th International SAMPE Symposium, May 10-13, 1993, 719-727.

[9] Soebroto, H. B., Hager, T., Pastore, C. M., Ko, F. K., Engineering Design of Braided Structural Fibreglas Composites, 35th International SAMPE Symposium, April 2-5, 1990, 687-696.

[10] Byun, J.-H., The analytical characterization of 2-D braided textile composites, Composites Science and Technology, 2000; 60 (5), 705-716.

[11] Huang, Z.M., The mechanical properties of composites reinforced with woven and braided fabrics, Composites Science and Technology, 2000; 60 (4), 479-498.

[12] Aggarwal, A., Ramakrishna, S., Ganesh, V.K., Predicting the in-plane elastic constants of diamond braided composites, Journal of Composite Materials, 2001; 35 (8), 665-688.

[13] Naik, R.A., Analysis of woven and braided fabric-reinforced composites, ASTM Special Technical Publication 1274, 1996, 239-263.

[14] Naik, R. A., Ifju, P. G., Masters, J. E., Effect of fiber architecture parameters on deformation fields and elastic moduli of 2-D braided composites, Journal of Composite Materials, 1994; 28 (7), 656-681.

[15] Huang, Z.-M., Fujihara, K., Ramakrishna, S., Tensile stiffness and strength of regular braid composites: Correlation of theory with experiments, Journal of Composites Technology and Research, 2003; 25 (1), 35-49.

[16] Carey, J., Munro, M., Fahim, A., Longitudinal elastic modulus prediction of a 2-D braided fiber composite, Journal of Reinforced Plastics and Composites, 2003; 22 (9), pp. 813-831.

[17] Raju, I.S., Wang, J.T., Classical laminate theory models for woven fabric composites, Journal of Composites Technology and Research, 1994; 16 (4), 289-303.

[18] Potluri, P., Manan, A., Francke, M., Day, R.J., Flexural and torsional behaviour of biaxial and triaxial braided composite structures, Composite Structures, 2006; 75 (1-4), pp. 377-386.

[19] Potluri, P., Manan, A., Mechanics of non-orthogonally interlaced textile composites, Composites Part A: Applied Science and Manufacturing, 2007, 38 (4), pp. 1216-1226.

[20] Ayranci C, Carey J., Elastic constants of braided thick-walled tubular composites, The sixth Canadian-international composites conference (CANCOM 2007), August 14-17 2007, Winnipeg, Manitoba, Canada.

[21] Yang, J. M., Ma, C. L., Chou, T.W-., Elastic Stiffness of Biaxial and Triaxial Woven Fabric Composites, 29th National SAMPE symposium, April 3-5, 1984, 292-303.

[22] Tsai, S.W., Hahn, H.T., Introduction to Composite Materials, Westport, CT: Technomic Publishing Co., Inc., 1980.

[23] Carey, J., Axial, flexural and torsional rigidities of two-dimensional braided fibre composite medical catheters, Ph.D. thesis, University of Ottawa (Canada), 2003, 222 pages.

[24] Flanagan, R.C. and Munro, M., High Energy Density Fibre Composite Rotors, Vol. 2, (1986), Department of Mechanical Engineering, University of Ottawa, Technical Report No UOME-FP-8603-1.

CHAPTER 4: EFFECT OF DIAMETER IN PREDICTING THE ELASTIC PROPERTIES OF 2D BRAIDED TUBULAR COMPOSITES

A version of this chapter was submitted to Journal of Composite Materials and was accepted for publication on 08 March 2010:

The paper was co-authored by: Cagri Ayranci, Jason P Carey

4.1. Introduction

Braided composites have been increasingly used to replace other materials due to their intrinsic advantages. Some applications are stiffness critical; hence, analytical and numerical models have been proposed to predict elastic properties, many of which were discussed in a review article detailing the literature until 2007, [1], and in more recent works [2 - 5].

Some have conducted parametric studies to determine the effects of constituents and geometric characteristics on elastic properties, identifying braid angle (θ), yarn aspect ratio (i.e. ratio of yarn width (W_y) to thickness (t)) , undulating yarn length (a_u), and variation in fiber and resin properties [6 - 11] as critical. All of the analytical work published in this field have studied or assumed flat unit cell braided composites. Although this may be a valid assumption for flat and tubular braided composites with large diameters, it is crucial to understand the effects of change in diameter on the properties for large and small diameter tubes.

An analytical model that recognizes the effects of mandrel diameter on the elastic constants of two-dimensionally braided tubular composites was developed and detailed in [12]. The model uses a curved unit cell to predict elastic constants where the radius of curvature of the curved unit cell is directly related to the mandrel diameter.

This paper outlines the extent of unit cell curvature effect on the longitudinal (E_{xx}) and shear (G_{xy}) elastic moduli, and in-plane Poisson's ratio (ν_{xy}) of braided tubular composites for stiffness critical applications. The experimental verification of findings for longitudinal elastic modulus is detailed in [12]. This

paper provides a comparison between predictive and in-house experimental results of shear modulus to verify the proposed model.

4.2. Proposed model

During the manufacturing of two-dimensionally braided tubular composites, half of the spools on the braiding machine travel on a circular pattern in clockwise direction, and the remaining half travel in counter clockwise direction during which all the spools follow a Maypole-type path to create the braided preform [13]. During this process, the bottom yarn of the overlapping strand pattern deposited on the mandrel is thicker than the top yarn due to the geometry of the placement of fibers (Figure 4.1). Analytical models available in the open literature use flat unit cells, Figure 4.2, to predict elastic constants, neglecting the overlapping strand thickness difference. The proposed model uses curved unit cell geometry, Figure 4.2, to account for the effects of the radius of curvature, i.e. *r* in Figure 4.3, on the elastic properties of the unit cell [12]. Radius of curvature (*r*) depends on the mandrel size used during the braiding process, and this, in return, affects the thickness of strands deposited on a mandrel.

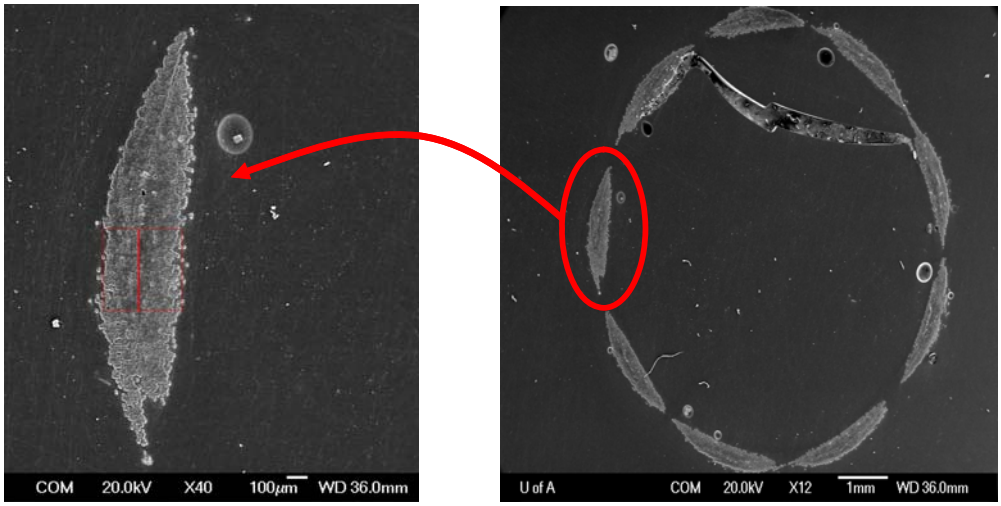

Figure 4.1: Scanning Electron Microscope (SEM) picture of a tubular braided composite. Right figure: cross-sectional view perpendicular to the longitudinal direction of the tube. Left figure: Zoomed-in view of the figure on the right, showing the differences in top and bottom yarns of a tubular braided structure.

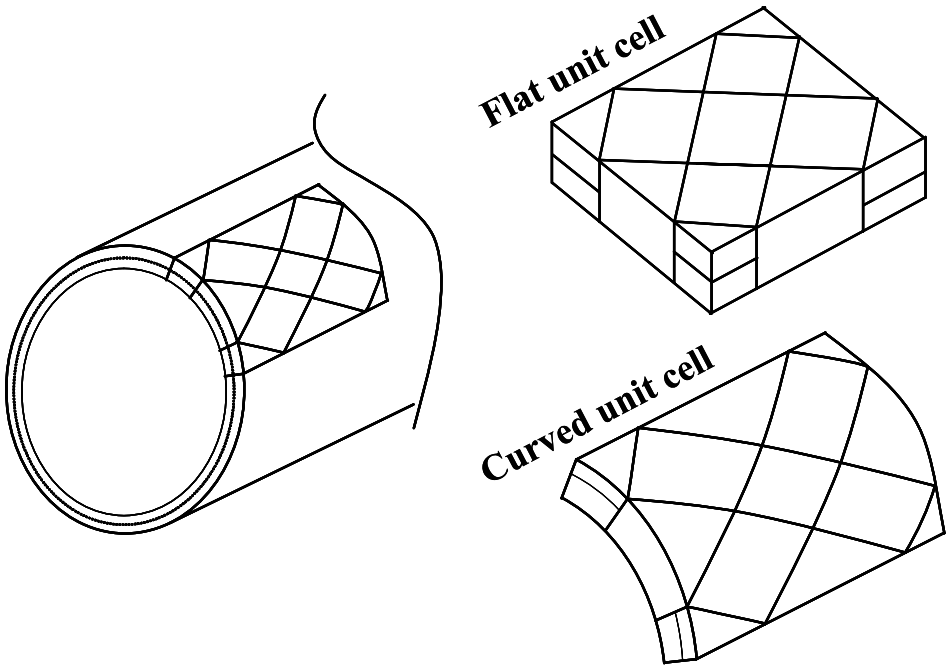

Figure 4.2: Schematic representation of a flat- and curved-unit cell.

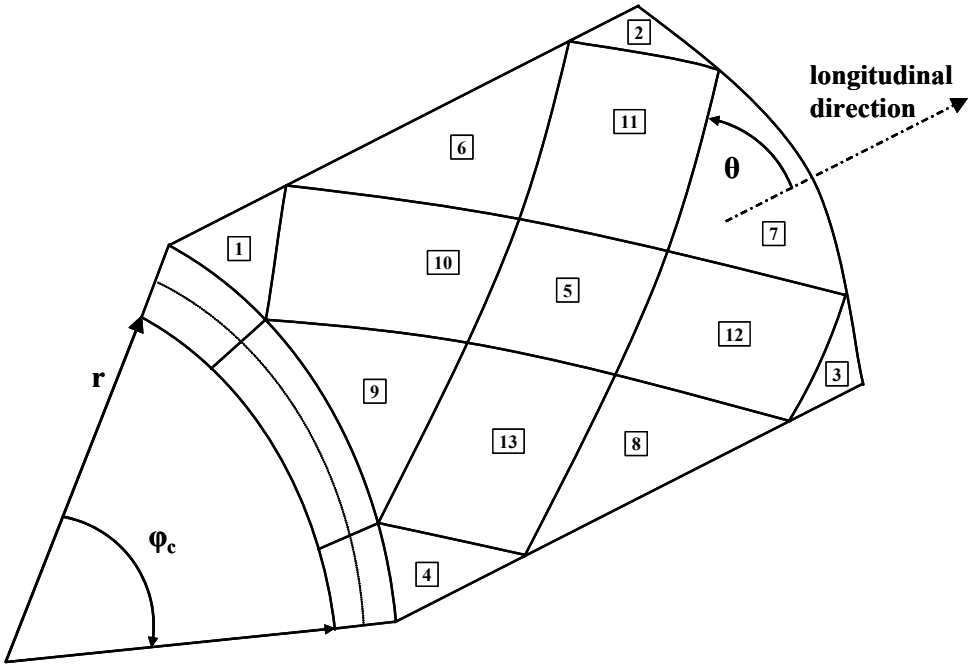

Figure 4.3: Schematic representation of a curved unit cell and the thirteen regions within the unit cell.

The unit cell is divided into three different regions (Figure 4.3), namely, crossover (regions 1-5), matrix-only (regions 6-9), and undulating (regions 10-13) regions. Similar to Raju and Wang [14] and Carey et al [15], a modified Classical Laminate Plate Theory (CLPT) is the basis of the model. Extensional stiffness, A, coupling stiffness, B, and bending stiffness matrices, D, of the three different regions are calculated separately, and then combined using a volume weighted averaging approach to obtain unit cell overall elastic constants.

In this paper, first the sensitivity of the proposed model to radius of curvature, and yarn thickness is outlined. Then, the proposed model is subjected to a literature based and experimental based verification.

4.3. Sensitivity

4.3.1. Effect of radius of curvature (Case study-1)

This study was conducted to outline the effects of unit cell curvature on elastic constants of tubular braided composites. In case study-1, only radius of curvature was varied while the remaining parameters were held constant to evaluate the effects of curvature. Yarn width and thickness were assumed 2 mm and 0.5 mm, respectively. Yarn properties used in this study are presented in Table 4.1. First, through an iterative study, for this particular case, it is found that the model becomes in-sensitive to change in curvature at a radius of curvature of 500 mm. The percent difference between the predicted results of 500 mm and 250 mm radius of curvature was found to be approximately 0.1%; therefore, a unit cell with 500 mm radius of curvature was accepted to be equivalent to a flat unit cell. Figure 4.4 shows the percent difference decrease in longitudinal elastic modulus predictions compared to the flat unit cell as a function of increase in radius of curvature. Very similar results in % difference of flat unit cell and curved unit cells is observed for shear modulus values; therefore the plot is not provided here. Figure 4.5, Figure 4.6, and Figure 4.7 outline the change in elastic properties versus braid angle as a function of radius of curvature (r) of the unit cell.

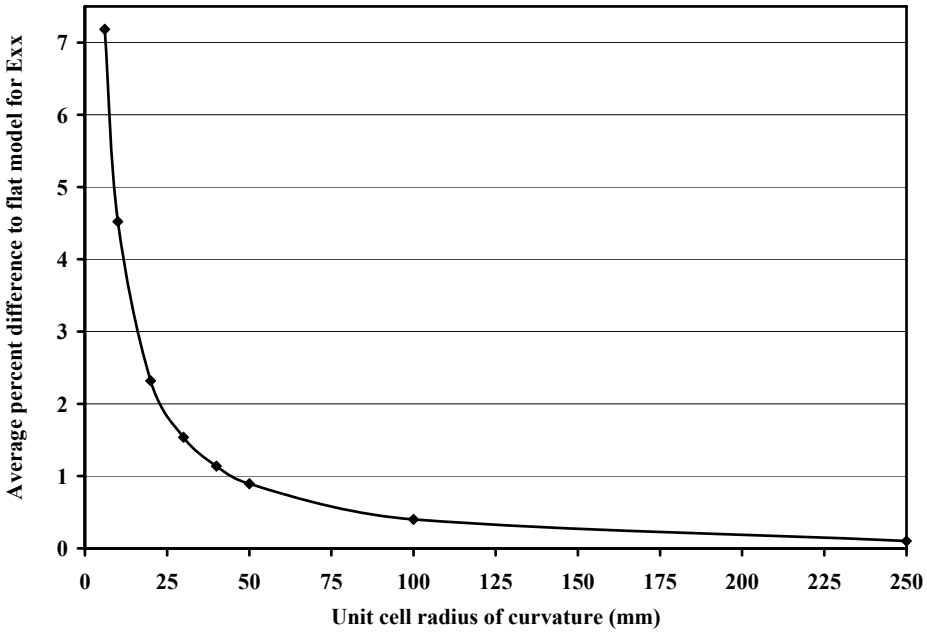

Figure 4.4: Average percent difference of flat versus curved model predictions for longitudinal elastic modulus.

Table 4.1: Elastic properties used in the calculations for Figure 4.4 to Figure 4.9.

	E_{11} (GPa)	E_{22} (GPa)	G_{12} (GPa)	ν_{12}	ν_{23}
Matrix (Epoxy Resin)	3.50	3.50	1.35	0.30	-
Yarn (Kevlar 49 – Epoxy)	79.40	5.49	2.14	0.33	0.29

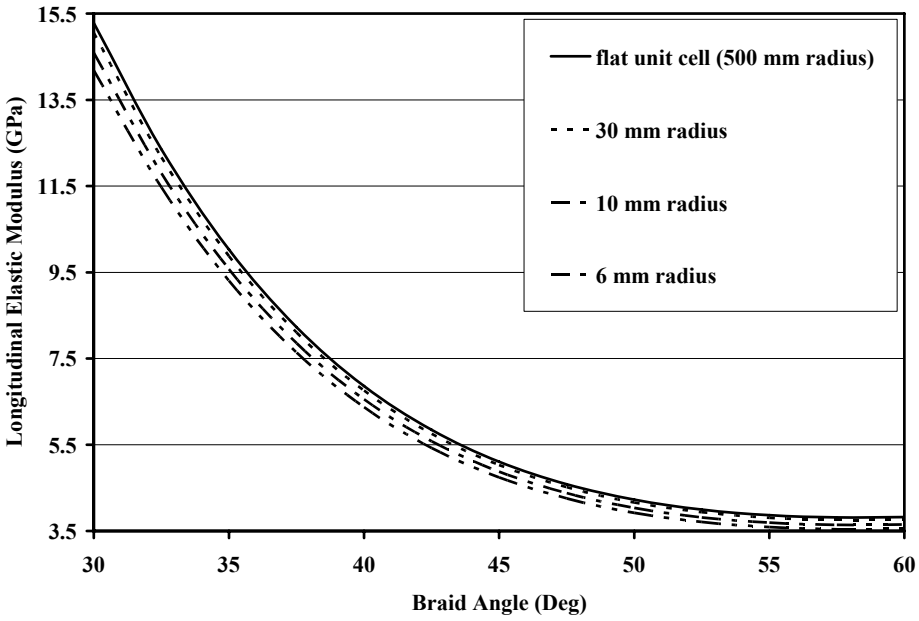

Figure 4.5: Effect of radius of curvature on longitudinal elastic modulus with respect to braid angle.

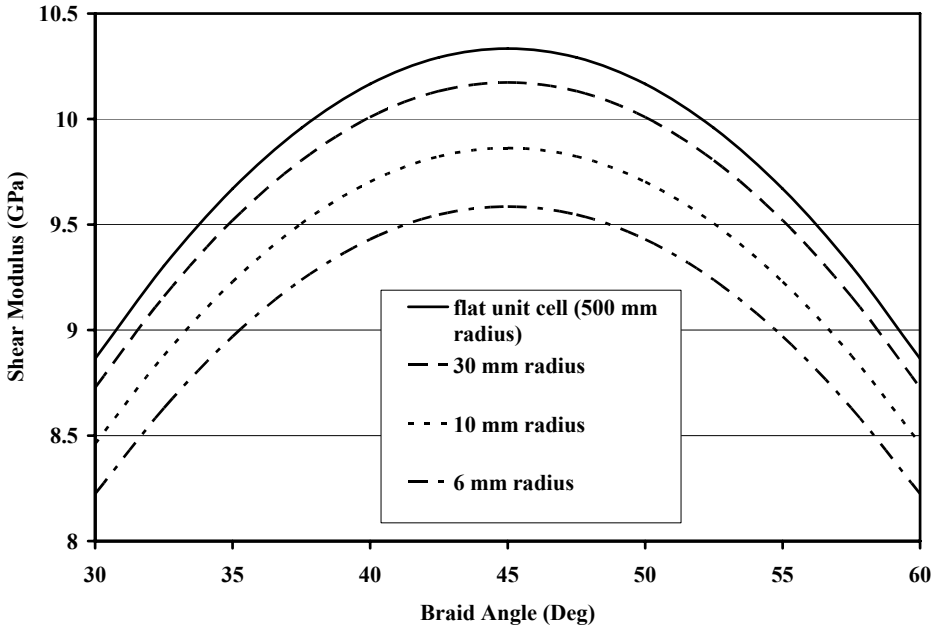

Figure 4.6: Effect of radius of curvature on shear modulus with respect to braid angle.

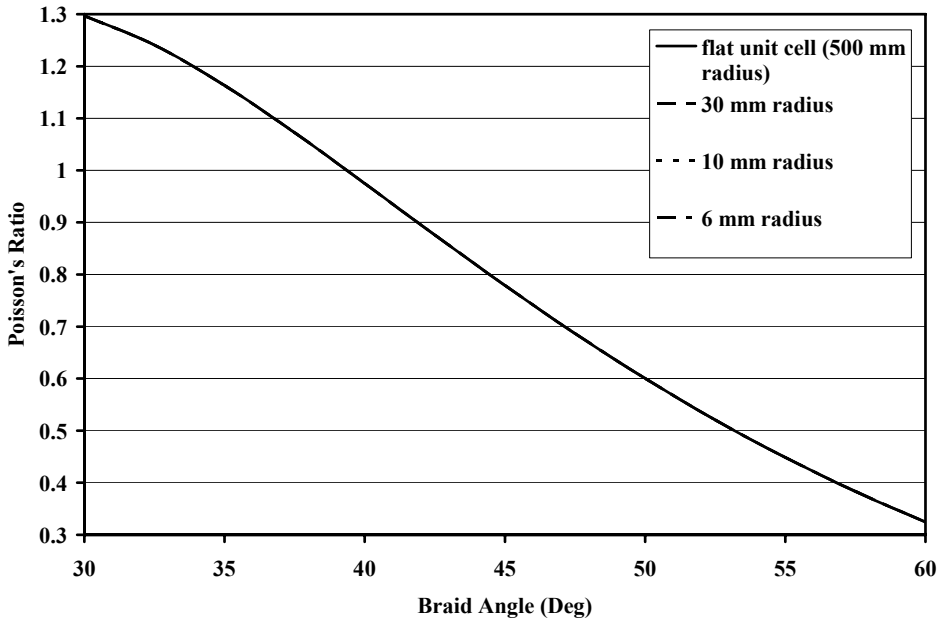

Figure 4.7: Effect of radius of curvature on Poisson's ratio with respect to braid angle (the three predictions overlap as the Poisson's ratio is insensitive to the change in unit cell curvature.).

Figure 4.5 shows the change in the longitudinal elastic modulus of two dimensionally braided structures as a function of radius of curvature. In the figure, the solid line represents flat unit cell (500 mm radius) predictions as a function of the braid angle. The remaining three dashed lines are for 30 mm, 10 mm and 6 mm radius of curvature unit cell predictions. As can be seen in the figure, as the diameter decreases the longitudinal elastic modulus decreases. For this case study, the flat and 30 mm unit cell predictions have approximately 1.54% difference throughout the braid angles 30 to 60 degrees. The effect of curvature is more pronounced as the radius decrease. This is observed as approximately 7.2% differences between the flat and 6 mm radius unit cell predictions.

Figure 4.6 shows the changes in shear modulus as a function of radius of curvature. Similar to elastic modulus results, flat, 30mm, 10 mm, and 6 mm radius unit cell predictions are plotted for angles between 30 and 60 degrees. Curved unit cell predictions with 30 mm radius are approximately 1.55% less than that of flat unit cell predictions. Differences between for the curved unit cell with 6 mm radius and the flat unit cell are approximately 7.2 % throughout the braid angle range.

Unlike the changes in the predictions of the moduli, no clear change in Poisson's ratio has been observed in any cases; predictions overlap (Figure 4.7).

4.3.2. Effect of yarn thickness (Case study-2)

It is also important to understand the effect of yarn geometry on the elastic properties; therefore, the data used for case study-1 was held constant with the exception of yarn thickness to conduct this study, which was reduced to 0.25 mm.

In case study-2, similar trends to that of case study-1 were observed. The longitudinal elastic (Figure 4.8) and shear moduli (Figure 4.9) values dropped gradually and Poisson's ratio was again insensitive as the unit cell radius of curvature was decreased from infinity to 6 mm. However, the percent differences in the predicted values were different as opposed to the first case study. The change in the longitudinal elastic (Figure 4.8) and shear modulus (Figure 4.9) values between the flat and 30 mm radius, and flat and 6 mm radius unit cell predictions were approximately 0.8% and 4%, respectively.

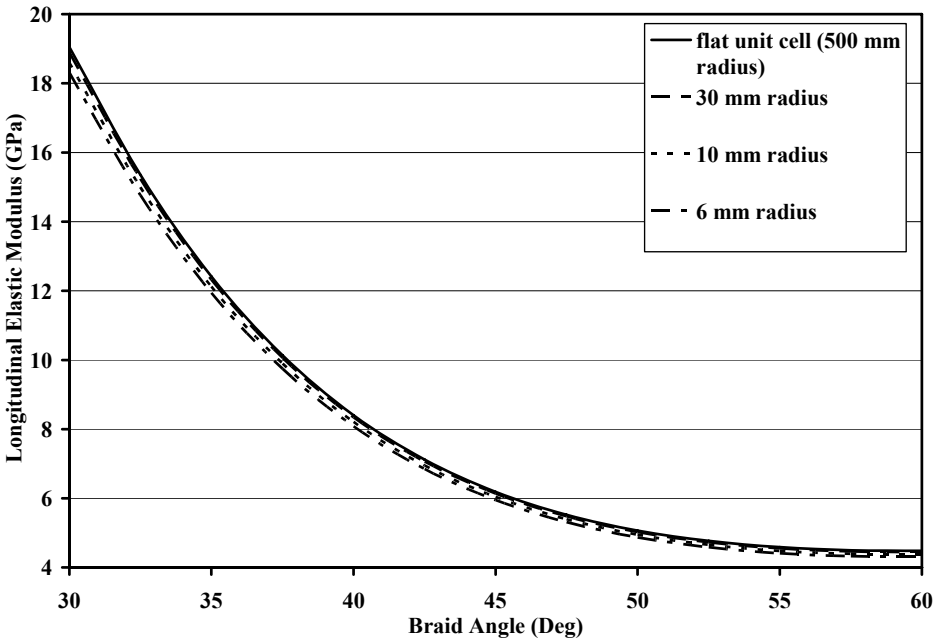

Figure 4.8: Effect of yarn thickness on longitudinal elastic modulus with respect to braid angle.

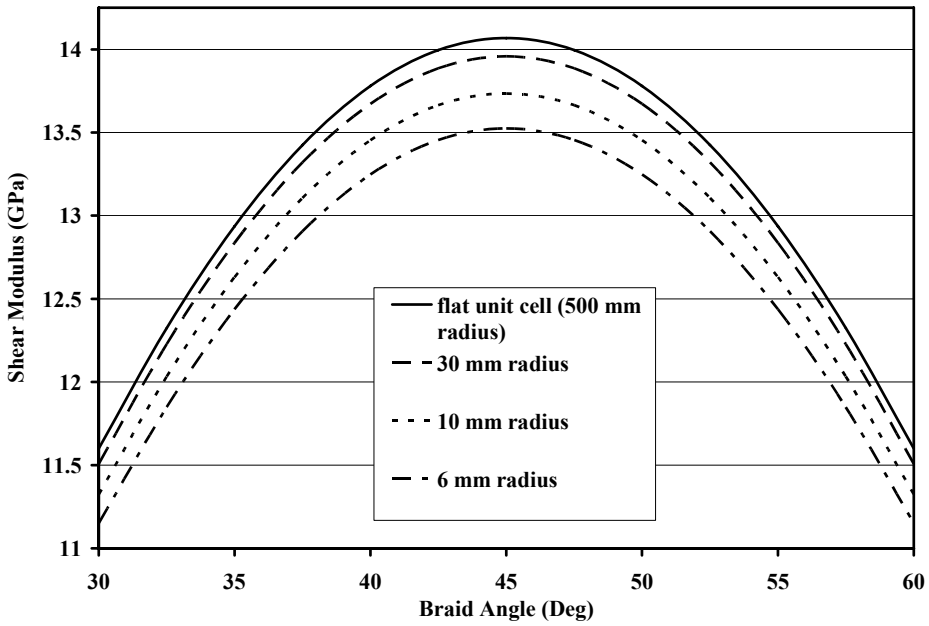

Figure 4.9: Effect of yarn thickness on shear modulus with respect to braid angle.

4.4. Literature based verification

Naik (1996) reported a study that predicts elastic constants of two-dimensionally braided composites using a flat unit cell as a function of braid angle [6]. The model was reported to be implemented in a personal-computer based code, TEXCAD. Elastic constants predictions of the proposed model are compared to Naik's findings [6] because of the clear description of the geometrical parameters used in his study allowing for a proper and repeatable comparison. These parameters were also being used in the proposed model making it easier to attempt to duplicate Naik's results using the proposed model. In the study, AS4 graphite fibers and Hercules 3501-6 epoxy matrix were used. Yarn width and thickness were chosen as 1.411 mm (provided) and 0.09 mm

(back calculated from the data provided by Naik), respectively. Table 4.2 outlines the yarn and matrix elastic properties.

Table 4.2: Properties of yarn and matrix used by Naik, R.A. (1996) [adopted from [6]].

	E_{11} (GPa)	E_{22} (GPa)	G_{12} (GPa)	ν_{12}	ν_{23}
Matrix (Hercules 3501-6 epoxy)	3.45	3.45	1.28	0.35	0.35
Yarn (AS4 graphite)	144.8	11.73	5.52	0.23	0.30

Note: Longitudinal, transverse, and thickness directions are represented by *1*, *2*, and *3*, respectively.

Naik's, results were read off a graph and presented in Figure 4.10 with the proposed model's predictions with a near infinite (r=500mm) unit cell curvature. This curvature was used as the proposed model becomes curvature independent at this radius (Figure 4.4) and thus allows for a direct comparison between models. As can be seen in Figure 4.10, elastic constants of the two models are in good agreement. A maximum difference of 4.95%, 1.62%, and 3.12% are found for E_{xx}, G_{xy}, and ν_{xy}, respectively.

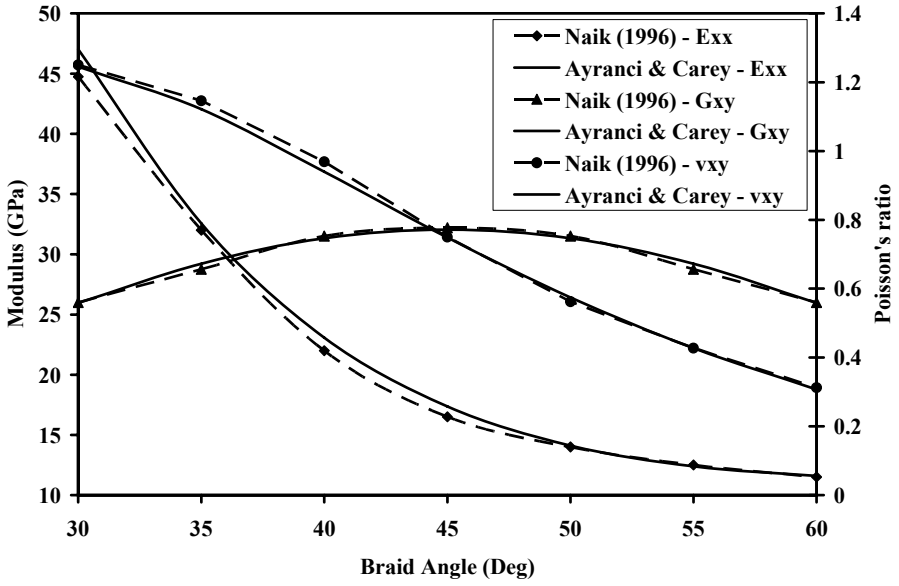

Figure 4.10: Comparison of longitudinal elastic modulus (Exx), shear modulus (Gxy), and Poisson's ratio (vxy) for the proposed model (Ayranci & Carey) versus Naik (1996).

4.5. Experimental verification

4.5.1. Methodology

Experimental verification of the model for longitudinal elastic modulus values was presented earlier [12]. The experimental results and analytical model predictions were in excellent agreement. Here, we compare and verify shear modulus predictions of the proposed curved model using in-house experiments. The experiments were conducted using three different diameter tubular braided specimens. For ease of discussion, the specimens are referred to as KLTO (Kevlar

- Large diameter - Torsion test specimen), KMTO (Kevlar -Medium diameter – Torsion test specimen), and KSTO (Kevlar - Small diameter - Torsion test specimen). Table 4.3 lists the geometric measurements taken from the specimens as well as the number of specimens tested for each diameter.

Table 4.3: Geometric measurements of the specimens used for validation.

	Number of Specimens	Braid Angle (θ, deg) (±Standard Deviation)	Strand width W_y (mm) (±Standard Deviation)	Outer Diameter OD, (mm) (±Standard Deviation)	Thickness t (mm) (±Standard Deviation)
KLTO	5	53.460 (±0.378)	1.984 (±0.050)	10.194 (±0.051)	0.285 (±0.008)
KMTO	5	51.56 0.(513±)	1.833 (±0.052)	8.591 (±0.034)	0.302 (±0.011)
KSTO	5	47.640 (±0.532)	1.773 (±0.060)	7.068 (±0.040)	0.303 (±0.011)

Epon 825/Ancamine 1482 curing agent matrix system and Kevlar 49 fibers were used in the preparation of the specimens (Table 4.4). The curing cycle reported by Flanagan and Munro, [16], was followed during the preparation. Three different sizes of Teflon mandrels were used as mandrel. Teflon was chosen for easy removal of the specimens from the mandrel after the curing process. The specimens were cut to length and attached to end fittings following the removal from the mandrels (Figure 4.11).

Table 4.4: Elastic properties used in the calculations for Figure 4.13 and specimens.

	E_{11} (GPa)	E_{22} (GPa)	G_{12} (GPa)	ν_{12}	ν_{23}
Epon 825 – Ancamine 1482	3.5	3.5	1.3	0.3	0.3
Kevlar 49 – Epoxy Lamina (Experimental properties based on [16])	79.7	5.9	1.5	0.33	-

Figure 4.11: Torsion specimens (from top to bottom: KSTO, KMTO, KLTO).

Specimens were tested under torsion loading (with compensation to assure no axial load was present) using a MTS-Torsion Master testing machine (MTS Systems Corporation Eden Prairie, MN, USA) equipped with a load cell of 2 Nm torsional load capacity (Figure 4.12). There is no specific ASTM standard for torsion testing of braided composite materials; therefore, the 0.03 degrees/second (approximately 2 degrees/minute) loading rate suggested in ASTM D 5448/D

5448M – 93 (Reapproved 2006) was followed (Standard Test Method for In-plane Shear Properties of Hoop Wound Polymer Matrix Composite Cylinders), to obtain a failure of the specimens within 1 to 10 minutes. Shear modulus of the specimens were calculated using:

$$G_{xy} = \frac{TL}{J\phi} \quad (1)$$

where *T, L, J,* and φ are applied torque, length of the specimen, polar moment of inertia, and angle of rotation in radians, respectively [17]. Careful measurements of the specimen end-fittings and moving parts of the testing machine were taken to back calculate the component of angular twist occurring in these parts due to the applied loads. This support structure angular twist was subtracted from the experimental value to increase the accuracy of the results and to isolate the angular twist of the braided tube. During the comparison of the experimental data to predicted data, it was assumed that predicted properties of the unit cell represent the overall properties of the tubular structure.

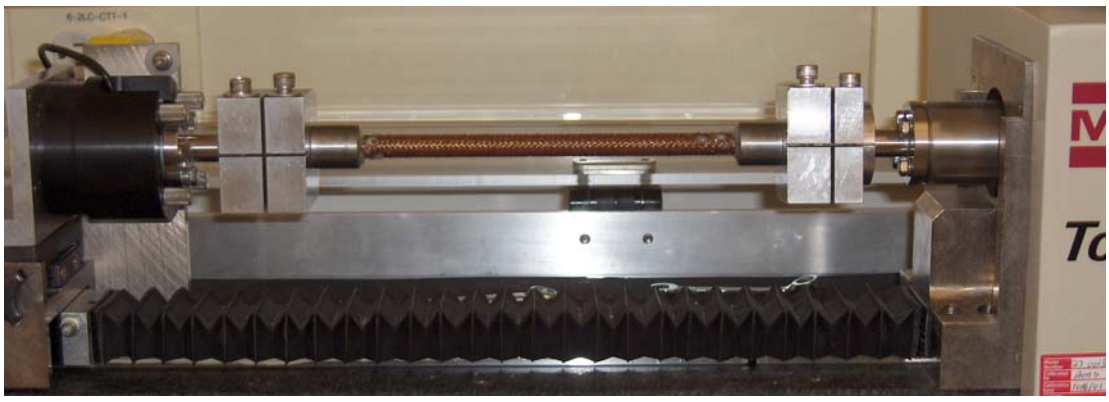

Figure 4.12: Specimen loaded on MTS TORSION-MASTER test apparatus.

4.5.2. Results

Figure 4.13 shows the shear modulus values for the KLTO, KMTO, and KSTO specimens and includes experimental results and corresponding curved-model prediction results for the dimensions listed in Table 4.3. In this figure, the error bars are used to show the standard deviations in the case of experimental findings, and the upper and lower predictions in the case of the curved model. The curved model predictions were obtained for the average values of the geometrical measurements for the unit cell. One standard deviation above and one standard deviation below the average unit cell measurements were used to obtain the upper and lower value predictions for the curved unit cell, respectively. The agreement between the experiments and the predictions are observed to be very good.

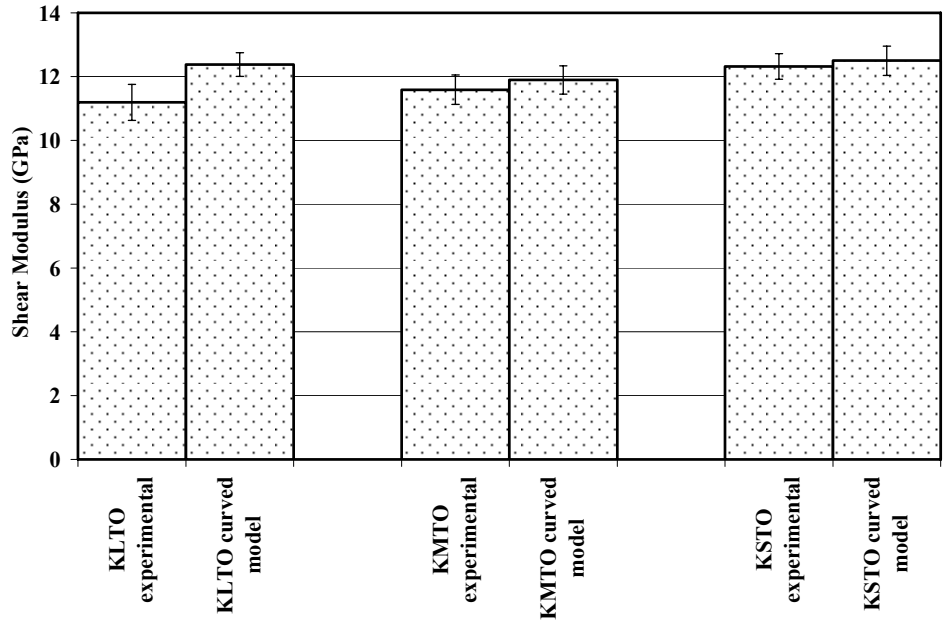

Figure 4.13: Experimental and corresponding curved model prediction results of KLTO, KMTO, and KSTO specimens. (Error bars indicate the standard deviations for the experimental results and upper/lower predictions in the curved model results.)

For KLTO specimens, average experimental shear modulus was 11.19 GPa (± 0.57 Standard Deviation) whereas the curved model predicted 12.38 GPa. The lower level prediction from the model for KLTO is 12.01 GPa. The upper value of the experimental finding of 11.76 GPa (i.e. 11.19+0.57=11.76) and the lower value prediction of the curved model (12.01 GPa) has only 2.1% difference which is a very good agreement compared to some reported differences that are above 10%, [10], between shear modulus predictions and experimental results.

For KMTO specimens, average experimental shear modulus was found as 11.59 GPa (± 0.46 Standard Deviation) whereas the curved model predicted 11.90 GPa. The predicted value falls within the spread of standard deviation of the experimental finding; hence, the results are in very good agreement.

For KSTO specimens, average experimental longitudinal elastic modulus was found as 12.32 GPa (± 0.40 Standard Deviation) whereas the curved model predicted 12.50 GPa. Predicted value falls within the spread of standard deviation of the experimental finding; hence, the results are in very good agreement.

4.6. Discussion

The observed differences in the predictions for longitudinal elastic and shear modulus may be an important window of tailorability for stiffness critical designs where accuracy is of importance, such as a braided catheter design [18].

It is important to explain the differences between the results of the predictions in case studies 1 and 2 reported in this paper. An increase in the predictions can be observed upon comparison of Figure 4.5 and Figure 4.8 for longitudinal elastic modulus values, and Figure 4.6 and Figure 4.9 for shear modulus values. In both case studies, the undulation length of the yarns was set to be two times the height of a yarn; hence, it is expected to see a slight increase in the moduli predictions when the yarn thickness was decreased from 0.5 mm to 0.25 mm as this results in a shorter undulation length. Also contributing to this increase is the steeper angle of undulation for the 0.5 mm yarn height case versus 0.25 mm yarn height case. As the slope of the yarn inclination increases, this acts as an off-axis effect and causes a decrease in the moduli values.

It may be argued from the two case studies that the decrease in radius of curvature of a unit cell cause a decrease in the longitudinal elastic and shear moduli values of a tubular braided composite. The effect of this decrease depends on the yarn thickness used in the braiding process as indicated in the two case studies.

Comparison of the proposed model with literature (Naik R.A. (1996)) outlines the relatively low difference in the predictions of the two models. This gives confidence in the results of the proposed model for flat braided structures (i.e. infinite radius of curvature). Although extreme care was taken during the measurements, small differences in the results may be attributed to the measurement errors, such as parallax error, as Naik's data was read off from the graph.

The experimental results discussed for the verification of the model have low standard deviation values due to the consistent experimental results. Strongly agreeing experimental and predictive results confirm the findings of the proposed model. The small differences in the model and the experimental findings may partially be attributed manual preparation of the specimens. The specimens used in this study were manually impregnated using the epoxy resin and cured in the oven. An automated manufacturing technique may minimize the small inconsistencies observed in the results. One other reason for the differences may be the assumption of rectangular yarn cross section used in the unit cell geometry. As can be seen in Figure 4.1, the actual cross section of the yarns may be slightly closer to an elliptical (lenticular) shape rather than a rectangular shape; however,

for this study, the yarn shape was chosen to be rectangular to slightly simplify the integrations used in the model.

As mentioned above some stiffness critical designs, such as braided catheters, due to their field of application need thorough understanding of their properties. Verification of the findings of this study via experimental results open a new design tailorability window for use of braided tubular products in stiffness critical applications.

4.7. Conclusions

This paper outlines the effects of change in radius of two-dimensionally braided tubular composites.

1. The effects of the curved unit cell on longitudinal elastic and shear moduli and Poisson's ratio results are outlined using two case studies. Up to 7.2% decrease in moduli values were observed.
2. The Poisson's ratio was found to be insensitive to the change in the unit cell in these case studies.
3. The longitudinal elastic and shear moduli and in-plane Poisson's ratio of two-dimensionally braided flat composites are predicted using the proposed model. The findings are compared to that of an available model in the literature and good agreement of results was observed.
4. The shear modulus predictions were compared to that of in-house experimental results and excellent agreement were observed.

5. Findings outlined in this work can be considered as valuable tools in the design of stiffness critical applications of two-dimensionally braided tubular composites.

4.8. References

[1] Ayranci C, Carey J. (2008). 2D braided composites: A review for stiffness critical applications, Composite Structures, 85 (1): 43-58.

[2] Tsai K-H, Hwan C-L, Chen W-L, Chiu C-H. (2008). A parallelogram spring model for predicting the effective elastic properties of 2D braided composites, Composite Structures, 83 (3): 273-283.

[3] Yuksekkaya ME, Adanur S. (2009). Analysis of polymeric braided tubular structures intended for medical applications, Textile Research Journal, 79 (2):99-109.

[4] Zhang P, Gui L-J, Fan Z-J. (2009). An analytical model for predicting the elastic properties of triaxially braided composites, Journal of Reinforced Plastics and Composites, 28 (15):1903-1916.

[5] Pickett, A.K., Sirtautas, J., Erber, A., "Braiding simulation and prediction of mechanical properties", Applied Composite Materials 16 (6), pp. 345-364, 2009.

[6] Naik RA. (1996). Analysis of woven and braided fabric-reinforced composites, ASTM Special Technical Publication 1274, 239-263.

[7] Huang ZM. (2000). The mechanical properties of composites reinforced with woven and braided fabrics, Composites Science and Technology, 60 (4):479-498.

[8] Aggarwal A, Ramakrishna S, Ganesh VK. (2001). Predicting the in-plane elastic constants of diamond braided composites, Journal of Composite Materials, 35 (8):665-688.

[9] Yan Y, Van Hoa S. (2002). Energy approach for prediction of mechanical behavior of 2-D triaxially braided composites Part II: Parameter analysis, Journal of Composite Materials, 36 (10):1233-1253.

[10] Carey J, Fahim A, Munro M. (2004). Predicting elastic constants of 2D-braided fiber rigid and elastomeric-polymeric matrix composites, Journal of Reinforced Plastics and Composites, 23 (17):1845-1857.

[11] Goyal D, Tang X, Whitcomb JD, Kelkar AD. (2005). Effect of various parameters on effective engineering properties of 2 × 2 braided composites, Mechanics of Advanced Materials and Structures, 12 (2):113-128.

[12] Ayranci, C., Carey, J.P., Predicting the longitudinal elastic modulus of braided tubular composites using a curved unit-cell geometry, Composites Part B: Engineering, 41 (3), 229-235, 2010.

[13] Ko FK, Pastore CM, Head AA. (1989). Formation of Industrial Braids, *(Atkins and Pearce) Handbook of Industrial Braiding,* page 3-1, Covington, Kentucky: Atkins and Pearce.

[14] Raju IS, Wang JT. (1994). Classical laminate theory models for woven fabric composites, Journal of Composites Technology and Research, 16 (4):289-303.

[15] Carey J, Munro M, Fahim A. (2003). Longitudinal elastic modulus prediction of a 2-D braided fiber composite, Journal of Reinforced Plastics and Composites, 22 (9):813-831.

[16] Flanagan RC, Munro M. (1986). High Energy Density Fibre Composite Rotors, Vol. 2, University of Ottawa, Technical Report No UOME-FP-8603-1.

[17] Popov EP. (1990). Torsion, *Engineering Mechanics of Solids*, Second Edition, page 224, Toronto: Prentice Hall.

[18] Carey J, Fahim A, Munro M. (2004). Design of braided composite cardiovascular catheters based on required axial, flexural, and torsional rigidities, Journal of Biomedical Materials Research - Part B Applied Biomaterials; 70 (1):73-81.

CHAPTER 5: ELASTIC PROPERTIES OF LARGE-OPEN-MESH 2D BRAIDED COMPOSITES: MODEL PREDICTIONS AND INITIAL EXPERIMENTAL FINDINGS

A version of this chapter was submitted to Polymer Composites and is accepted:

The paper was co-authored by: Cagri Ayranci, Daniel Romanyk, Jason P Carey

5.1. Introduction

Two dimensional (2D) braiding has been utilized as an automated composite material preform manufacturing technique for decades and used in a broad variety of applications [1]. 2D braided preforms are most commonly manufactured using a Maypole type braiding machine, [2], where half of the continuous fiber loaded carriers move in clockwise direction and the remaining half move in counter-clockwise direction. During this motion, the carriers follow a serpentine path to create the necessary braid architecture. The majority of 2D braided composite applications require closed-mesh structures to minimize the matrix-only and undulating regions in an attempt to maximize the stiffness and strength of the structures as seen in braided structural columns, pressure vessels, aviation applications, sports equipment [3 - 5].

There are also some stiffness critical applications that may require open-mesh structures; such as braided catheters and stents [6, 7]. Utilization of braiding for medical applications is fairly recent compared to other traditional braiding applications. Very few researchers, [8 - 14], included open-mesh structures in their work; therefore, experimental data is very limited for large-open mesh structures, which maybe a valuable tool in the design of medical braided structures.

Tan et al (1997), [8], developed a theoretical model for "*open-packing woven fabric unit cells*" to investigate open-mesh woven fabrics linear elastic properties. Authors, [8], utilized data published by Naik and Shembekar (1992), [15], and compared their results to that of a finite element analysis (FEA) model.

They reported that the FEA model findings were 50% higher than their theoretical model for the shear modulus values, and the authors suggested that this may be due to the fact that the FEA model assumes an iso-strain condition as opposed to the iso-stress condition assumed by their theoretical model. Works of Tan et al (1997) and Naik and Shembekar (1992) were both for woven fabric composites; hence, effect of undulation length with respect to the braid angle was not investigated.

Aggarwal et al (2001) [9], highlighted effects of change in gap space between braided yarns within the unit cell through a parametric study as part of an analytical model developed. Authors looked at the ratio of undulation length and yarn width. They investigated ratios only between 0 and 0.4.

Zhao and Hoa (2003) and Zhao et al (2003) published two papers on open-hole triaxial woven fabrics typically used for satellite applications [10, 11]. These papers were investigating triaxially braided structures; therefore, a direct comparison of the results with this study is not possible.

5.2. Motivation

In this paper the effect of undulation length on elastic properties of 2D braided tubular composites will be investigated and experimental and theoretical findings will be compared; in addition, the applicability of the proposed model to stent-like structures due to the recently improving use of braided composites in medical stent applications will be investigated.

Most available models predict elastic properties of braided structures by isolating and analyzing a repeating element in the structure, a unit cell, and

assuming properties predicted using this approach reflects the properties of the overall structure.

Figure 5.1 shows a schematic representation of an isolated unit cell of a 2D braided tubular structure. Three main regions that exist are shown, namely; crossover, undulation, and matrix-only regions. Figure 5.2 shows top views of schematic representation of unit cells for a braided structure used in this paper, where Figure 5.2 (a) and (b) are examples of a closed-mesh (or tight mesh) and open-mesh unit cell, respectively. The crossover regions of Figure 5.2 (a) and (b) are identical. Increasing the undulation length (a_u) from Figure 5.2 (a) to (b) also causes an increase in the matrix-only regions (shown by the dark triangles in Figure 5.2 (b)) of the unit cell. Hence, it is reasonable to expect changes in the elastic properties of a braided structure as the undulation length increases.

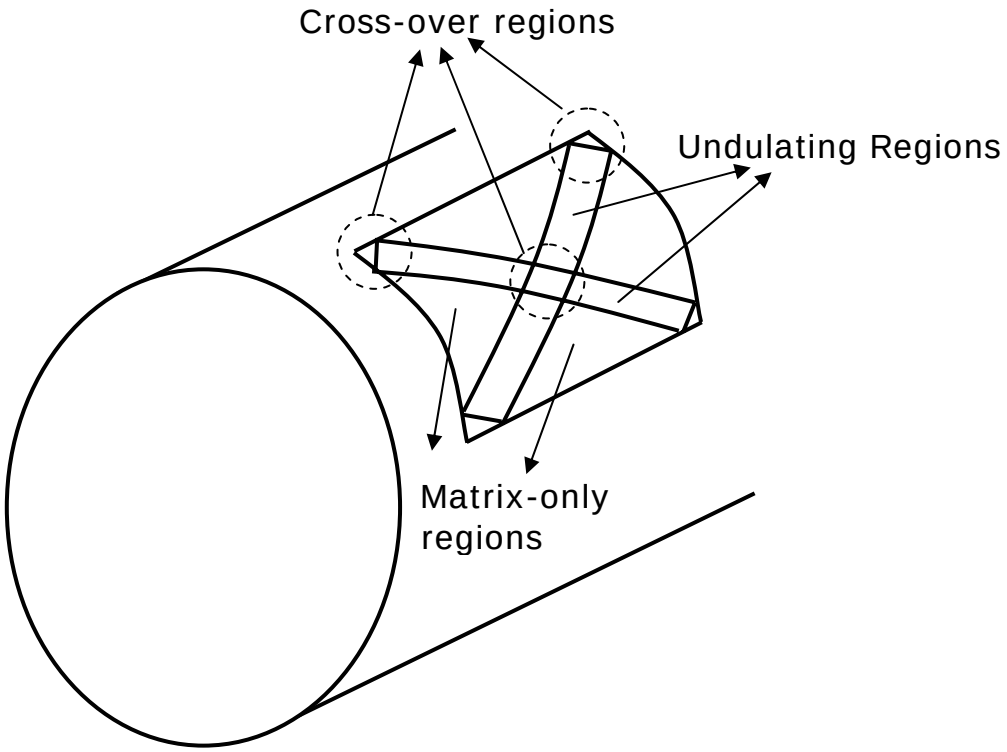

Figure 5.1: Schematic representation of an isolated unit cell on a 2D braided tubular structure.

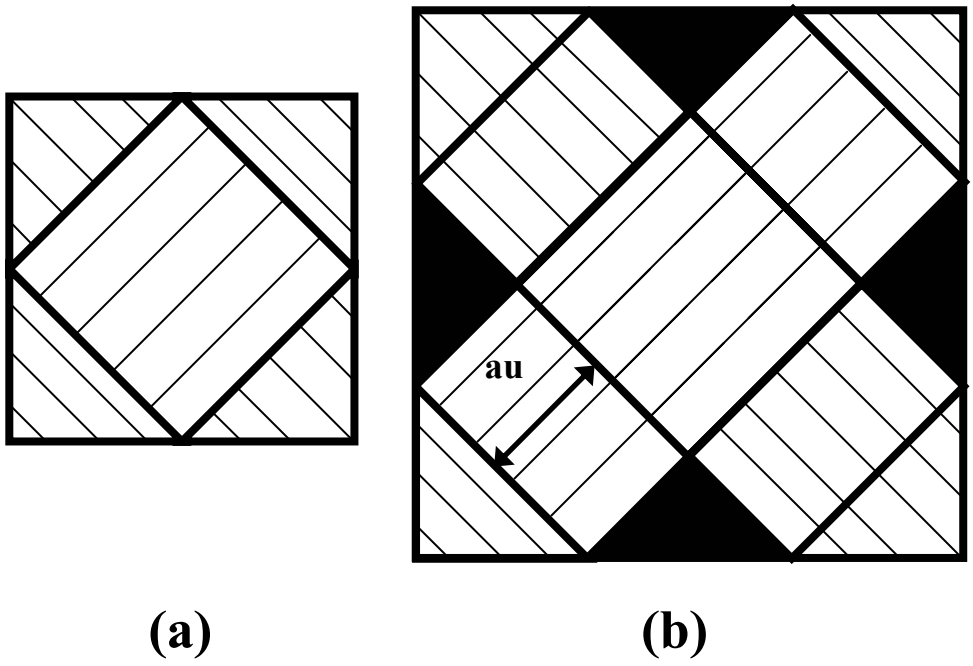

Figure 5.2: Top views of schematic representation of unit cells for a braided structure used in this paper. (a) closed-mesh (or tight-mesh) and (b) open-mesh unit cell.

The published data in the open literature for the investigation of the effect of the undulation length on braided structures is very limited. Almost all of the predictive models published in this field so far have been developed and verified using closed-mesh (or near closed-mesh) structures. Some researchers mention that their developed models take into account the undulation length; however, the model verification of these models are mostly done using experimental results of closed-mesh specimens (i.e. minimal undulation length) or near-closed-mesh specimens such as Aggarwal et al's work [9]. An experimental study that clearly

addresses the effect of a_u on elastic properties is a gap that needs to be filled in the literature and could be useful for research and development and design purposes.

As aforementioned, most likely applications of open-mesh braided composites would be in the medical field, such as braided tubes, braided composite catheters, and braided stents, one of the other applications may be braided garden hoses. It is therefore also important to understand the limitations of the curved-model used to predict the elastic properties of the said composites, and understand how the model behaves if the structure is an open-mesh structure without matrix-only regions (i.e. stent-like structure). Stents are commonly used in the medical fields and there are a number of researchers, such as Yuksekkaya and Adanur [7], working on braided polymeric stents. Understanding the applicability of the model to stent-like structures is important.

5.3. Open-mesh Composites - Effect of undulation length on elastic properties

5.3.1. Analytical model

The predictive analytical model used in this study takes into account the radius of curvature of the unit cell and close- and open-mesh unit cell variants was published earlier [16]. Here, for completeness purposes, the model is explained briefly. The model analyzes the unit cell (Figure 5.1) using a modified Classical Laminate Plate Theory (CLPT) approach. The extensional stiffness, $\boldsymbol{A}$, coupling stiffness, $\boldsymbol{B}$, and bending stiffness, $\boldsymbol{D}$, matrices of the three main regions in the unit cell are individually calculated using micromechanical models for the given

fiber-matrix combination and transformation matrices for the given geometrical properties of the placement of fibers in the unit cell. The calculated $\boldsymbol{A}$, $\boldsymbol{B}$, and $\boldsymbol{D}$ matrices of the individual regions are assembled using a volume averaging approach to calculate the overall unit cell properties.

The possible effects of a change in one or more of the unit cell regions can be immediately realized by investigating Figure 5.2 (a) and (b): as $\boldsymbol{a_u}$ increases, from Figure 5.2 (a) to Figure 5.2 (b), the ratio of volume occupied by matrix-only regions (with low stiffness properties) and crossover regions (with relatively higher stiffness properties due to the existing fibers) changes.

5.3.2. Analytical model results

In this section, effects of change in $\boldsymbol{a_u}$ of a unit cell, as predicted by the model, is presented for longitudinal elastic ($\boldsymbol{E_{xx}}$) and shear ($\boldsymbol{G_{xy}}$) moduli, and Poisson's ratio ($\boldsymbol{\nu_{xy}}$) in Figure 5.3. A Kevlar-epoxy composite system has been used for this study, and the properties of the constituents are included in Table 5.1. The yarn width and the thickness ($\boldsymbol{t_m}$) of the unit cell were taken as 4 mm and 1.5 mm, respectively. The unit cell was assumed to have a radius of curvature of 25 mm.

Table 5.1: Elastic constants used in the model for predictions.

Material	**Elastic constants**			
Constituent	**E_{f11} (GPa)**	**E_{f22} (GPa)**	**G_{f12} (GPa)**	**ν_{f12}**
Kevlar 49 fiber	130	7.3	2.86	0.35
Carbon fiber*	220	13.8	9.0	0.2
S2-glass	96.5	96.5	39.2	0.23
	E_m	**-**	**G_m**	**ν_m**
Epon825/Ancamine1482 resin	3.5	-	1.3	0.3
Lamina (V_{f0} =60%)	**E_{11} (GPa)**	**E_{22} (GPa)**	**G_{12} (GPa)**	**ν_{12}**
Kevlar 49/epoxy	79.7	5.9	1.5	0.33
Carbon/epoxy	133	7.9	3.9	0.24
S2-glass/epoxy	59.3	15.8	6.0	0.26

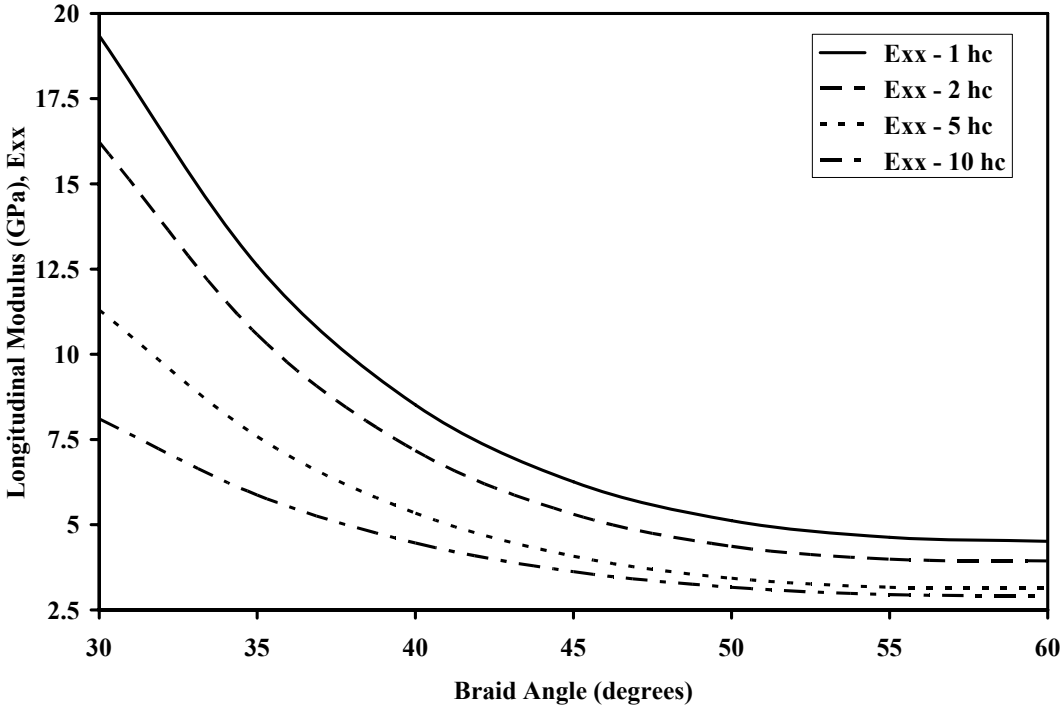

Figure 5.3 (a)

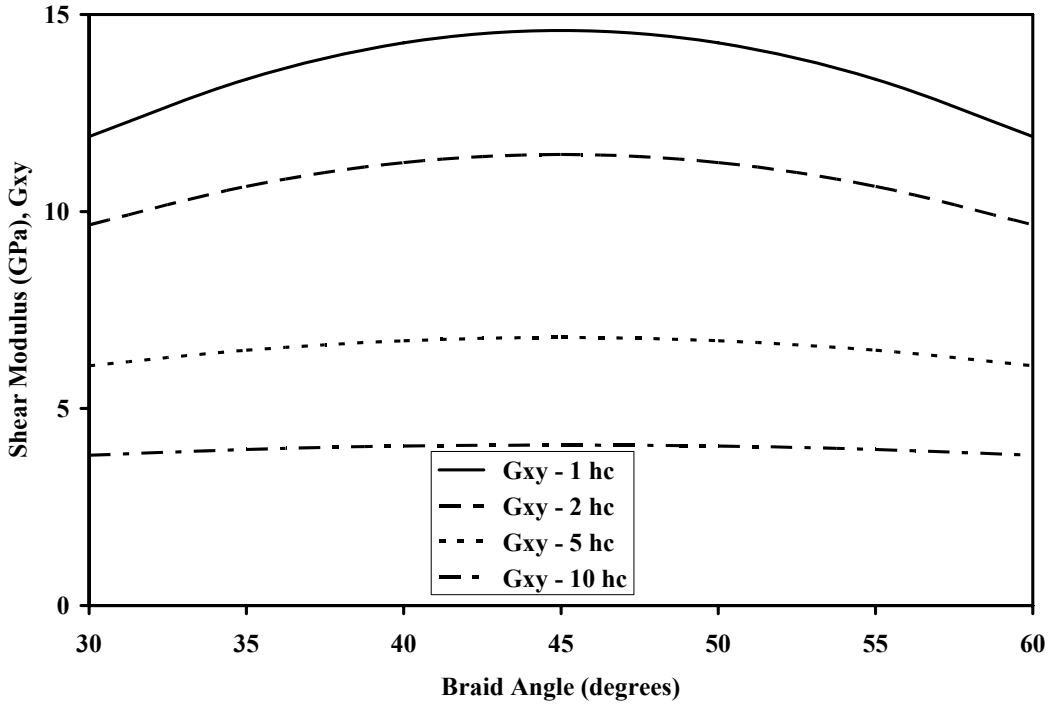

Figure 5.3 (b)

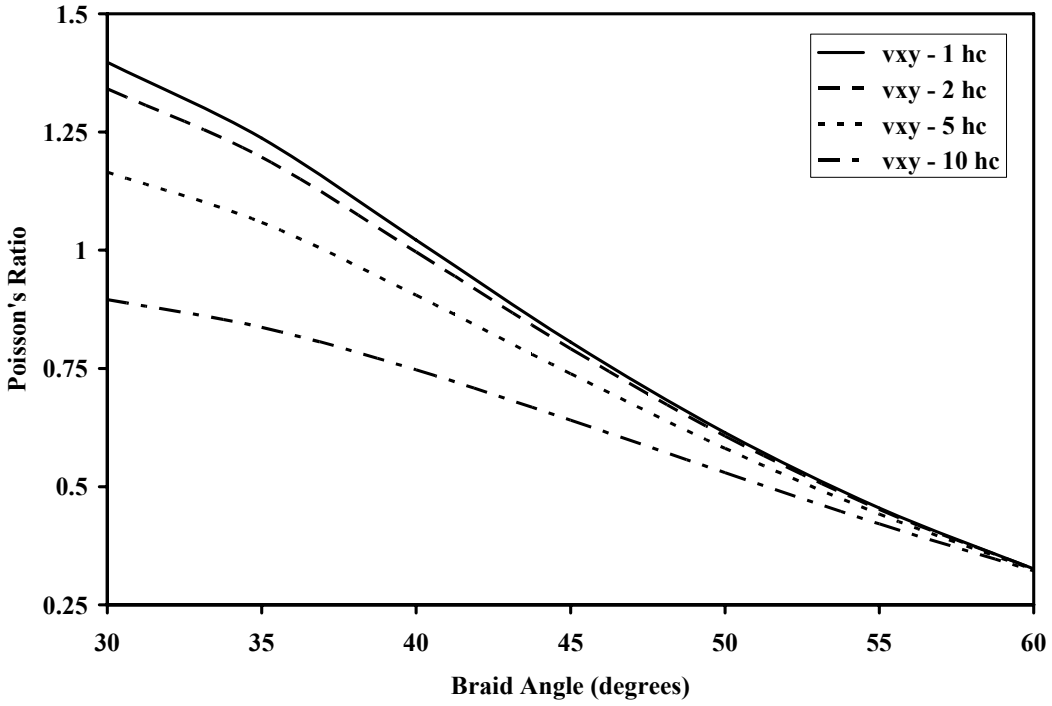

Figure 5.3 (c)

Figure 5.3: Predicted effect of undulation length (au) on (a) the longitudinal elastic modulus, (b) shear modulus, (c) Poisson's ratio as a function of braid angle.

Throughout this parametric study (Figure 5.3), only the parameter a_u was varied between one yarn thickness ($1h_c$) and $10h_c$ and the remaining parameters were kept constant. This change in a_u corresponds to an increase in the ratio of matrix-only region area to the overall unit cell projected area. The average ratios calculated were 0.024, 0.071, 0.226 and 0.415 for $1h_c$, $2h_c$, $5h_c$ and $10h_c$ cases,

respectively. It is reasonable to accept the $1\boldsymbol{h_c}$ unit cell to be a fully-closed mesh and $10\boldsymbol{h_c}$ unit cell to be a large-open mesh structure. In all three figures of Figure 5.3, as $\boldsymbol{a_u}$ increases, a considerable decrease in the predicted values was observed. Hence, it maybe important to highlight the percent differences between $1\boldsymbol{h_c}$ and $10\boldsymbol{h_c}$ unit cell cases, as the extreme scenario, in all three figures of Figure 5.3.

For the results shown in Figure 5.3 (a), at 30 degree braid angle, 58% difference was found between the $\boldsymbol{E_{xx}}$ values of $1\boldsymbol{h_c}$ and $10\boldsymbol{h_c}$ undulation length cases; where the elastic modulus was 19.3 GPa and 8.1 GPa $\boldsymbol{E_{xx}}$ for the $1\boldsymbol{h_c}$ and $10\boldsymbol{h_c}$ undulation length cases, respectively. This percent difference gradually decreased down to 35% as braid angle was increased from 30 to 60 degrees.

In Figure 5.3 (b), for $\boldsymbol{G_{xy}}$ values, at 30 degree braid angle, 68% difference was found between the $\boldsymbol{G_{xy}}$ values of $1\boldsymbol{h_c}$ and $10\boldsymbol{h_c}$ undulation length cases. This percent difference gradually increased to 72% as braid angle was increased from 30 to 45 degrees (45 to 60 degree range was the mirror image of 30 to 60 degrees). It is also worth noting that the model became increasingly insensitive to the changes in braid angle as the $\boldsymbol{a_u}$ increased. This can be seen in the almost-horizontal line of the $10\boldsymbol{h_c}$ undulation length case in Figure 5.3 (b).

In Figure 5.3 (c), for $\boldsymbol{\nu_{xy}}$ values, at 30 degree braid angle, 35% difference was found between the $\boldsymbol{\nu_{xy}}$ values of $1\boldsymbol{h_c}$ and$10\ \boldsymbol{h_c}$ undulation length cases. This percent difference gradually decreased to 1% as braid angle was increased from 30 to 60 degrees.

5.4. Experimental verification

A set of in-house experiments were conducted to validate the predicted results of the open-mesh composites. Three most commonly used fiber types were chosen; namely; Kevlar, Carbon, and S2-Glass with an Epon 825/Ancamine 1482 curing agent matrix system epoxy based matrix material was chosen (Table 5.1). A picture of the specimen with attached end fittings is shown in Figure 5.4 (a).

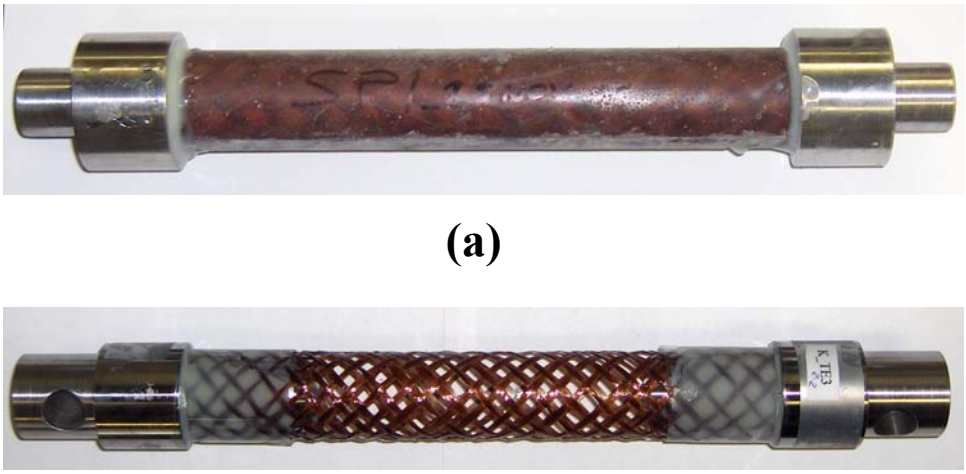

(a)

(b)

Figure 5.4: (a) Open mesh braided specimen with end fittings, (b) Open mesh specimen without matrix-only regions (stent-like structure).

5.4.1. Methodology

Longitudinal elastic modulus was determined as a result of tensile tests. The gathered data were used to calculate the E_{xx} from the slope of the stress-strain

curves. An MTS 810 material testing system equipped with a 100 kN maximum load cell and MTS 634.12E-24 extensometer were used for the experiments that were done with a loading rate of 1mm/min (ASTM D 3039/D 3039M – 08, Standard Test Method for Tensile Properties of Polymer Matrix Composite Materials).

The shear modulus was determined with torsion test experiments using an MTS-Torsion Master testing machine (MTS Systems Corporation Eden Prairie, MN, USA) equipped with a load cell of 2 Nm torsional load capacity. No international testing standard exists for torsion testing of open-mesh braided composite materials; therefore, the 0.03 degrees/second (approximately 2 degrees/minute) loading rate suggested in ASTM D 5448/D 5448M – 93 (Reapproved 2006) was followed (Standard Test Method for In-plane Shear Properties of Hoop Wound Polymer Matrix Composite Cylinders), to obtain a failure of the specimens within 1 to 10 minutes. The data gathered during the tests were used to calculate the shear modulus using Equation (1):

$$G_{xy} = \frac{TL}{J\phi} \tag{1}$$

where *T, L, J,* and φ are applied torque, length of the specimen, polar moment of inertia, and angle of rotation in radians, respectively [17]. Dimensions of the specimen end-fittings, manufactured from 4140 Steel for minimal deflection during testing, and moving parts of the testing apparatus were carefully measured to back calculate the amount of angular twist occurring in these parts during

testing. Later, the calculated angular twist of the parts, other than the specimen, was subtracted from the measured angular twist to increase the accuracy of the results and isolate the angular twist of the braided tube.

5.4.2. Results

5.4.2.1. Open-mesh composites

Table 5.2 presents the dimensional measurements of the tensile-test specimens used for all three types of braided composites (i.e. Kevlar-, Carbon, S2/Glass- epoxy composites). In this table, and in all the other tables used in this manuscript, θ, ID, OD, t, W_y refer to braid angle, inner and outer diameter, thickness of the braided tube, and width of a braiding strand, respectively. Figure 5.5 shows experimental $\boldsymbol{E_{xx}}$ findings with standard deviation, and predicted $\boldsymbol{E_{xx}}$ findings that were calculated using the curved-unit cell model for the given dimensions. Average, upper and lower predictions of the curved-unit cell model were also calculated for the $\boldsymbol{E_{xx}}$ and presented in the figure. The average values of the geometrical measurements were used to obtain average-model predictions. The upper and lower predictions were obtained using one standard deviation above and one standard deviation below the average unit cell measurements, respectively.

Table 5.2: Average dimensions with ± standard deviations for Exx specimens (adopted from [12]).

Specimen type	Samples	θ (deg)	ID (mm)	t (mm)	W_y (mm)	a_u (mm)
Kevlar/ epoxy	5	44.19 ± 1.63	24.71 ± 0.28	1.51 ± 0.15	3.81 ± 0.68	1.50 ± 0.32
Carbon/ epoxy	5	41.80 ± 0.11	24.54 ± 0.19	1.58 ± 0.09	3.40 ± 0.22	2.00 ± 0.51
S2-glass/ epoxy	4	46.00 ± 1.30	24.53 ± 0.47	1.48 ± 0.04	3.34 ± 0.54	3.89 ± 0.08

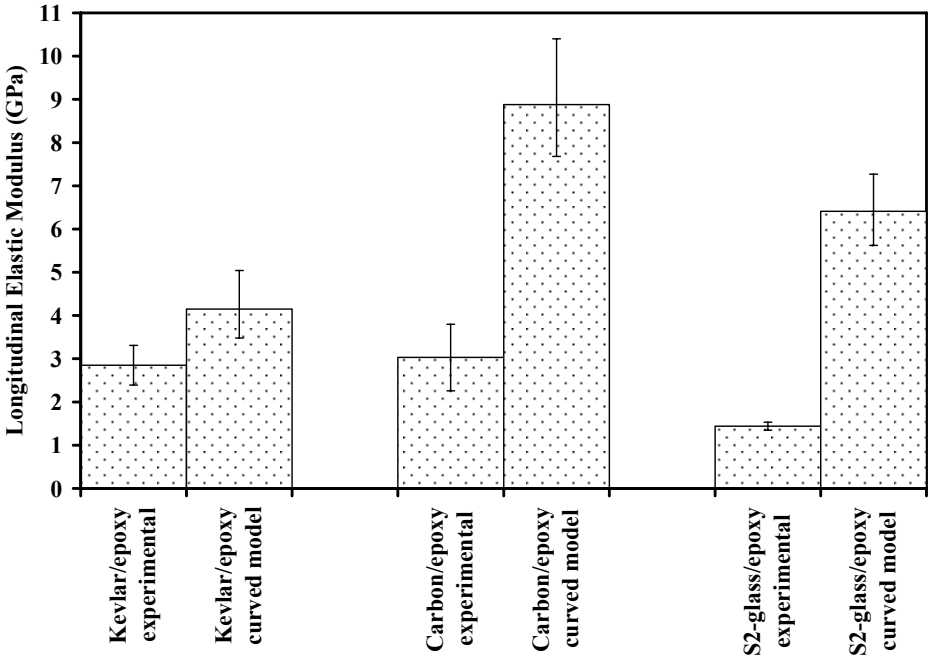

Figure 5.5: Experimental and predicted Exx values for the three composite systems of open mesh structures (experimental results were adopted from [12]).

In Figure 5.5, average experimental and curved-model predicted E_{xx} values for Kevlar-epoxy specimens are 2.85 GPa and 4.15 GPa, respectively. The

ratio of predicted and experimental findings is 1.46. Average experimental and curved-model predicted E_{xx} values for Carbon-epoxy specimens are 3.03 GPa and 8.88 GPa, respectively. The ratio of predicted and experimental findings is 2.93.

Average experimental and curved-model predicted E_{xx} values for S2-Glass-epoxy specimens are 1.44 GPa and 6.41 GPa, respectively. The ratio of predicted and experimental findings is 4.45.

Table 5.3 presents the dimensional measurements of the torsion-test specimens used for all three types of braided composites. Figure 5.6 outlines the experimental G_{xy} findings (along with their standard deviation) and predicted G_{xy} findings that were calculated using the curved-unit cell model for the given dimensions. The calculations of the average, upper and lower predictions of the curved-unit cell model were done using the same technique above for E_{xx}.

Table 5.3: Average dimensions with ± standard deviations for Gxy.

Specimen type	Samples	θ (deg)	OD (mm)	t (mm)	W_y (mm)	a_u (mm)
Kevlar/ epoxy	5	50.56 ± 2.16	27.56 ± 0.13	1.27 ± 0.11	4.70 ± 0.27	4.34 ± 0.70
Carbon/ epoxy	3	41.93 ± 1.15	27.72 ± 0.06	1.05 ± 0.04	3.72 ± 0.33	3.85 ± 0.43
S2-glass/ epoxy	5	38.89 ± 0.72	27.65 ± 0.04	1.04 ± 0.01	3.51 ± 0.43	3.78 ± 0.52

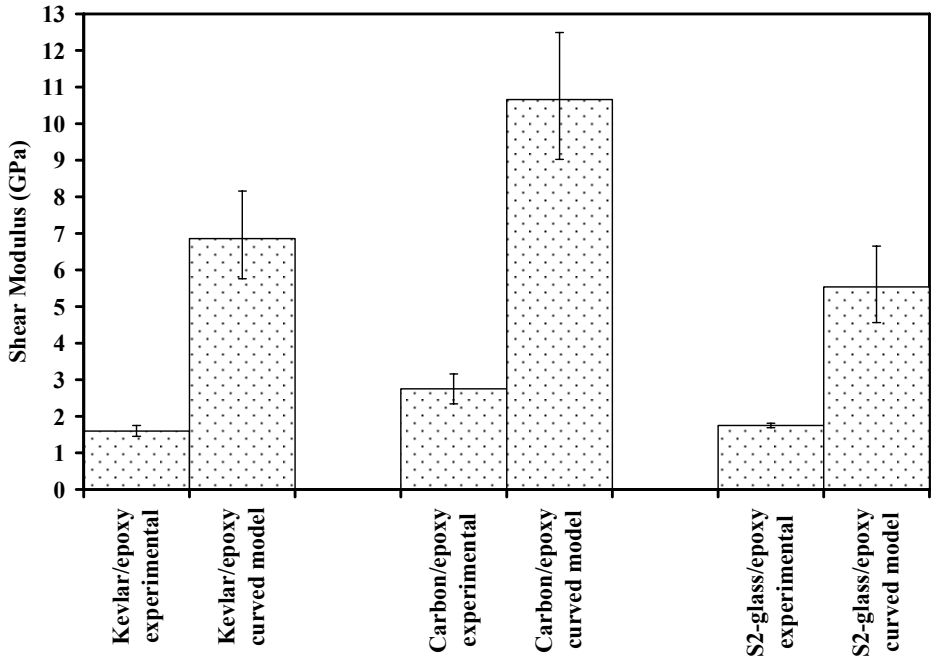

Figure 5.6: Experimental and predicted Gxy values for the three composite systems for open mesh structures.

As seen in Figure 5.6, average experimental and curved-model predicted G_{xy} values for Kevlar-epoxy specimens are 1.60 GPa and 6.86 GPa, respectively. The ratio of predicted and experimental findings is 4.29. Average experimental and curved-model predicted G_{xy} values for Carbon-epoxy specimens are 2.75 GPa and 10.66 GPa, respectively. The ratio of predicted and experimental findings is 3.88. Average experimental and curved-model predicted G_{xy} values for S2-Glass-epoxy specimens are 1.75 GPa and 5.54 GPa, respectively. The ratio of predicted and experimental findings is 3.17.

5.4.2.2. Open-mesh Composites without matrix-only regions (stent-like structures)

Comparison of the predictive model and the experimental results for stent like structures were done conducting tensile and torsion tests and calculating E_{xx} and G_{xy} results. Figure 5.4 (b) shows one of the open mesh braided composite specimens without-matrix only regions prepared for this purpose. Table 5.4 outlines the geometric dimensions of the specimens. Only Kevlar-epoxy composites were used in this preliminary study.

Table 5.4: Average specimen dimensions and experimental and predicted Exx and Gxy values (with ± standard deviations) for open mesh specimens without matrix-only regions (i.e. stent-like structures).

Specimen type	Number of Samples	θ (deg)	OD (mm)	t (mm)	W_y (mm)	a_u (mm)
Tensile test specimens (for E_{xx} calculations)	6	43.48 ± 1.94	26.00 ± 0.13	0.302 ± 0.01	1.84 ± 0.11	6.31 ± 0.65
Torsion test specimens (for G_{xy} calculations)	5	37.3± 4.26	26.07 ± 0.09	0.29 ± 0.02	1.97 ± 0.24	6.88 ± 0.33

Figure 5.7 outlines the experimental and predicted results of E_{xx} and G_{xy} values. During the experimental and predictive model calculations for the longitudinal elastic and shear moduli, the hollow sections of the stent-like

structure was omitted because the structure does not have any matrix-only regions (Figure 5.4 (b)). The predictive model calculations were done by assigning zero values to the extensional stiffness, $\boldsymbol{A}$, coupling stiffness, $\boldsymbol{B}$, and bending stiffness, $\boldsymbol{D}$, matrices of the matrix-only regions. The hollow sections were not taken into account in the calculation of $\boldsymbol{E_{xx}}$ and $\boldsymbol{G_{xy}}$ results (i.e. cross sectional area was determined by omitting the contribution of the hollow sections).

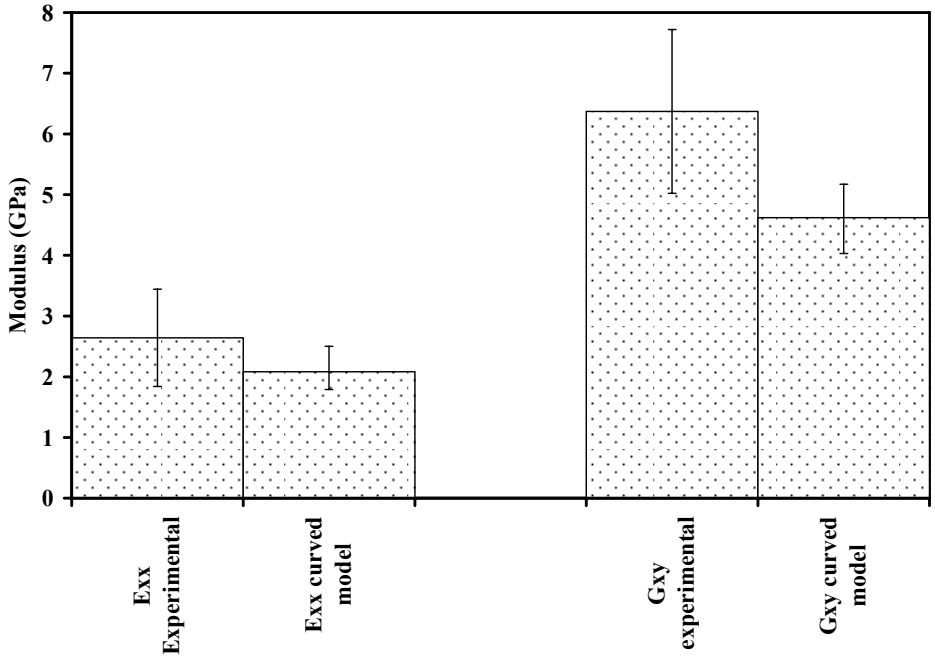

Figure 5.7: Experimental and curved-model predictions of Exx and Gxy of Kevlar-epoxy composites with open mesh and without matrix-only regions (stent-like structure).

Experimental $\boldsymbol{E_{xx}}$ results were found to be 2.64 GPa (± 0.8 GPa Standard Deviation) whereas the model predicted the average $\boldsymbol{E_{xx}}$ as 2.08 GPa, with upper and lower bound $\boldsymbol{E_{xx}}$ predictions of 2.5 GPa and 1.79 GPa for the given dimensions, respectively.

Experimental G_{xy} results were found to be 6.37 GPa (± 1.35 GPa Standard Deviation) whereas the model predicted the average G_{xy} as 4.62 GPa for the dimensions, with again the upper and lower bound G_{xy} predictions of 5.17 GPa and 4.03 GPa for the given dimensions, respectively.

5.5. Discussion

The curved-unit cell predictive model that was used for this study has been verified in a previous study, [16], by the authors for closed-mesh braided structures. Figure 5.5 and Figure 5.6 clearly indicate that the model is over-predicting compared to the experimental results if the structures are open-mesh braided composites, i.e. large a_u. The high ratio between predicted and experimental results (for E_{xx}: 1.46, 2.93, 4.45 for Kevlar, Carbon, S2-Glass-epoxy composites, respectively; and for G_{xy}: 4.29, 3.88, 3.17 for Kevlar, Carbon, S2-Glass-epoxy composites, respectively) indicate a need for an explanation for differences between the experimental and analytical results for open-mesh structures.

The analytical model used for this study, similar to most models in the field, assumes a uniform-strain approach for the unit cell under investigation. Hence, upon application of a load, the model assumes different regions of the unit cell experience identical strain. This is schematically shown in Figure 5.8 (a) for a closed-mesh structure. In Figure 5.8 (a), the figure on the left hand side is a closed-mesh structure with zero strain (i.e. no load has been applied) and the figure on the right hand side is the same unit cell but elongated due to an applied load. In this figure, it is acceptable to assume a uniform strain upon loading as the

adjacent regions of the unit cell have similar elastic properties due to the minimal undulating and matrix-only regions.

On the other hand, Figure 5.8 (b) shows a schematic representation of an open-mesh unit cell structure (exaggerated drawing for demonstration purposes). In Figure 5.8 (b), left hand side is the original unit cell (i.e. no load has been applied), and right hand side is the elongated unit cell. Upon application of a tensile load to an open-mesh unit cell, it is not unreasonable to expect a non-uniform strain (possibly due to bending of the undulating yarns) that is similar to the one shown in the right hand side of Figure 5.8 (b). A similar concept was observed and discussed by Zhao et al 2003, [11], for their triaxial woven fabric composites. Reasons behind the expectation of this type of deformation are due to the fact that, unlike the closed-mesh unit cell, the adjacent regions of the open-mesh unit cell do not have similar elastic properties (eg. the non-reinforced matrix-only regions versus the crossover regions) and also, possible off-loading-axis alignment of the yarns may introduce additional bending moments to the structure which may also be contributing to the differences in the experimental and predicted results.

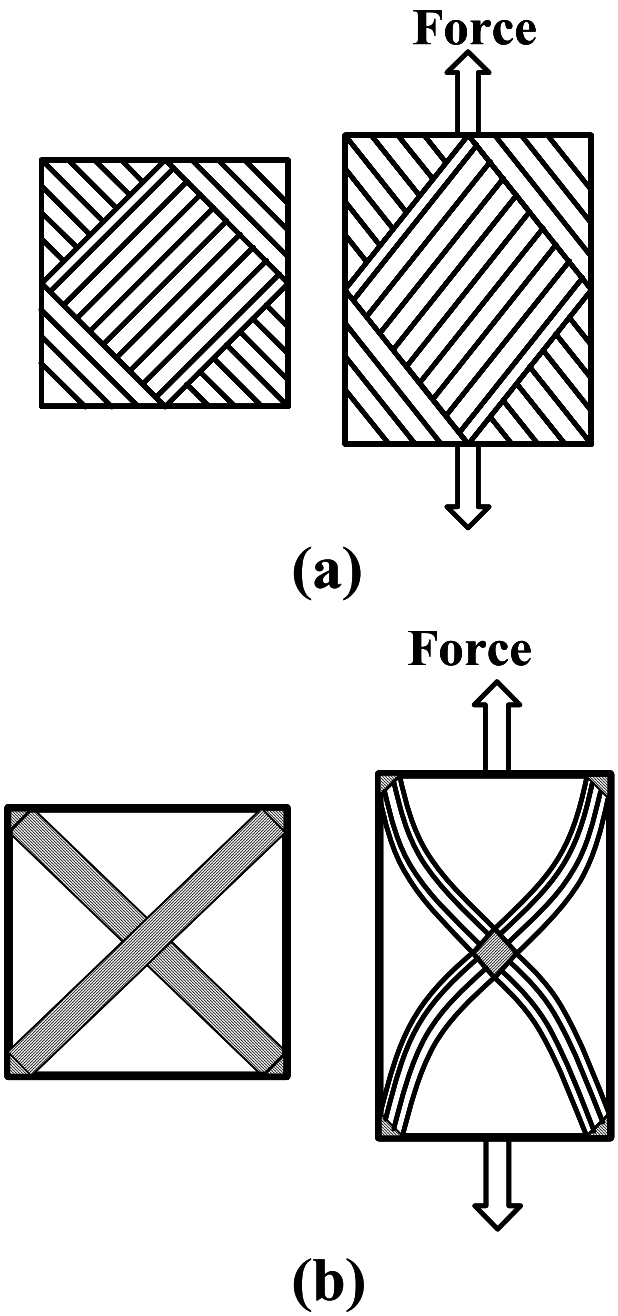

Figure 5.8: (a) Schematic representation of a closed mesh structure. Left hand side: no load is applied; Right hand side: loaded and stretched unit cell. (b) Schematic representation of an open mesh structure (exaggerated view). Left hand side: no load is applied; Right hand side: loaded and stretched unit cell.

Experimental elastic modulus (***E***) was calculated as the slope of stress (***σ***)-strain (***ε***) curve using Equation 2:

$$E = \frac{\sigma}{\varepsilon} \tag{2}$$

During the experiments, if the strain recorded is larger (than predicted by the model) due to the aforementioned reasons (i.e. non-uniform strain) and schematic explanation in Figure 5.8 (b), it can be seen from Equation 2 that the elastic modulus would be determined lower than the model. A similar explanation for the shear loading can be imagined for the $\boldsymbol{G_{xy}}$ results. Hence, as the $\boldsymbol{a_u}$ increases in open mesh structures; such as braided tubular structures, braided composite catheters, it may be necessary to use a correlation factor for the model's predictions to compensate for the original uniform-strain assumption of the model. Unfortunately, it was not possible to draw a conclusive correlation factor due to the lack of large data bank available at this point; however, it is suspected that undulation length, braid angle, thickness of the specimen, and strand thickness, and fiber/epoxy choice may all contribute to the difference in results, because the model is highly sensitive to all these parameters. The correlation factor may be determined by a detailed controlled parametric experimental study where only one parameter at a time is changed to understand the effects. The ratios of predicted versus experimental findings should be the start point for the correlation factor determination.

For the stent-like structures, upon investigation of Figure 5.7, it is seen that the experimental and predicted results are in agreement. Although the average predicted and experimental E_{xx} results have approximately 21 % difference (2.64 GPa versus 2.08 GPa), the predicted E_{xx} results fall within the spread of experimental findings. The average predicted and experimental G_{xy} results have approximately 27% difference (6.37 GPa versus 4.62 GPa), but the upper value of the G_{xy} prediction (5.17 GPa) falls within the spread of the experimental data (i.e. due to 6.37±1.35 GPa the spread is from 5.02 GPa to 7.72 GPa). Although the percent differences in both E_{xx} and G_{xy} cases are relatively high, having the spread of experimental and predictive results overlap gives confidence in the model.

It is also important to mention the possible contribution of interface shearing to the differences in results of the stent-like structures. There are hollow sections in the structure; therefore, when a load is applied, the undulating strands tend to align parallel to the loading direction. This re-alignment may cause excessive shear forces between the interface of the top and bottom yarns of the crossover regions which in return may be contributing to the differences in analytical and experimental results.

The analytical model used for this study is very sensitive to changes in dimensions and other parameters. The specimens used for this work were prepared using hand manufacturing technique (i.e. braided preform was impregnated by manual application of resin). This technique may have caused some misalignment in the fiber yarn directions leading to a large spread of data (especially in the case of stent-like structures). Hence, if the manufacturing

technique is improved (i.e. automated), it is believed that the model can be used for stent-like structures successfully. This will be addressed in future work.

The selection of extensometer gage length may also be an important factor as every unit cell on the structure may not be identical due to the hand manufacturing technique used for the specimens. For both open mesh specimens and stent-like specimens this may have an effect on the results.

5.6. Conclusions

This paper outlines the effects of having an open-mesh versus closed-mesh structure for specifically biomedical applications of braided composites.

1. Effects of undulation length on elastic properties of braided composites are outlined using an analytical model.
2. Experimental results for longitudinal elastic ($\boldsymbol{E_{xx}}$) and shear ($\boldsymbol{G_{xy}}$) moduli of three different types of open-mesh braided composites (Kevlar-, Carbon-, and S2 Glass-Epoxy braided tubes) were investigated.
3. Predicted versus experimental $\boldsymbol{E_{xx}}$ and $\boldsymbol{G_{xy}}$ results are compared and it was observed that the model that was previously proven for closed-mesh braided structures has always over-predicted compared to the experimental findings.
4. Findings of the study suggests a need for a correlation factor for most of the CLPT based analytical predictive models that are successfully used for closed-mesh structures in the field.
5. Findings also suggest the need for further investigation of the elastic properties/behavior of open mesh braided composites.

6. Finally, preliminary experiments with open-mesh braided specimens without matrix-only regions (i.e. stent-like structures) are conducted. Experimental and predictive results are in agreement.

5.7. References

[1] Ayranci C, Carey J. (2008). 2D braided composites: A review for stiffness critical applications, Composite Structures, 85 (1): 43-58.

[2] Ko FK, Pastore CM, Head AA. (1989). Formation of Industrial Braids, (Atkins and Pearce) Handbook of Industrial Braiding, page 3-1, Covington, Kentucky: Atkins and Pearce.

[3] Brookstein D. Structural applications of advanced braided composites. In: Proceedings SPE/APC'88. Advanced polymer composites for structural applications. Los Angeles, 14–17 November; 1988. p.415–24.

[4] White ML. Tubular braided composite main rotor blade spar. J Am Helicopter Soc 1982(N4):45–8.

[5] Casale N, Bristow D, Pastore CM. Design and fabrication of a braided composite monocoque bicycle frame. In: High-Tech fibrous materials (ACS symposium series 457); 1991. p. 90–101.

[6] Carey, J., Fahim, A., Munro, M., Design of braided composite cardiovascular catheters based on required axial, flexural, and torsional rigidities, 2004, Journal of Biomedical Materials Research - Part B Applied Biomaterials 70 (1), pp. 73-81.

[7] Yuksekkaya ME, Adanur S. (2009). Analysis of polymeric braided tubular structures intended for medical applications, Textile Research Journal, 79 (2):99-109.

[8] Tan, P., Tong, L., Steven, G.P. (1997). A three-dimensional modelling technique for predicting the linear elastic property of opened-packing woven fabric unit cells, Composite Structures 38 (1-4), pp. 261-271.

[9] Aggarwal, A., Ramakrishna, S., Ganesh, V.K. (2001). Predicting the in-plane elastic constants of diamond braided composites, Journal of Composite Materials 35 (8), pp. 665-688.

[10] Zhao, Q., Hoa, S.V., (2003). Triaxial Woven Fabric (TWF) composites with open holes (Part I): Finite element models for analysis, Journal of Composite Materials 37 (9), pp. 763-789.

[11] Zhao, Q., Hoa, S.V., Ouellette, P. (2003). Triaxial woven fabric (TWF) composites with open holes (Part II): Verification of the finite element models, Journal of Composite Materials 37 (10), pp. 849-873.

[12] Carey, J., Awid, T., McCracken, P., Experimental Validation of Predictions for Open Mesh Braided Fibre Composites, Fifth Canadian-International Composite Conference, August 16-19, (2005), Vancouver.

[13] Carey, J., Munro, M., Fahim, A. (2005). Regression-based model for elastic constants of 2D braided/woven open mesh angle-ply composites, Polymer Composites 26 (2), pp. 152-164.

[14] Ayranci, C., Carey J., Elastic Properties of Large-Open-Mesh Diamond-Braided Tubular Composites: Comparison of Predictive and Experimental Findings, SAMPE Baltimore, MD. May 18 - 21 , 2009, 13 page manuscript.

[15] Naik, N.K., Shembekar, P.S. (1992). Elastic behavior of woven fabric composites: I-lamina analysis, Journal of Composite Materials 26 (15), pp. 2196-2225.

[16] Ayranci, C., Carey, J.P., Predicting the longitudinal elastic modulus of braided tubular composites using a curved unit-cell geometry, Composites Part B: Engineering, 41 (3), 229-235, 2010.

[17] Popov EP. (1990). Torsion, Engineering Mechanics of Solids, Second Edition, page 224, Toronto: Prentice Hall.

CHAPTER 6: EXPERIMENTAL VALIDATION OF A REGRESSION-BASED PREDICTIVE MODEL FOR ELASTIC CONSTANTS OF OPEN MESH TUBULAR DIAMOND-BRAID COMPOSITES

A version of this chapter was submitted to Polymer Composites and is currently under review:

The paper was co-authored by: Cagri Ayranci, Jason P Carey

6.1. Introduction

Braided composites are increasingly used for structural, aerospace, military and biomedical applications. The advantages of braids, such as properties variations through reinforcement positioning, increased toughness and greater resistance to delamination, production of complex parts and cost, have long been identified [1-3]. Although discussed to certain degree by various authors, the prediction of the elastic constants of large open mesh braided composites has not been clearly characterized.

Braided composites are formed by a series of angle-ply overlapping fiber strands. There are three main types of 2D braids: the single-overlapping diamond braid, the double overlap, or regular braid, and the triple strand overlapping Hercules braid. The focus of this work is the investigation of open-mesh diamond braids that have relatively large resin rich regions. A schematic view of the unit cell used for this study is shown in Figure 6.1 where resin rich regions, R_6 to R_9, between overlapping strands, R_1 to R_5, and undulating strands, R_{10} to R_{13}, are illustrated. A closed-cell braided composite, compared to an open-mesh braided composite, has no or minimal resin rich regions. Open-mesh braided composites can be utilized in low stiffness critical applications that require various levels of axial, flexural and torsional reinforcement.

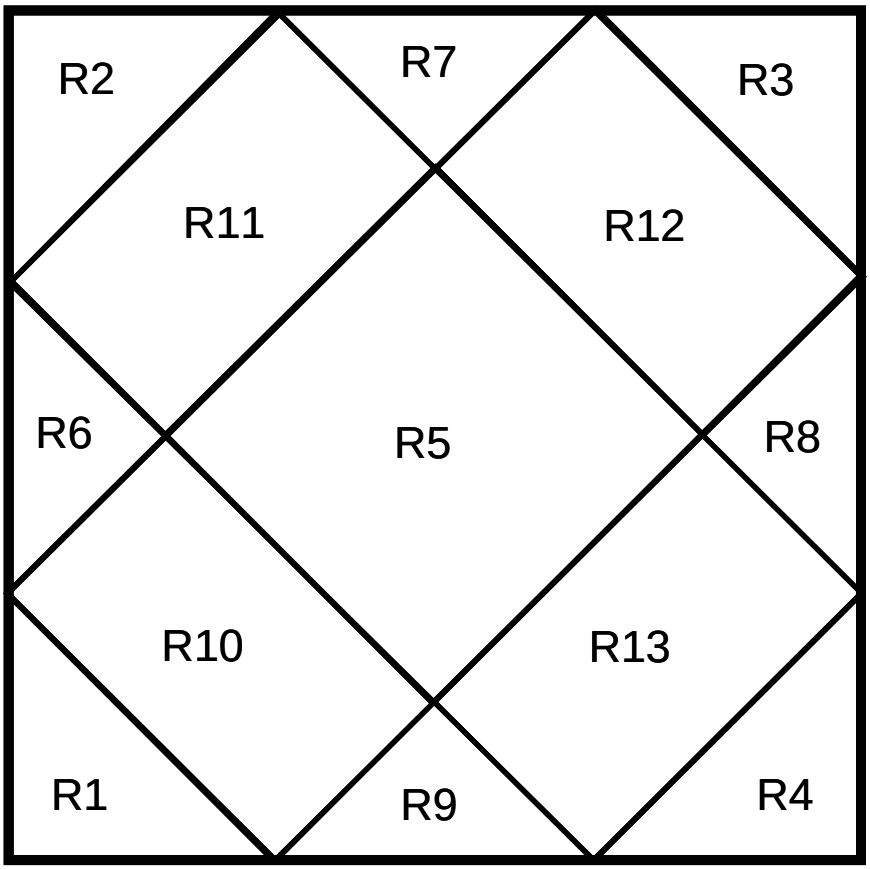

Figure 6.1: Open mesh single overlap braided unit cell; R1-R5 strand overlap; R6-R9 resin rich areas; R10-R13 undulating strand regions.

The development of braided composites was presented by Ko et al [4]. Dynamic and geometric variables for the production of different braid

configurations have been established [1, 5]. Conventionally, during the production of braided composites first the preform is produced as seen in Figure 6.2 (a). The preform is then coated with resin and cured following a strict resin-specific curing cycle and finally removed from the mandrel Figure 6.2 (b). This process is successfully utilized for manufacturing closed mesh braids impregnated by resin that form rigid tubes of interlocked fibers. Figure 6.2 (b) shows a closed mesh braided Kevlar 49/epoxy composite with a 25.4mm diameter.

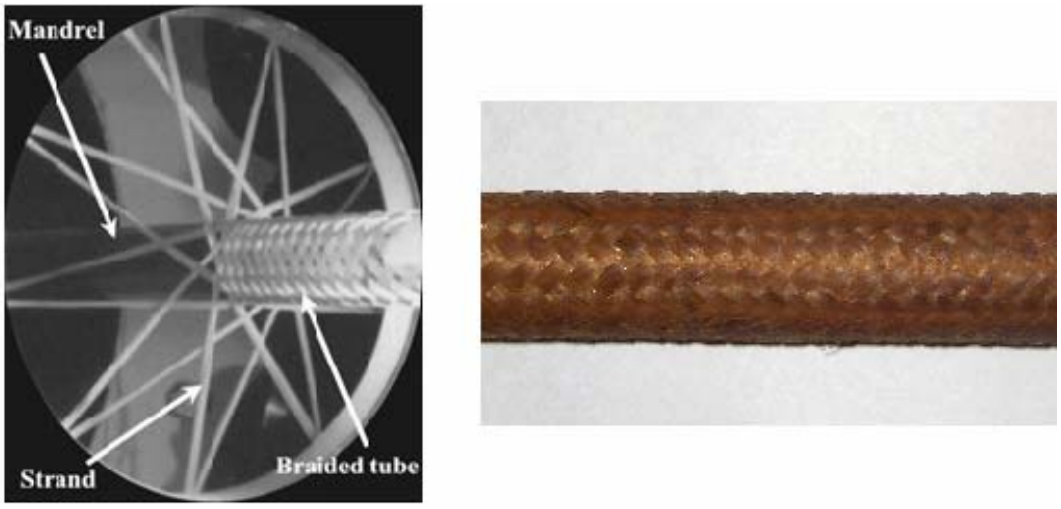

(a) (b)

Figure 6.2: (a) braided preform production; (b) cured closed mesh braided composite tube.

Elastic behavior of unidirectional composites, laminates and closed mesh braids has been detailed in previous works. It was shown [3, 6] that elastic constants for closed mesh composite materials were lower than that of laminates.

It was further shown that as the fiber volume fraction decreases, or the more open the braid configuration, the elastic constants continue to decrease; the limit of which has not been evaluated [6].

A number of models have been proposed to predict the elastic properties of laminate woven and braided composites. In 1997 Tan et al reviewed a number of these models [7]. These models can be listed as: Classical Laminate Plate Theory (CLPT) based models [8 - 11], the Fabric Geometry Model (FGM) [4], Finite Element Analysis (FEA) [12] and the Four-Cell Method (FCM) [13] that were used to predict longitudinal elastic (E_x), transverse elastic (E_y), and shear (G_{xy}) moduli as well as major Poisson's ratio (ν_{xy}) of the said composites. A thorough review of these models was presented in Ayranci and Carey (2008) [14].

Carey et al [6] developed an empirical Regression-Based Design Model (RBDM) for prediction of open and closed mesh braid elastic constants. Authors, [6], claimed the RBDM model to be simpler and computationally less time consuming. Authors reported the RBDM to be successful at predicting the longitudinal elastic modulus (less than 4 % error) and showed similar success as previous works at predicting the shear modulus of closed mesh braids. Carey et al [6] presented four empirical equations, that were based on linear regression analysis, to predict E_x, E_y, G_{xy} and ν_{xy} for braided/woven composites as a function of the laminate elastic constants at the same braid/weave angle (E^0_x, E^0_y, G^0_{xy}, ν^0_{xy}), as well as the braid/weave (V_{fo}) and laminate (V_f) fiber volume fractions for various braid configurations and with various material combinations. Equations

(1) to (3), repeated for completeness, are the equations for three in-plane elastic constants. The longitudinal elastic modulus of a θ angle plied composite is:

$$E_x(\theta) = E_x^0(\theta)\left(\frac{V_{fo}}{V_f}\right) \quad (1)$$

The transverse elastic modulus of a θ angle plied composite is:

$$E_y(\theta) = E_y^0(\theta)\left(\frac{V_{fo}}{V_f}\right) \quad (2)$$

The shear modulus of a θ angle plied composite is:

$$G_{xy}(\theta) = G_{xy}^0(\theta)\left[m\left(\frac{V_{fo}}{V_f}\right) + b\right] \quad (3)$$

where the slope, m, was defined following a Halpin-Tsai formulation [15]. Carey et al [6] was not able to determine an expression for the shear modulus regression equation's intercept; however they concluded that the intercept was a function of the resin properties.

The results of the major Poisson's ratio could not be predicted by a simple regression as in the earlier cases [6]. Authors found the influence of the resin to be more significant as a rigid epoxy matrix showed a gradual decrease of $\nu_{xy}(\theta) \ / \ \nu_{xy}^0(\theta)$ with decreasing V_{fo}/V_f as well as a decrease in $\nu_{xy}(\theta) \ / \ \nu_{xy}^0(\theta)$ as the braid angle neared 45°, while using a flexible polyurethane matrix only showed a slight decrease of $\nu_{xy}(\theta) \ / \ \nu_{xy}^0(\theta)$ with a decrease of V_{fo}/V_f [6].

V_{fo} / V_f of an open mesh braid can be calculated using the following equation developed for tube geometry:

$$\frac{V_{fo}}{V_f} = \frac{4L_e^2 \sin(\theta) \cos(\theta) + 2W_y a_u}{X \cdot Y} \tag{4}$$

where, W_y, h_c, a_u, t and θ are the strand width, the wet strand thickness, the undulation length, the tube wall thickness and the braid angle, respectively. The parameter L_e is defined as a function of W_y and braid angle as $L_e = W_y / \cos(2\theta - \pi / 2)$.

Figure 6.3 show typical $E_x(\theta) / E_x^0(\theta)$ versus V_{fo} / V_f (Figure 6.3 (a)) and $G_{xy}(\theta) / G_{xy}^0(\theta)$ versus V_{fo} / V_f (Figure 6.3 (b)) plots [16]. The longitudinal and transverse elastic moduli figures should be identical.

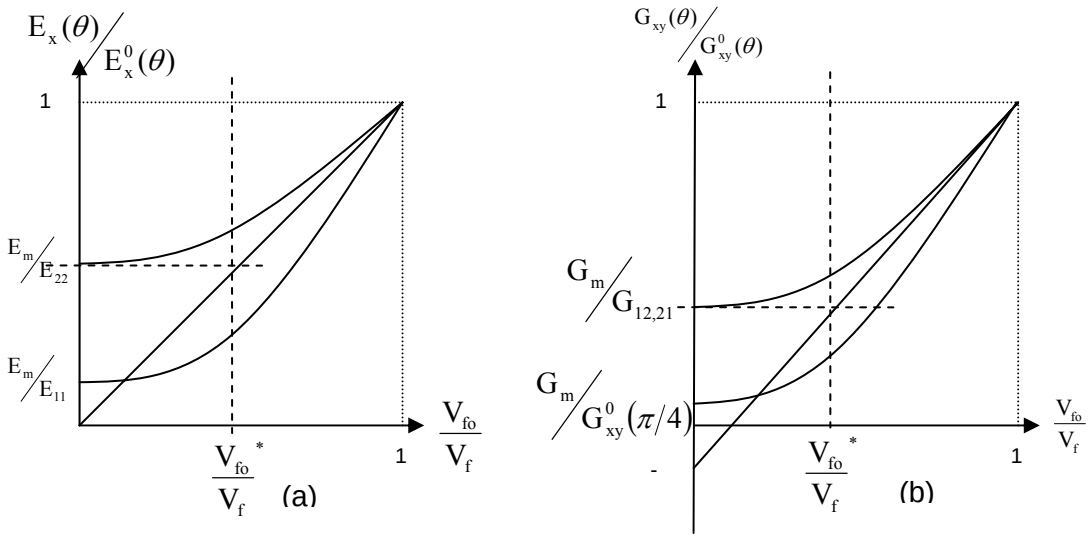

Figure 6.3: (a) Longitudinal elastic and (b) shear moduli to laminate ratios versus V_{fo}/V_f. $(V_{fo}/V_f)^*$ represents the lower linearity limit (LLL). [adopted from [16]].

As discussed originally, [6], the longitudinal elastic modulus and shear modulus cannot have their physical intercepts at 0 and -b, respectively, as determined by the RBDM for a fiber/rigid epoxy resin composite. The data approaches horizontal asymptotic values below a value of V_{fo}/V_f which will be termed the lower linearity limit (LLL), $\left(\frac{V_{fo}}{V_f}\right)^*$, for which the model should work [6, 16].

Carey et al discussed the physical significance of a $V_{fo}/V_f = 0$ for both longitudinal elastic and shear moduli [6]. The intercepts of Figure 6.3 (a) will vary from a value of E_m/E_{11} at a braid angle of 0° to E_m/E_{22} at a braid angle of 90°,

where E_{11} is the longitudinal elastic modulus and E_{22} is the transverse elastic modulus of a fiber composite lamina.

Similarly, for shear modulus, the intercept (Figure 6.3 (b)) will range between G_m/G_{12} or G_m/G_{21}, for laminate angles between 0° and 90°, respectively and $G_m/ G^0_{xy}(\pi/4)$ for a cross-ply laminate at 45°. It should be noted that G_{12} and G_{21} are the same.

From the review of the literature, it was found that the prediction of elastic constants of open-mesh diamond braids has not been adequately studied. The objective of this work is to further validate the longitudinal elastic and shear moduli regression equations using experimental data from in-house experiments as well as from the literature; determine the LLL for the RBDM model equations; and, assess the findings of the regression based predictive model for E_x, E_y and G_{xy} for large open mesh composites.

6.2. Specimens production and Methodology

The experimental results of the open-mesh braided composites used in this study were published earlier by the same authors for verification of an analytical model [17].

Reinforced tubing is used for various applications, such as flexible piping [18], catheters [19] and other medical applications. On the other hand, very limited data is available in the open literature regarding the production, testing and prediction of properties of open mesh composites. Anderson [20] reported on a degradable mandrel for thermoset and thermoplastic composites ; however, this method requires a new mandrel for every specimen. Semsarzadeh et al. [21]

proposed use of a rotating mold for a collapsible mandrel to be used for jute reinforced polyester structures.

Carey et al [22] stated that an ideal production method should produce geometrically accurate tubes, excellent surface smoothness, avoid crack formation and voids, ensure the integrity of the resin rich areas, be reusable and simple to use. Following the curing, removal of braided tubular composites from the mandrel is difficult. Although use of a mold release agent is helpful, adhesion and mechanical keying of the composite to the mandrel is unavoidable. Removal of the cured specimen from the mold requires large shear forces. Carey et al, [22] stated that use mold release was shown to be effective in the case of most closed mesh tubes, but production of open mesh braids using low viscosity thermoset epoxy resins was difficult. In open mesh braids, geometrical accuracy and surface smoothness of matrix-only regions can not be achieved easily, and result in cracks, voids, or complete failure of matrix-only regions. Specimens have regularly broken during production due to the fragility of the resin in pilot tests [22].

The test specimens of the study were produced using a steel mandrel with Teflon outer-liner. The reason for not using a Teflon-only mandrel was the fact that when the specimens are put into the oven at 110 degrees Celcius, the residual stresses in the Teflon-only mandrel caused it to warp. This was eliminated by inserting a steel mandrel inside a thin Teflon tube (i.e. the outer-liner). A mold assembly was designed, [22], to capture the resin during the curing process and to obtain a smooth and dimensionally accurate exterior surface. The mandrel /mold

assembly is illustrated in Figure 6.4. The mold was machined from two blocks of steel. The inner surfaces of the mold were ground for dimensional accuracy and smoothness. The mandrel is aligned using two alignment rings. The function of these rings is to keep the mandrel centered in the mold. The mold is aligned using simple dowel pins. The specimens were cured in the oven and after removal from the mold, the specimens were easily removed from the mandrel utilizing the advantages offered by the Teflon mandrel.

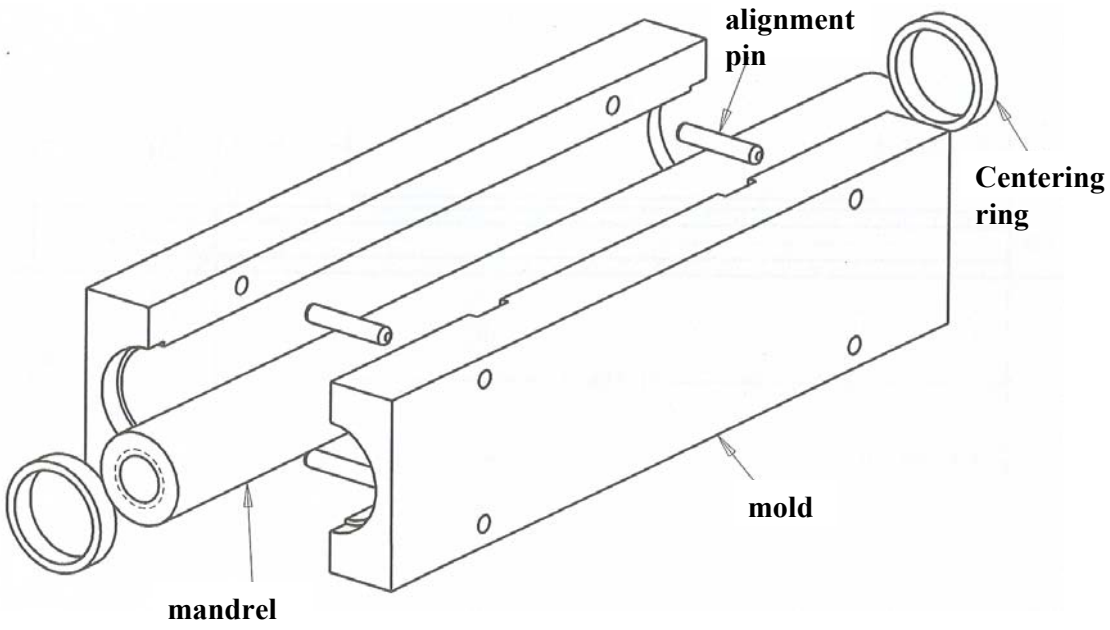

Figure 6.4: Schematic representation of the mold and the mandrel used for the production of the specimens [adopted from [22]].

Excellent quality specimens were produced using this method. The matrix only regions of the specimens had excellent integrity and dimensional accuracy. Also, excellent fiber impregnation and inner and outer surface quality was achieved. In a small number of the specimens air bubbles (Figure 6.5) was observed.

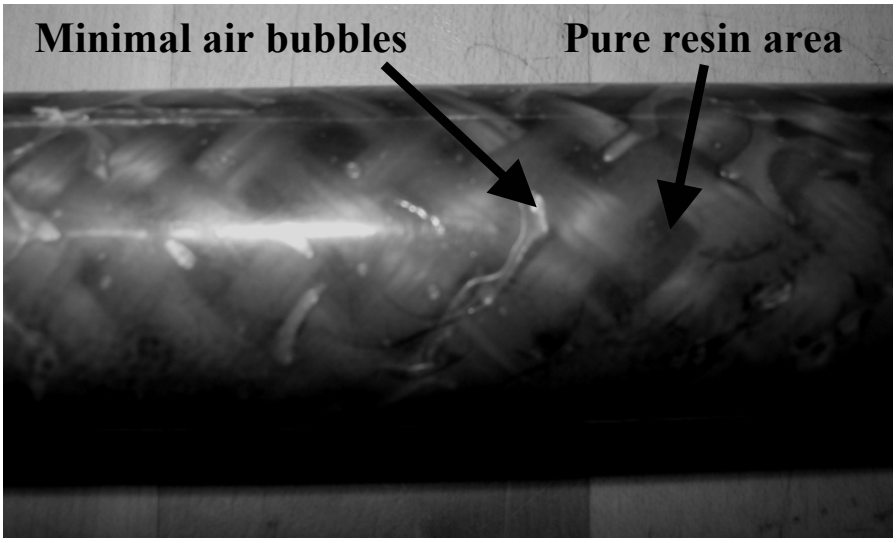

Figure 6.5: Sample specimen with small air bubbles on the outer surface. The resin rich area integrity is conserved with smooth surface and the high dimensional accuracy [adopted from [16]].

Figure 6.6 shows an actual sample test specimen (Figure 6.6 (a)) along with the Teflon mandrel and the two halves of the mold (Figure 6.6 (b)) used for the production of the specimens.

(a)

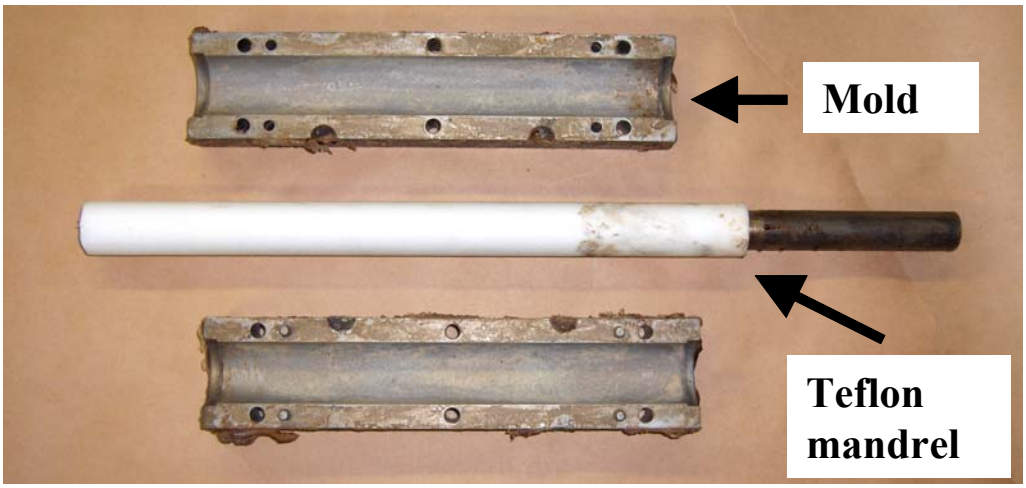

(b)

Figure 6.6: An actual sample test specimen (a) and the actual mold halves and the Teflon mandrel (b).

Three different composite material specimens (Kevlar/epoxy, Carbon/epoxy and S2-glass/epoxy) were constructed to evaluate the tensile longitudinal and shear elastic behavior of open mesh braids. Constituent and lamina properties are listed in Table 6.1. Curing schedule specified for the epoxy resin in the work by Flanagan and Munro [23] was followed.

Table 6.1: Constituent and lamina elastic constants. ("*"Provided by manufacturer; "" back calculated using Halpin-Tsai [15]; "***" experimental, see reference; "****" micromechanical models)**

Material	**Elastic constants**			
Constituent	**E_{f11} (GPa)**	**E_{f22} (GPa)**	**G_{f12} (GPa)**	**ν_{f12}**
Kevlar 49 fiber	130*	7.3 [23] **	2.86*	0.35*
Carbon fiber*	220	13.8	9.0	0.2
S2-glass*	96.5	96.5	39.2	0.23
	E_m		**G_m**	**ν_m**
Epon 825/ Ancamine 1482 resin*** [23]	3.5	-	1.3	0.3
Lamina (V_{f0} =60%)	**E_{11} (GPa)**	**E_{22} (GPa)**	**G_{12} (GPa)**	**ν_{12}**
Kevlar 49/epoxy*** [23, 24]	79.7	5.9	1.5	0.33
Carbon/epoxy****	133.4	7.9	3.9	0.24
S2-glass/epoxy****	59.3	15.8	6.0	0.26

For the tensile tests, an MTS 810 material testing system, with an MTS 20E-3, 100 kN maximum load cell and MTS 634.12E-24 extensometer were used to measure the tensile load-strain curves at a strain rate of 1mm/min. For the torsion tests, an MTS-Torsion Master testing machine (MTS Systems Corporation

Eden Prairie, MN, USA) with a load cell of 2 Nm torsional load capacity was used [17]. Specimens were twisted with a loading rate of 0.03 degrees/second.

6.3. Results and discussion

6.3.1. Experimental findings

Specimen information is listed in Table 6.2 and a picture of a typical specimen, with resin rich areas highlighted, is found in Figure 6.5. The small standard deviations in the specimen dimensions listed in Table 6.2 demonstrates the success in producing repeatable and high quality specimens. Some specimens had a minimal number of air pockets within the resin rich areas. The three types of fibers (Kevlar, Carbon, S2-glass) provide a greater range of V_{fo}/V_f for comparison of RBDM model and the experimental results.

Table 6.2: Specimen information and average (± standard deviation) dimensions as defined in equation 4.

Tensile test specimens						
Specimen type	**Samples**	**θ (deg)**	**ID (mm)**	**t (mm)**	**W_y (mm)**	**a_u (mm)**
Kevlar/ epoxy	5	44.19 ± 1.63	24.71 ± 0.28	1.51 ± 0.15	3.81 ± 0.68	1.50 ± 0.32
Carbon/ epoxy	5	41.80 ± 0.11	24.54 ± 0.19	1.58 ± 0.09	3.40 ± 0.22	2.00 ± 0.51
S2-glass/ epoxy	4	46.00 ± 1.30	24.53 ± 0.47	1.48 ± 0.04	3.34 ± 0.54	3.89 ± 0.08
Torsion test specimens						
Specimen type	**Samples**	**θ (deg)**	**OD (mm)**	**t (mm)**	**W_y (mm)**	**a_u (mm)**
Kevlar/ epoxy	5	50.56 ± 2.16	27.56 ± 0.13	1.27 ± 0.11	4.70 ± 0.27	4.34 ± 0.70
Carbon/ epoxy	3	41.93 ± 1.15	27.72 ± 0.06	1.05 ± 0.04	3.72 ± 0.33	3.85 ± 0.43
S2-glass/ epoxy	5	38.89 ± 0.72	27.65 ± 0.04	1.04 ± 0.01	3.51 ± 0.43	3.78 ± 0.52

Average longitudinal elastic moduli (standard deviation) results of the experimental study were 2.85 (0.46) GPa, 3.03 GPa (0.77), and 1.44 (0.09) GPa for Kevlar/Epoxy, Carbon/Epoxy, and S2-Glass/Epoxy systems, respectively. Average shear moduli results of the experimental study were 1.6 (0.15) GPa, 2.75 (0.41) GPa, and 1.75 (0.06) GPa for Kevlar/Epoxy, Carbon/Epoxy, and S2-Glass/Epoxy systems, respectively.

6.3.2. Regression model predictions

6.3.2.1. Longitudinal elastic modulus

Very limited published documents available in the literature provide all of the necessary information from their experimental procedure, or have the correct braid/weave architecture, to compare with the current RBDM; therefore, the following findings from the previous experimental results by the authors [11] and the experimental results presented earlier are plotted in Figure 6.7 for comparison of experiments and regression based model findings.

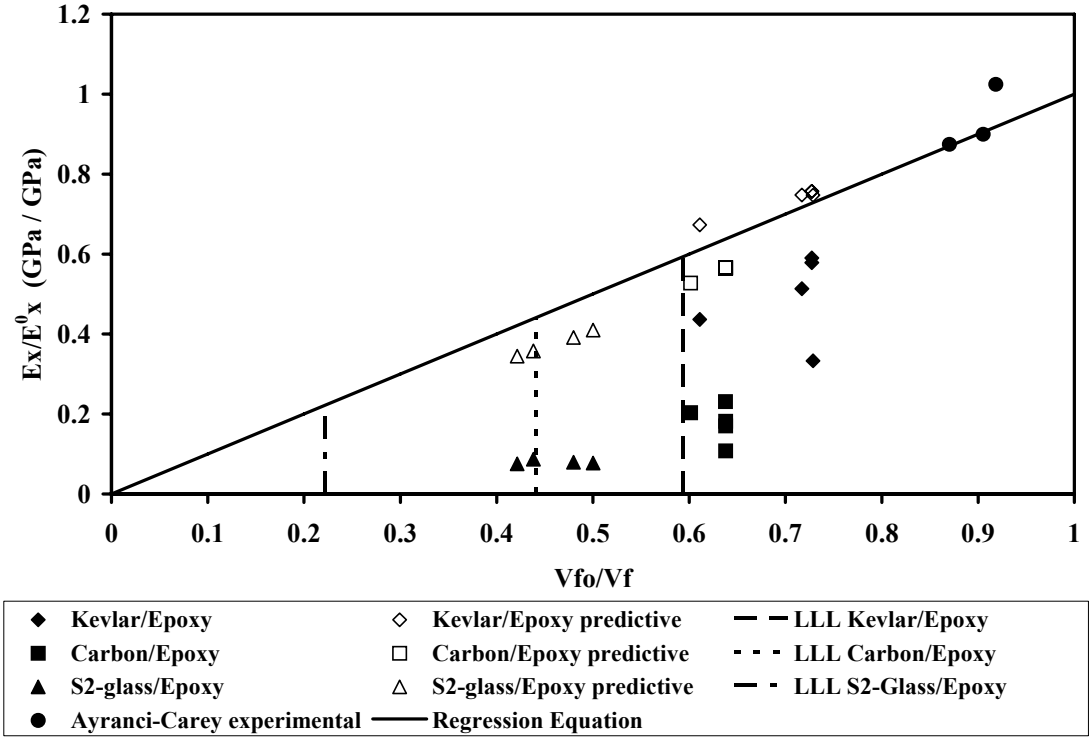

Figure 6.7: Comparison of the RBDM predictions (the regression equation predictions) for longitudinal elastic modulus (Equation 1) and experimental data. Also, LLL are presented.

In the previous work of the authors, [11], specimens with three different diameters were tested, five specimens per diameter. Average findings for each diameter are repeated using the legend name "Ayranci-Carey experimental" in Figure 6.7. The results were 0.90, 0.87, 1.02 (GPa/GPa) for E_x/E^0_x values versus 0.91, 0.87, 0.92 for V_{fo}/V_f , respectively. The specimens were closed-mesh braided Kevlar/epoxy tubular composites.

The findings presented earlier in this paper (Section 3.1) for the three types (Kevlar-, Carbon-, S2-Glass/Epoxy) of open mesh braided composites are also presented in Figure 6.7 by using the legend names "Kevlar/Epoxy", "Carbon/Epoxy", and "S2-Glass/Epoxy". Additionally, in Figure 6.7, predicted results of E_x/E^0_x for these specimens using the measured geometry are included (legend names: "Kevlar/Epoxy predicted", "Carbon/Epoxy predicted", and "S2-Glass/Epoxy predicted"). The predictions were done for comparison purposes using an analytical model presented by the authors earlier [11].

6.3.2.2. Shear modulus

Previous shear modulus experimental results [17] were reproduced using the legend name "Ayranci-Carey experimental" in Figure 6.8. Secondly, the findings presented above for the three types of open mesh braided composites are presented using the legend names "Kevlar/Epoxy", "Carbon/Epoxy", and "S2-Glass/Epoxy". Additionally, predicted results of G_{xy}/G^0_{xy} for the same specimens using the measured geometry are included (legend names "Kevlar/Epoxy predicted", "Carbon/Epoxy predicted", and "S2-Glass/Epoxy predicted"). The predictions were done using an analytical model presented by the authors earlier [11]. This was done for comparison purposes.

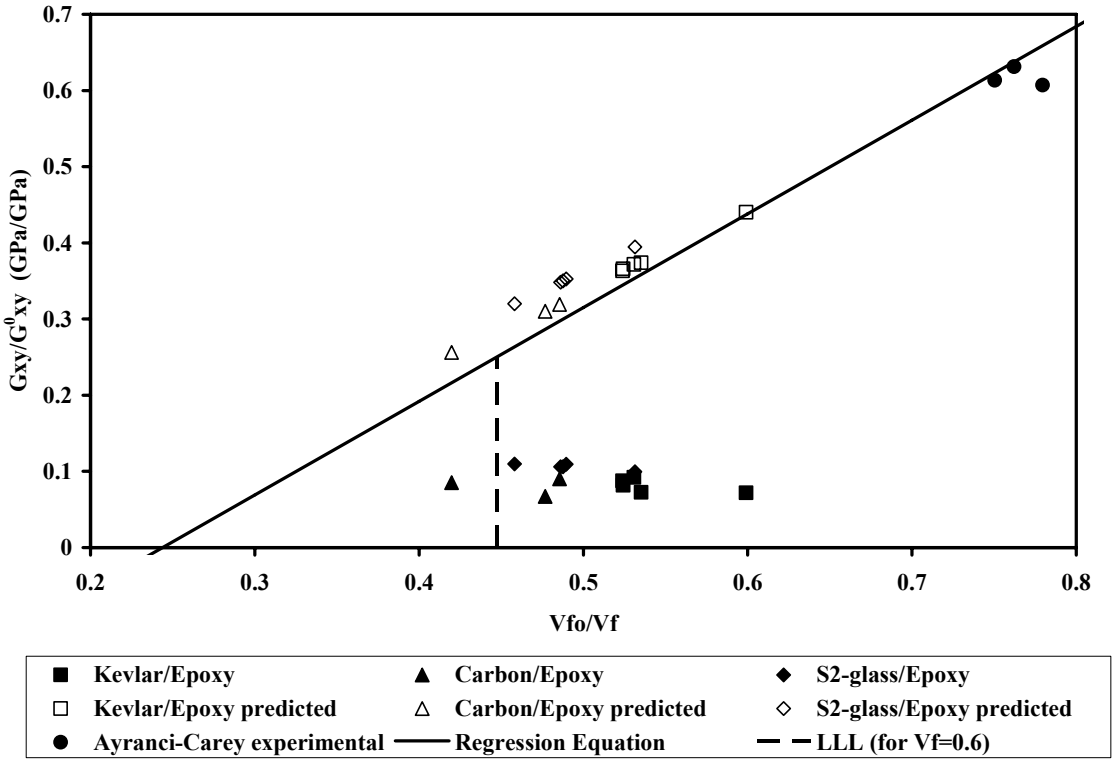

Figure 6.8: Comparison of the RBDM predictions (the regression equation predictions) for shear modulus (Equation 3) and experimental data. Also, LLL is presented.

6.3.2.3. Lower linearity limit (LLL)

This work also wished to establish the LLL for RBDM based on constituent material properties for the longitudinal elastic and shear moduli regression equations. Initial development of the formulae presented here was presented earlier [16] and is repeated here for completeness purposes. Micromechanical models have long been developed for lamina longitudinal (E_{11}) and transverse (E_{22}) elastic moduli. The longitudinal elastic modulus is typically

calculated from a rule of mixtures formula (equation (5)), while the transverse modulus is calculated from the Halpin-Tsai formulation (equation (6)) [15].

$$E_{11} = E_f V_f + E_m(1 - V_f) \tag{5}$$

$$E_{22} = E_m \frac{1 + \xi\eta V_f}{1 - \eta V_f} \tag{6}$$

where

$$\eta = \left(\frac{E_f}{E_m} - 1\right) \Big/ \left(\frac{E_f}{E_m} + \xi\right)$$

and ξ is typically 2 for square or round fibers.

In order to define the LLL, the upper limit of the two intercepts seen in Figure 6.3 (a) will be selected as selecting a value lower than E_m/E_{22} extends the region in which the linear regression is valid. In order to adopt a safe design model, it is assumed that the fiber and resin elastic moduli, E_f and E_m, respectively, and the laminate fiber volume fraction are known. This naturally leads to the boundary:

$$\left(\frac{V_{fo}}{Vf}\right)^* = \frac{E_m}{E_{22}} \tag{7}$$

Investigation of Equation (7) reveals that the LLL is dependent of constituent properties. This characteristic is essential for the RBDM to be a simpler model. For the Kevlar, Carbon and S2-glass test cases the LLL were calculated as 0.59, 0.44, and 0.22 (Figure 6.7), respectively, for laminate fiber volume fraction of 0.6. Below the LLL, it is expected that there is a point were the fiber strands are no longer effective reinforcements, in the same way that a minimum fiber volume fraction is necessary to have an effective lamina strength [25]. Hence it may be suggested that for longitudinal and transverse elastic moduli the range of values for which the RBDM is valid is:

$$\frac{E_m}{E_{22}} \leq \frac{V_{fo}}{V_f} \leq 1 \tag{8}$$

Since the LLL is defined using the upper horizontally asymptotic value, E_m/E_{22}, of Figure 6.3 (a), an analysis of the possible range of intercepts for Figure 6.3 (a) was performed using equations (5) and (6) to give an indication as to where the lower asymptotic value, E_m/E_{11}, would be located on the figure. This range of difference between E_m/E_{22} and E_m/E_{11} is plotted in Figure 6.9 for different ratios of E_m/E_f at three typical laminate fiber volume fractions, $V_f = 0.5$, 0.6 and 0.7. Using a typical elastic modulus for epoxy, 3.5GPa, for E_m and using a wide range for the fiber elastic modulus, E_f, (20GPa to 230 GPa to include commonly used fibers such as graphite (E_{11}=230 GPa), Kevlar (E_{11}=130 GPa) and Glass fiber (E_{11}=72 GPa)) a range of E_m/E_f was selected. From Figure 6.9 it was

found that the range between the intercepts in Figure 6.3 will not exceed 0.325 if V_f remains between the commonly used range of 0.5 to 0.7.

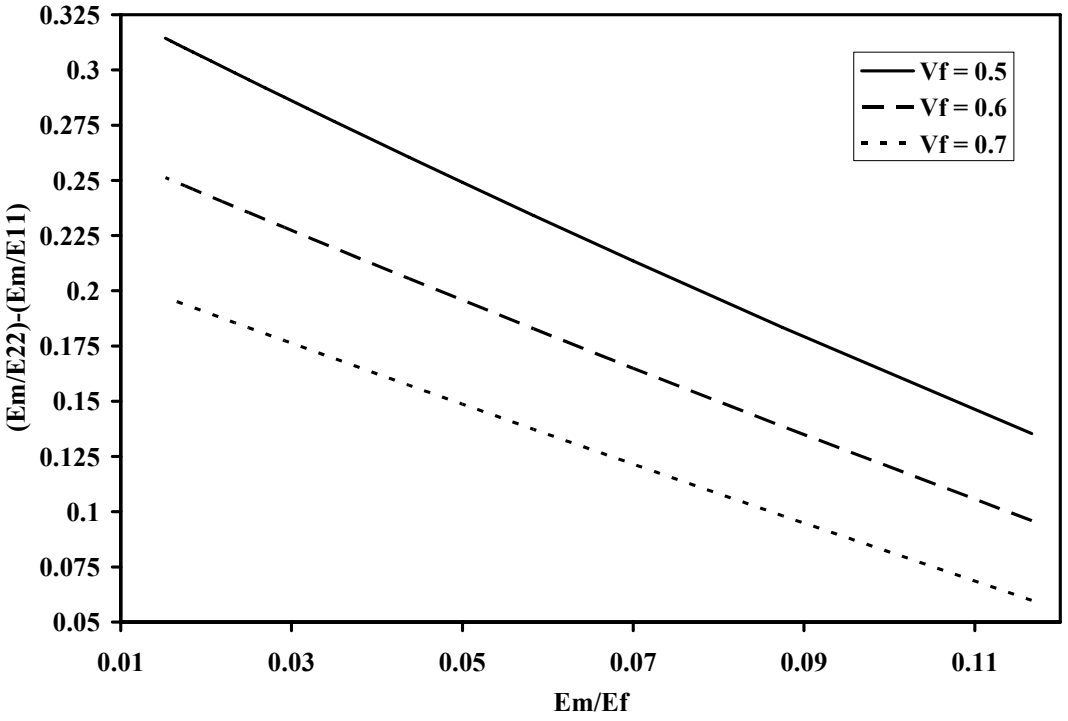

Figure 6.9: Difference between upper and lower intercepts for longitudinal elastic modulus versus Em/Ef at three different laminate volume fractions.

A number of micromechanical models are available for lamina in-plane shear modulus, G_{12}. According to a comparison by Barbero [26] between experimental results and predictions of various models, the matrix dominated

cylindrical assemblage model (Equation 9) [27] provides the best predictions if $G_m << G_f$.

$$G_{12} = G_m \frac{1 + V_f}{1 - V_f} \tag{9}$$

Similar to the longitudinal modulus case, selecting the upper limit of G_m/G_{12} to be the safest point at which for the LLL, $(V_{fo}/V_f)^*$ is calculated by equating equations (3) and (9) such that:

$$\frac{G_m}{G_{12}} = \frac{1 - V_f}{1 + V_f} = \left[m\left(\frac{V_{fo}}{V_f}\right)^* + b \right] \tag{10}$$

which leads to:

$$\left(\frac{V_{fo}}{V_f}\right)^* = \frac{1}{m}\left[\frac{1 - V_f}{1 + V_f} - b\right] \tag{11}$$

where, m was defined earlier. This can be seen in Figure 6.3 (b). For Kevlar, Carbon and S2-glass test cases the LLL were calculated as 0.45, Figure 6.8, for laminate fiber volume fraction of 0.6. Again, below the LLL, it is expected that the findings will show that there is a point were the fiber strands appear to no longer be effective reinforcements [25]. The range of values for which the RBDM is valid for shear modulus is:

$$\frac{1}{m}\left[\frac{1 - V_f}{1 + V_f} + b\right] \leq \frac{V_{f0}}{V_f} \leq 1 \qquad (12)$$

6.4. Discussion

The regression based model was initially developed for closed- and open-mesh braids, but it was only verified using experimental data of closed-mesh braids [6]. The closed mesh data used in Figure 6.7, legend name "Ayranci-Carey experimental", proves the validity of model for closed-mesh braids once more as the experimental results agree well with the Regression equation line plotted on Figure 6.7. On the other hand, the open-mesh braid experimental data presented in Figure 6.7 do not agree with the regression model as well as the closed-mesh braid results. However, the third set of data, that was obtained using an analytical model (legend names: "Kevlar/Epoxy predicted", "Carbon/Epoxy predicted", and "S2-Glass/Epoxy predicted"), presented in Figure 6.7 again agree well with the regression based model for all three types of the open-mesh braided composites (Kevlar/Epoxy, Carbon/Epoxy, and S2-Glass/Epoxy).

The regression based model was originally structured using E_x/E^0_x versus (Vfo/V_f) for a range of braid angles between 29.5 degrees and 62.5 degrees. Using regression equations for a number of angles in between this range, lead to the formation of the final formulae (Equation 1). The predictions for the two extreme cases, of 29.5 degrees and 62.5 degrees, used for this process are repeated here for the sake of the discussion, Figure 6.10. As seen in Figure 6.10, the E_x/E^0_x range

covered by the assigned regression equation (Equation 1) for any given value of (Vfo/V_f) narrows down as the (Vfo/V_f) approaches to unity. Hence, it may be reasonable to expect that the regression model to be more accurate as the braid structure gets closer to closed-mesh. Naturally, the opposite can be argued as the braid structure becomes more open-mesh (i.e. for Vfo/V_f values of 0.65 and lower.).

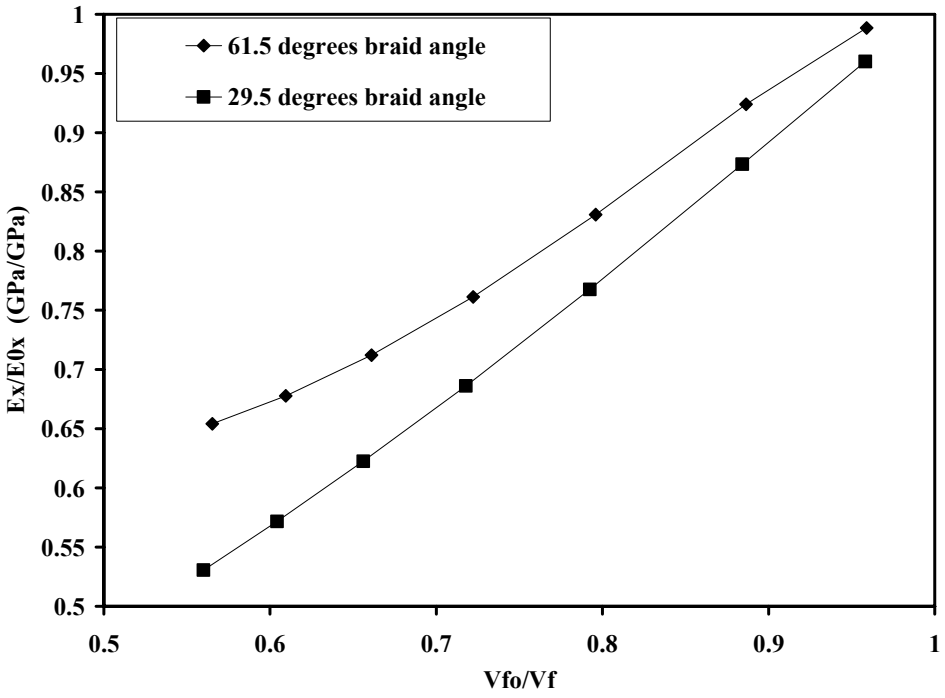

Figure 6.10: Repeated data from the original regression based paper [6].

Investigation of Figure 6.7 shows the Kevlar/, Carbon/, and S2-Glass/Epoxy open mesh composites had average Vfo/V_f values of 0.7, 0.63, and 0.46, respectively. Hence, similar to the discussion above, the results are closer to

the regression line as the V_{fo}/V_f gets larger; i.e. S2-Glass/Epoxy specimens have the smallest V_{fo}/V_f and are furthest away from the regression line, where as the Kevlar/Epoxy specimens are the closest. The spread of all data presented in Figure 6.7 also shows a narrowing trend (similar to Figure 6.10) as the V_{fo}/V_f gets larger.

Other reasons behind the differences between the regression model and the experimental findings may be due to one of the basic assumptions used in the original development of the regression based model: the unit cell was assumed to be under uniform strain upon application of load. This assumption may be correct for closed-mesh braided structures, where regions R_6 to R_{13} are very small compared to regions R_1 to R_5 (Figure 6.1), as regions with similar elastic properties are adjacent to each other. On the other hand, the assumption may be incorrect as the structure becomes open-mesh, because, as the undulation length increases, the elastic properties of the adjacent regions may not be similar to each other if one considers the low elastic modulus properties of matrix-only regions (R_6 to R_9). Hence, upon application of a load, it may be reasonable to expect non-uniform deformations between the regions of a unit cell. This may result in a different loading mode such as bending of the undulating regions that are lacking lateral support due to the low modulus matrix-only regions.

An alternative or additional possibility, is that this could be seen as an analogous situation to geometric stress concentration factors, although verification of this statement would require a specific target-study on such effects the following discussion should provide theoretical support to the proposed notion.

The tubular open-mesh tensile test specimens were roughly 25 mm in diameter. Upon loading, due to the elongation, the structure is expected to decrease in diameter. If the structure was assumed to decrease down to 24 mm during a test, it may be argued the stress concentration developed in the structure may be approximated from the commonly used stress concentration factor diagrams for round stepped shafts under longitudinal loading. Norton gives the formula for the stress concentration factor of such a shaft as [28]:

$$Kt = A\left(\frac{r}{d}\right)^{b} \tag{13}$$

where A and b are geometric parameters and r is the radius of the step, and d is the smaller (stepped down) diameter (24 mm for the case in hand). Using the assumed parameters above and assuming $r = d / 10$, parameters A and b are found as 1.00480 and -0.17076, respectively. Hence, the stress concentration factor is found approximately as 1.48. The ratio between the average of the open-mesh braid Kevlar/Epoxy longitudinal elastic modulus and the model prediction was roughly 1.46 which is very close to the stress concentration factors calculated above. The ratio between the average of the open-mesh Carbon/Epoxy and model prediction, and S2-Glass/Epoxy and the model prediction was 2.93 and 4.45, respectively. This can be explained in part by the brittleness of carbon and glass as compared to Kevlar; intensity of stress concentration factors is higher in brittle materials. Furthermore, the differences could be indicative of localized behaviors

at the strand-resin rich region interface between two brittle materials (fiber and resin).

Similar to the longitudinal elastic modulus results, the closed mesh data used in Figure 6.8 for shear modulus results, legend name "Ayranci-Carey experimental", proves the model validity for closed-mesh braids once more as the experimental result agrees well with the Regression equation line plotted on Figure 6.8. On the other hand, the open-mesh braid experimental data presented in Figure 6.8 do not show good agreement with the regression model as well as the closed-mesh braid results. However, the third set of data, that was obtained using an analytical model (legend names: "Kevlar/Epoxy predicted", "Carbon/Epoxy predicted", and "S2-Glass/Epoxy predicted"), presented in Figure 6.8 again agrees well with the regression based model for all three types of the open-mesh braided composites (Kevlar/Epoxy, Carbon/Epoxy, and S2-Glass/Epoxy).

The calculated LLL values are shown in Figure 6.7 and Figure 6.8. Almost all of the experimental data are at or above the LLL limit calculated; however, similar to Figure 6.3 (a) and (b), the spread deviation from the regression line increases as the V_{fo}/V_f gets closer to the LLL and show asymptotic behavior as predicted lending credence to the proposed approach.

6.5. Conclusions

Experimental verification of a previously developed regression-based model was conducted for simpler initial design calculation purposes of braided composite materials. The results of the model match well with experimental

findings for close-mesh braided composites; however, for open-mesh braided composites the results show differences. In the paper, possible reasons for this behavior are discussed. The lower linearity limit (LLL) of the model for different fiber-matrix systems were calculated and discussed. These initial experimental results comparison suggest a full characterization of the model can be possible by increasing the experimental data pool in the literature which is currently very limited.

6.6. References

[1] Brunnschweiller, D., Braids and Braiding, Journal of the Textile Institute Proceedings, 45: 9, 668-686, 1953.

[2] Brunschweiller, D., The Structure and Tensile Properties of Braids. Journal of the Textile Institute Transactions, 45:1, T55-T77, 1954.

[3] Aggarwal, A., Ganesh, V.K. and Ramakrishna, S. (2001). Predicting the in-plane elastic constants of diamond braided composites. Journal of Composite Materials, 35(8): 665–688.

[4] F. K. Ko, C.M. Pastore, and A. A. Head, Atkins and Pearce Handbook of Industrial Braiding, Covington, Kentucky: Atkins and Pearce, (1989).

[5] Du, Guang-Wu, Popper, Peter, Chou, Tsu-Wei, "Process model of circular braiding", American Society of Mechanical Engineers, Materials Division (Publication) MD 19, pp. 119-133, (1990).

[6] Carey J, Munro M, Fahim A, Regression-Based Model for Elastic Constants of 2-D Braided/Woven Open Mesh Angle-Ply Composites, Polymer Composites, 26(2), 152-164 (2005).

[7] Tan, P., Tong, L. and Steven, G.P. (1997). Modelling for predicting the mechanical properties of textile composites – A review. Composites Part A, Applied Science and Manufacturing 28 (11), pp. 903-922.

[8] Ishikawa, T. and Chou, T.-W., Stiffness and Strength Behavior of Woven Fabric Composites, Journal of Materials Science, 17 (11), 3211-3220 (1982).

[9] Raju, I.S. and Wang, J.T., Classical Laminate Theory Models for Woven Fabric Composites, Journal of Composites Technology and Research, 16(4), 289-303 (1994).

[10] Carey J, Munro M, Fahim A, Longitudinal Elastic Modulus Prediction of a 2-D Braided Fiber Composite, Journal of Reinforced Plastics and Composites, 22(9), 813-832 (2003).

[11] Ayranci, C., Carey, J.P., Predicting the longitudinal elastic modulus of braided tubular composites using a curved unit-cell geometry, Composites Part B: Engineering, 41 (3), 229-235, 2010.

[12] Nakai A., Hamada H., Hoa, S.V., Influence of braiding structure on torsional properties of braided composite tube, American Society of Mechanical Engineers, Pressure Vessels and Piping Division (Publication) PVP 326, pp. 125-130, (1996).

[13] Tabiei, A., and Yi, W., Comparative Study of Predictive Methods for Woven Fabric Composite Elastic Properties, Composite Structures, 58 (1),149-164 (2002).

[14] Ayranci, C., Carey, J., 2D braided composites: A review for stiffness critical applications, Composite Structures 85 (1), pp. 43-58, (2008).

[15] Halpin, J.C. and Tsai, S.W., Effects of Environmental Factors on Composite Materials, AFML-TR 67-423, 1969.

[16] Carey, J., Awid, T., McCracken, P., Experimental Validation of Predictions for Open Mesh Braided Fibre Composites, Fifth Canadian-International Composite Conference, August 16-19, (2005), Vancouver.

[17] Cagri Ayranci, Daniel Romanyk, Jason P Carey , Elastic properties of large-open-mesh 2D braided composites: model predictions and initial experimental findings, submitted to Polymer Composites and accepted for publication on 23 March 2010.

[18] web source, Reinforced Polyurethane Tubing, visited on 02 February 2010, "http://www.eldonjames.com/html/polyb.html".

[19] Carey, J., Fahim, A., Munro, M., Design of Braided Composite Cardiovascular Catheters Based on Required Axial, Flexural and Torsional Rigidities, Journal of Biomedical Materials Research Part B: Applied Biomaterials, 70 (1), 73-81 (2004).

[20] Anderson, M. H., Internal cavity-forming process for high-temperature polymer composites, Society of Manufacturing Engineers Technical Papers Ser EM, EM89-107 (1989).

[21] Semsarzadeh, Mohammad A., Lotfali, Abdol R., Mirzadeh, Hamid, Jute reinforced polyester structures, Polymer Composites 5 (2), pp. 141-142, (1984).

[22] Carey, J., McCracken, P., Awid, T., Production and Failure Testing of Open Mesh Braided Fibre Composites, The Fifth Canadian-International Composite Conference, August 16-19, Vancouver.

[23] Flanagan, R.C., Munro M., High Energy Density Fiber Composite Rotors, Volume 2, Department of Mechanical Engineering, University of Ottawa, Technical Report no UOME-FP-8603-1, 1986.

[24] Quenneville, G.-M., Determination of Shear Properties of Fiber Composite Materials, Fourth Year Undergraduate Thesis, Department of Mechanical Engineering, University of Ottawa, Ottawa, Canada (1986).

[25] Agarwal, B.D. and Broutman L.J., Analysis and Performance of Fiber Composites, 2nd Edition, Wiley-Interscience, (1990).

[26] Barbero, E. J., Introduction to Composite Materials Design, Taylor and Francis, (1999).

[27] Hashin, Z. and Rosen, B.W., the Elastic Moduli of Fiber Reinforced Materials, Journal of Applied Mechanics, June, 223-230 (1964).

[28] Norton, R.L., Machine Design, An Integrated Approach, 2nd edition, Prentice Hall, 2000.

CHAPTER 7: SUMMARY, CONCLUSIONS, AND FUTURE WORK

The studies were conducted to provide an accurate model predict elastic properties of braided composite tubes to be used for braided medical catheters and other low stiffness requirement designs.

First, an analytical model that recognizes the effects of curvature on the unit cell of braided tubular composites as a function of the diameter of the tubular composite was developed. The model predictions were compared to and validated using a flat-model prediction available in the literature by setting a large-enough diameter for the curved-unit cell predictions to obtain comparable results. In a particular case study, results of curved- versus flat-model showed up to 4.7 % difference which may be an important difference for a catheter design. In another case study, between curved- and flat-model predictions, approximately 7.2% differences were observed for both the longitudinal elastic and shear moduli properties. On the other hand, Poisson's ratio was found to be insensitive to the changes in the diameter of the braided tubular composites. Findings of longitudinal elastic and shear moduli of the curved-model were validated using experimental findings. For this purpose, tensile and torsion experiments were conducted for three different diameter braided composites. Excellent agreements were observed between the predicted and experimental results for both longitudinal and shear modulus.

Properties of open-mesh braided tubular composites were predicted and compared to that of closed-mesh braided tubular composites using the developed analytical model. This was done by gradually increasing the undulation length in the unit cell. It was observed that elastic properties decrease as the undulation length increase. Results were compared to that of an in-house experiments that were conducted using three different fiber/matrix composite system, namely, Kevlar/Epoxy, Carbon/Epoxy, and S2-Glass/Epoxy. Analysis of the results showed that, as predicted by the analytical model, decrease in elastic properties were observed; however, comparison of experimental and predicted results showed that the decrease in the results of experimental findings were higher than the ones predicted. A conclusive correlation between experimental and predicted results was not reached. Possible reasons for this behavior were discussed and an experimental study was suggested to obtain a correlation factor. Preliminary experiments with open-mesh braided specimens without matrix-only regions (i.e. stent like structures) were also carried out. The proposed analytical model predictions and experimental results for these stent-like structures were in agreement.

Finally, experimental verification of a previously developed regression-based model was done using the closed mesh experimental data (Chapters 3 and 4) and experimental data collected for the open-mesh structures (Chapter 5). Good agreement with the closed-mesh results was obtained; however, differences in open-mesh results were observed. The possible reasons between differences in the

findings were discussed. Also, Lower Linearity Limits (LLL) of the model for different fiber/matrix systems were determined.

Contributions

This PhD study contributed to the field of study in numerous ways:

1. The developed curve model is more accurate then previous models, and provides a better tool to the designers to achieve more accurate designs for such a crucial device that is used in human body. The model investigates the effects of tube diameter, via unit cell radius of curvature, on the elastic properties of tubular braided composites that have not been previously done in the literature.

2. Via parametric studies, the important parameters that have direct effect on the elastic properties of the braided composites have been determined. This again is a crucial tool for the designers to achieve better results.

3. Effect of undulation length on elastic properties of braided catheters is underlined using the developed model. Catheters, due to their nature, may need changing rigidities throughout their lengths. One of the limited ways to achieve this is to change the braid angle. Having control over one more parameter, undulation length, is very important to give flexibility to the designer.

4. Currently very limited experimental data are available in the literature about open mesh braided composites. Direct comparison results showed that the decrease in properties due to increase in undulation length is actually higher than the predicted values which highlighted an important gap in the literature that needs to be closed.

5. Further validation of a previously developed practical design model, regression based model, was conducted. Also, lower linearity limit for the predictions of this model was determined which tells the designers the theoretical limitations of the model.

Future Work

The findings of this PhD thesis study contributes greatly to the improvement of braided catheter design. As a result of this work, there is a need for further investigations in following new areas:

1. Catheters have small inner and outer diameters, as an example approximately 1 mm inner diameter and 2mm outer diameter. As a follow up to the works presented in Chapters 3 and 4, further investigation and validation of the model with real catheter size specimens are required.

2. Using the developed model and experimental findings, design curves that specify critical braid diameters as a function of strand geometry should be plotted.

3. Effect of curvature induced state of strain of the strands and fiber-matrix interface interactions on the model predictions should be investigated to further improve the model. Experimental results can be further analyzed using the curvature induced state of strain of the strands due to unit cell curvature.

4. The model was developed assuming use of un-twisted strands. Effect of twisted strands on the elastic properties should be analyzed.

5. The uniform strain assumption that was used in the model needs to be further investigated as it is suspected that the differences between the

experimental and predicted results for open-mesh braided structures may be related to this assumption.

6. As a follow up on the work discussed in Chapters 5 and 6, an experimental study needs to be conducted to fully characterize the behavior and properties of open-mesh composites. The experimental data pool in the literature is currently very limited prohibiting a successful attempt to suggest a correlation factor between the open-mesh experimental results and model predictions.

This is possible using a fully automated manufacturing technique. Homogenously impregnated, defect free specimens with high dimensional tolerances should be produced and tested to minimize the spread in data. Undulation length of the specimens must be gradually increased to plot practical design curves.

7. This manufacturing technique is most likely extrusion as it satisfies the criteria listed above and it is the manufacturing technique used in conventional catheters. However, use of extrusion brings another challenge into the future work of braided catheters: homogeneous and complete impregnation of fibers. Current thermoplastic materials used for conventional catheters have relatively high melt viscosity values compared to thermoset materials. Higher melt viscosities prevent thermoplastic matrix from fully and homogeneously impregnating fibers used in the braiding process. To avoid this, a few preventive measures may be taken such as use of special fillers that decrease matrix viscosity, or pre-impregnate and cure the braided preform using a compatible thermoset resin, and then coat it using the thermoplastic matrix.

8. Catheters are commonly subjected to axial compression type of loading; hence, critical load, P_{cr}, that results in buckling of the braided tubular structures should be determined using overall unit cell length and undulation length.

9. The buckling mode of failure should be investigated as a function of curvature in the braided strands.

10. Development of 3-Dimensional non-contact strain measurement systems may be extremely valuable during test for braided composites. Use of extensometers or strain gages has their limitations, such as limited gage length or attaching the strain gage to an uneven surface due to the texture of the specimens. It may be especially very helpful in characterization of open-mesh braided structure properties, because it may help to identify the response of undulation lengths, such bending of the undulation length, upon loading.